



UNIVERSITAT DE
BARCELONA

Design, synthesis and evaluation of the biological properties of colistin analogues

Judith Solé Solé

ADVERTIMENT. La consulta d'aquesta tesi queda condicionada a l'acceptació de les següents condicions d'ús: La difusió d'aquesta tesi per mitjà del servei TDX (www.tdx.cat) i a través del Dipòsit Digital de la UB (diposit.ub.edu) ha estat autoritzada pels titulars dels drets de propietat intel·lectual únicament per a usos privats emmarcats en activitats d'investigació i docència. No s'autoritza la seva reproducció amb finalitats de lucre ni la seva difusió i posada a disposició des d'un lloc aliè al servei TDX ni al Dipòsit Digital de la UB. No s'autoritza la presentació del seu contingut en una finestra o marc aliè a TDX o al Dipòsit Digital de la UB (framing). Aquesta reserva de drets afecta tant al resum de presentació de la tesi com als seus continguts. En la utilització o cita de parts de la tesi és obligat indicar el nom de la persona autora.

ADVERTENCIA. La consulta de esta tesis queda condicionada a la aceptación de las siguientes condiciones de uso: La difusión de esta tesis por medio del servicio TDR (www.tdx.cat) y a través del Repositorio Digital de la UB (diposit.ub.edu) ha sido autorizada por los titulares de los derechos de propiedad intelectual únicamente para usos privados enmarcados en actividades de investigación y docencia. No se autoriza su reproducción con finalidades de lucro ni su difusión y puesta a disposición desde un sitio ajeno al servicio TDR o al Repositorio Digital de la UB. No se autoriza la presentación de su contenido en una ventana o marco ajeno a TDR o al Repositorio Digital de la UB (framing). Esta reserva de derechos afecta tanto al resumen de presentación de la tesis como a sus contenidos. En la utilización o cita de partes de la tesis es obligado indicar el nombre de la persona autora.

WARNING. On having consulted this thesis you're accepting the following use conditions: Spreading this thesis by the TDX (www.tdx.cat) service and by the UB Digital Repository (diposit.ub.edu) has been authorized by the titular of the intellectual property rights only for private uses placed in investigation and teaching activities. Reproduction with lucrative aims is not authorized nor its spreading and availability from a site foreign to the TDX service or to the UB Digital Repository. Introducing its content in a window or frame foreign to the TDX service or to the UB Digital Repository is not authorized (framing). Those rights affect to the presentation summary of the thesis as well as to its contents. In the using or citation of parts of the thesis it's obliged to indicate the name of the author.

DISSERTATION

**Design, synthesis and evaluation
of the biological properties
of colistin analogues**

Judith Solé Solé

**Program of doctorate in Organic Chemistry
Department of Inorganic and Organic Chemistry
Section of Organic Chemistry
Faculty of Chemistry
University of Barcelona**

**Francesc Rabanal Anglada
Department of Inorganic and Organic
Chemistry
Section of Organic Chemistry
Faculty of Chemistry
University of Barcelona**

**Yolanda Cajal Visa
Department of Pharmacy and
Pharmaceutical Technology, and Physical
Chemistry
Faculty of Pharmacy and Food Sciences
University of Barcelona**

“An expert is a man who has
made all the mistakes which
can be made, in a narrow field”

Niels Bohr

En primer lloc vull agrair a en Francesc Rabanal que em donés la oportunitat de dur a terme aquesta tesi doctoral, per la seva ajuda i motivació durant tot aquest procés. Gràcies Yolanda Cajal per ajudar-me, no únicament en la part més 'bio', sinó durant tot aquest viatge, la teva alegria es transmet i fa que cada dia sigui més amè. Agraïments infinits per la Roser Segovia, per ensenyar-me quasi bé totes les tècniques experimentals que he dut a terme, i per donar-me suport durant tota la tesi (que no han estat pocs anys precisament). Tot i tenir les nostres diferències has estat una gran companya i m'has ajudat moltíssim.

Agraeixo a la meva família tot el suport que m'han donat, i sense els quals, possiblement, no seria la persona que soc ara ni hauria pogut recórrer aquest camí. Al meus tiets Marutxi i Enrique, i la meva cosina Ruth, per cuidar-me com una filla més i haver tingut tanta paciència amb mi, sé que no era una nena fàcil... A en Pol i l'Eva, els meus 'germanets', créixer amb vosaltres ha estat tota una aventura. Per altra banda, estic molt agraïda també als meus avis Francina i Xavier, per cuidar-me sempre, per ser com bàsicament els meus altres pares, i per obrir-me les portes de casa seva incondicionalment. No m'oblido del meu tiet David... puc recordar perfectament qui em tallava les ungles cada diumenge de petita, qui em va ensenyar a anar amb bicicleta, qui em treia de l'aigua perquè no m'ofegués, i qui s'ha desviscut, bàsicament, per fer-me riure i ajudar-me sempre. Tambien dar las gracias a mis suegros Pepi y Antonio por tratarme como si fuera de casa. Tots vosaltres heu cregut sempre en mi i m'heu fet millor persona.

No m'oblido de la gent important que m'he creuat al llarg de la meva vida i que d'alguna manera o altra m'han marcat o ajudat. Eva, Alina i Carola, tot i haver seguit camins diferents, sense vosaltres no estaria on estic ara. Menció especial per la Concepció, que no només m'obria sempre casa seva, sinó que va aconseguir que la Química fos suficientment interessant com per iniciar la meva aventura en aquest àmbit. A l'Irene, la Lucia, la Sara, l'Edu, l'Eric, en Rubén i en Pol per totes les quedades i bons moments. A la Marina, la Cris i l'Alberto, pels jajas, les viciades i les nits de festa, indispensables per sobreviure al dia a dia.

També vull agrair a totes les fieras que han passat per casa: Nala, Wendy, Samsi, Kaly, Tell, Honey, Ares, Xena, Quinoa, Vampy, Salem i per descomptat, en Luce (Lucifer), per tots els bons moments que m'han regalat.

No m'oblido d'en Xavi, sense qui possiblement no hauria acabat el Grau de Química... ni hagués sobreviscut a l'any d'Erasmus... també em vas ajudar durant el Màster, i la tesi no podia ser diferent. Crec que la idea queda clara. La nostra dinàmica de fer-nos la punyeta, competir fins la sacietat i motivar-nos l'un a l'altre han ajudat a que aquest projecte no hagi quedat a mitges. Gràcies per ser el meu Bro i el meu support troll incondicional desde que ens vam conèixer a Física II.

Per últim, agraeixo a l'Antonio Serrano per ser bàsicament el meu pilar i sense el qual de ben segur no hagués acabat aquest projecte... Gràcies per la teva paciència infinita i per animar-me sempre en els meus projectes, per molt sòrdids que puguin arribar a ser.

ABBREVIATIONS AND APPENDICES

ABBREVIATIONS

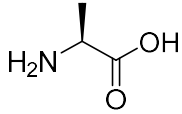
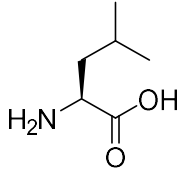
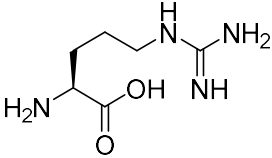
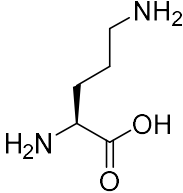
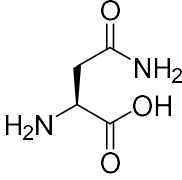
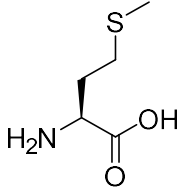
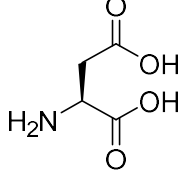
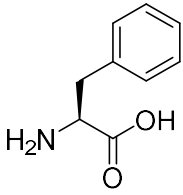
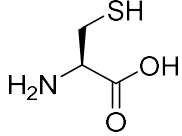
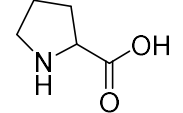
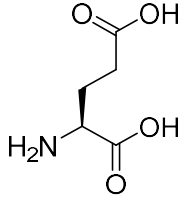
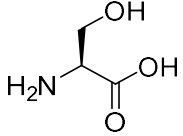
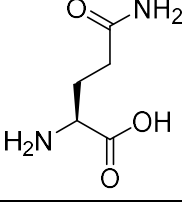
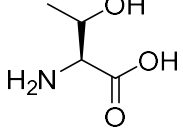
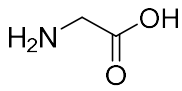
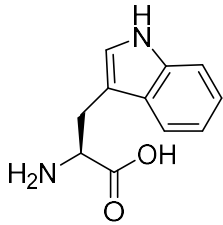
2-CTC	2-Chlorotrityl chloride resin
AA	Amino acid
<i>A. baumannii</i>	<i>Acinetobacter baumannii</i>
ABC	ATP Binding Cassette
Abu	α -Amino-n-butyric acid
ACN	Acetonitrile
ADME	Absorption, Distribution, Metabolism and Excretion
AMPs	Antimicrobial peptides
ANTS	1-Aminonaphthalene-3,6,8-trisulfonic acid
AS	Animal Score
ATCC	American Type Culture Collection
AUC	Area under the curve
BHA	Benzhydrylamine hydrochloride resin
Boc	<i>tert</i> -Butoxycarbonyl
cfu	Colony-forming unit
Chol	Cholesterol
CL	Cardiolipin
C_{max}	Maximum concentration
CMS	Colistin methanesulfonate
Dab	L-2,4-Diaminobutyric acid
DAdec	D-2-Aminodecanoic acid
DAoc	D-2-Aminooctanoic acid
Dap	2,3-Diaminopropionic acid
DCM	Dicloromethane
DHPS	Dihydropteroate synthase
DIEA	diisopropylethylamine
DIPCDI	Diisopropylcarbodiimide
DMAP	4-dimethylaminopyridine
DMF	dimethyl formamide
DMSO	dimethyl sulfoxide
DNA	Deoxyribonucleic acid
DPX	N-N'-p-xylenebis(pyridinium bromide)

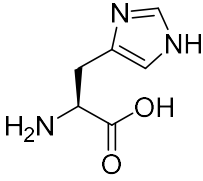
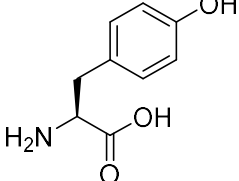
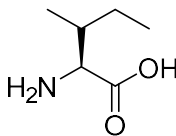
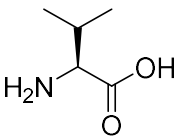
<i>E.coli</i>	<i>Escherichia coli</i>
eq	Equivalent
EUCAST	European Committee on Antimicrobial Susceptibility Testing
F	Fluorescence
Fmoc	9-Fluorenylmethoxycarbonyl
FRET	Fluorescence resonance energy transfer
GS	Group Score
GUVs	Giant unilamellar vesicles
h	hour
HATU	<i>N</i> -[(Dimethylamino)-1 <i>H</i> -1,2,3-triazolo-[4,5- <i>b</i>]pyridin-1-ylmethylene]- <i>N</i> -methylmethanaminium hexafluorophosphate <i>N</i> -oxide
HFIP	Hexafluoroisopropanol
HOBt	Hydroxybenzotriazole
HPLC	High-performance liquid chromatography
IM	Inner membrane
LADME	Liberation, Absorption, Distribution, Metabolism and Excretion
LPS	Lipopolysaccharide
LUVs	Large unilamellar vesicles
MATE	Multidrug and Toxic compound Extrusion family
MBC	minimum bactericidal concentration
MFS	Major facilitator superfamily
MHB	Mueller Hinton Broth
MIC	Minimum inhibitory concentration
min	Minute
MLD	Minimum Lethal Dose
MLVs	Multilamellar vesicles
mRNA	Messenger ribonucleic acid
MVs	Multivesicular vesicles
MW	Molecular weight
NA	Not aplicable
NBD-PE	1,2-dimyristoyl- <i>sn</i> -glycero-3-phosphoethanolamine- <i>N</i> -(7-nitro-2-1,3-benzoxadiazol-4-yl)
ND	Not determined

Nva	Norvaline
OD	Optical density
OM	Outer membrane
<i>P. aeruginosa</i>	<i>Pseudomonas aeruginosa</i>
PC	Phosphatidylcholine
PE	Phosphatidylethanolamine
PG	Phosphatidylglycerol
PI	Phosphatidylinositol 4,5-bisphosphate
PK	Pharmacokinetics
POPC	1-Palmitoyl-2-oleoyl-sn-glycero-3-phosphocholine
POPE	1-Palmitoyl-2-oleoyl-sn-glycero-3-phosphoethanolamine
POPG	1-Palmitoyl-2-oleoyl-sn-glycero-3-phospho-(1'-rac-glycerol)
PS	Phosphatidylserine
PxB	Polymyxin B
PxE	Colistin
Rh-PE	1,2-dioleoyl-sn-glycero-3-phosphoethanolamine-NB sulfonyl) - (lissamine rhodamine)
RNA	Ribonucleic acid
RND	Resistance-Nodulation-cell Division family
<i>S. aureus</i>	<i>Staphylococcus aureus</i>
SM	Sphingomyelin
SUVs	Small unilamellar vesicles
SP	Sphingolipids
SPPS	Solid phase peptide synthesis
tBu	tert-Butyl
TEM	Transmission electron microscopy
TES	Triethylsilane
TFA	Trifluoroacetic acid
TFE	2,2,2-trifluoroethanol
T_{max}	Time of maximum concentration
TIS	Triisopropylsilane
Ttr	Thiothreonine or thiolate threonine
tRNA	Transfer ribonucleic acid
TSA	Tryptone soya agar

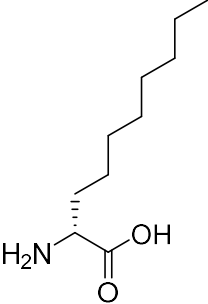
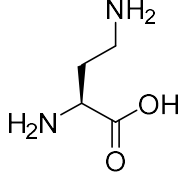
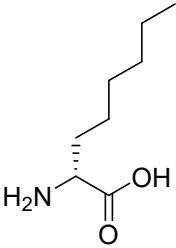
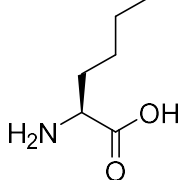
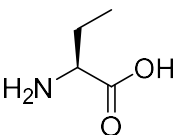
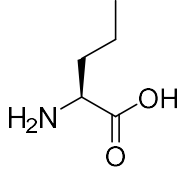
TSB	Tryptone soya broth
UV-VIS	Ultraviolet-visible

Appendix 1. Structure of the most common amino acid residues, with their 3 and 1 letter codes.

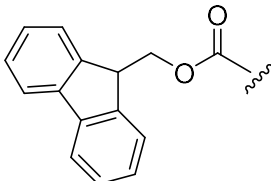
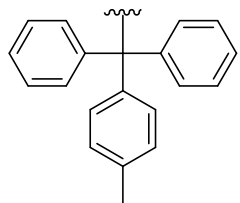
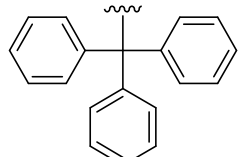
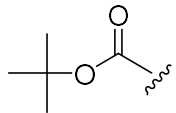

Amino Acid	Structure	Amino Acid	Structure
Alanine Ala A		Leucine Leu L	
Arginine Arg R		Lysine Lys K	
Asparagine Asn N		Methionine Met M	
Aspartic acid Asp D		Phenylalanine Phe F	
Cysteine Cys C		Proline Pro P	
Glutamic acid Glu E		Serine Ser S	
Glutamine Gln Q		Threonine Thr T	
Glycine Gly G		Tryptophan Trp W	

Histidine His H		Tyrosine Tyr Y	
Isoleucine Ile I		Valine Val V	

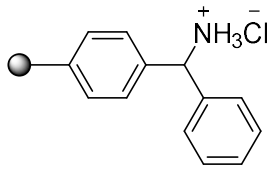
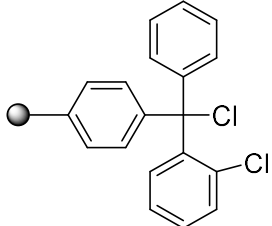
Appendix2. Structure of the non-proteogenic amino acid residues used in this thesis, with their abbreviation.

Amino Acid	Structure	Amino Acid	Structure
D-2-Aminodecanoic acid D-Adec		L-2,4-Diaminobutyric acid Dab	
D-2-Amino-octanoic acid D-Aoc		L-Norleucine Nle	
L-2-Aminobutyric acid Abu		L-Norvaline Nva	

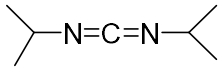
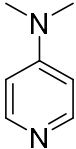
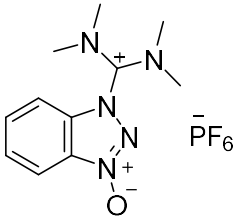
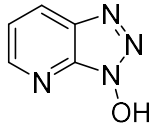

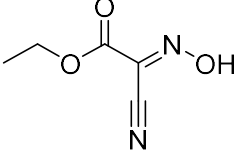
Appendix 3. Structure of the protecting groups used in this thesis, with their abbreviation.

Protective Group	Structure
9-Fluorenylmethoxycarbonyl Fmoc	
4-Methyltrityl Mtt	
Trityl Trt	
<i>tert</i> -Butoxycarbonyl Boc	
<i>tert</i> -Butyl ^t Bu	

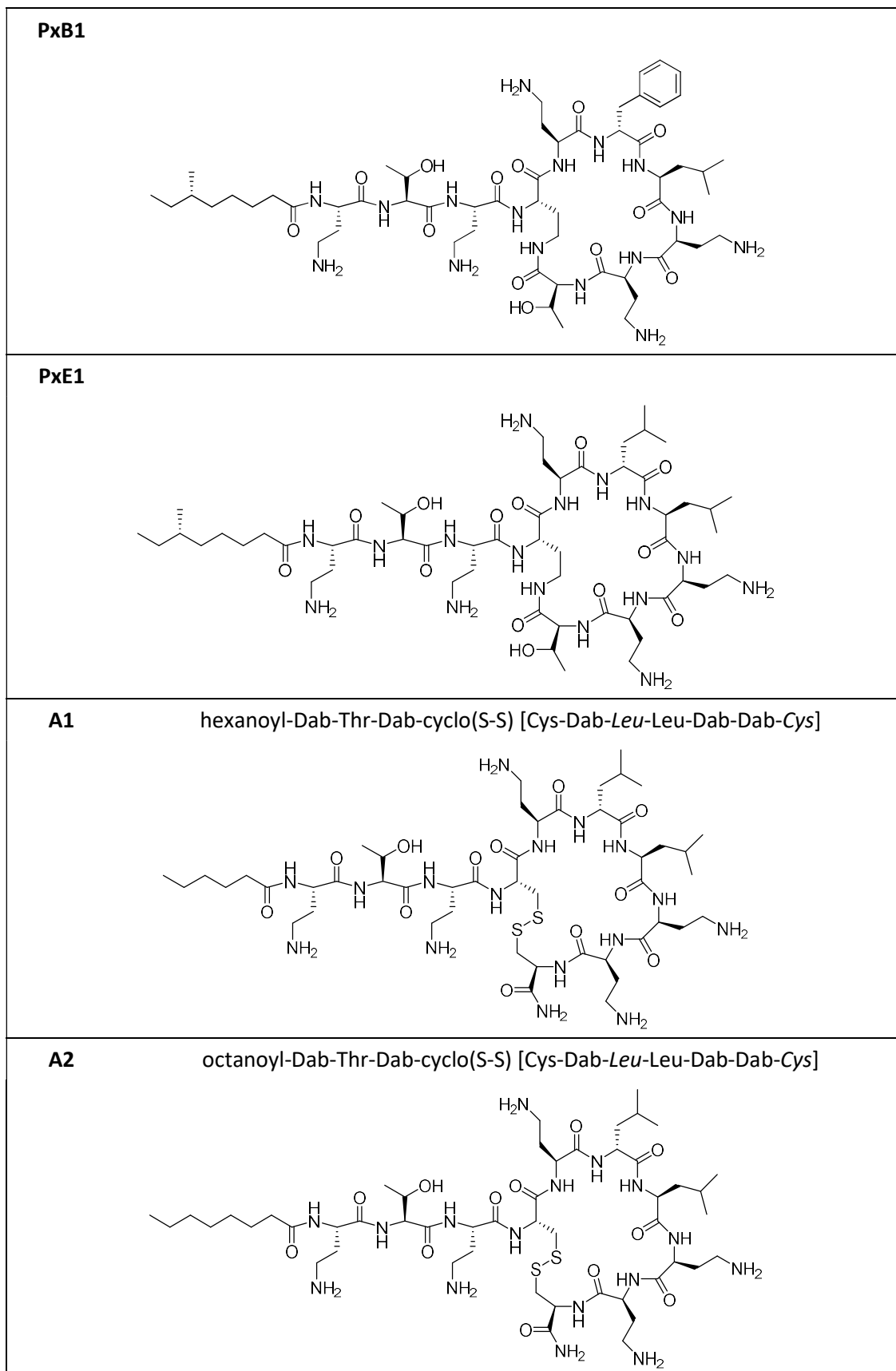
Appendix 4. Structure, name and abbreviation of the polymeric supports used in this thesis.

Polymeric Support	Structure
Benzhydrylamine Hydrochloride resin BHA	
2-Chlorotrityl chloride resin 2-CTC	

Appendix 5. Structure, name and abbreviation of the coupling reagents used in this thesis.

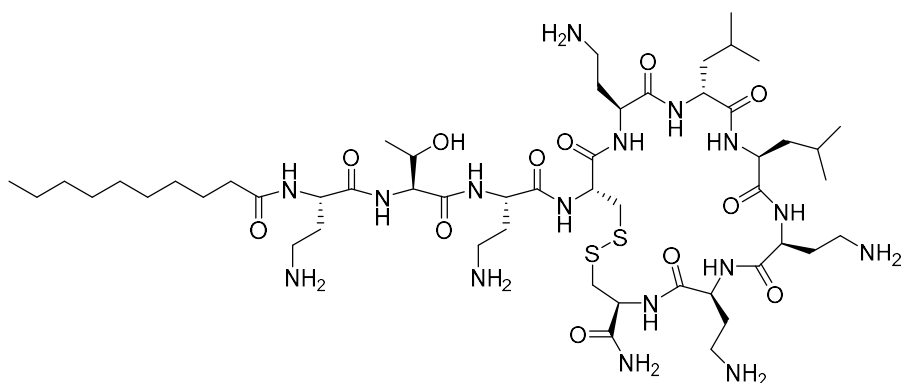
Coupling Agent	Structure
<i>N,N'</i> -Diisopropylcarbodiimide DIC	
<i>N,N</i> -Dimethyl-4-aminopyridine DMAP	
1-[Bis(dimethylamino)methylene]-1H-1,2,3-triazolo[4,5-b]pyridinium 3-oxide hexafluorophosphate HATU	
1-Hydroxy-7-azabenzotriazole HOAt	
<i>N</i> -Hydroxybenzotriazole HOBt	
Ethyl (2 <i>Z</i>)-2-cyano-2-(hydroxyimino)acetate (K-Oxyma)	

Appendix 6. Structure and sequence of the synthetic analogues used in this thesis. Amino acid residues are in three-letter code, D-amino acids are denoted in *italics* and underlined residues denote an ester bond formation.

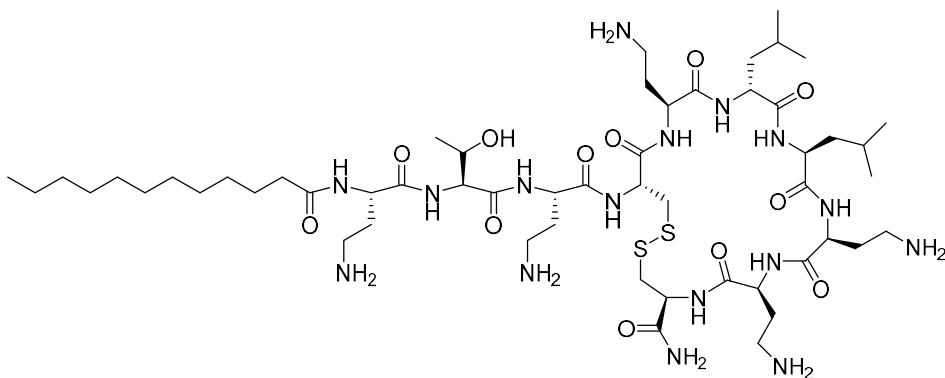


A3

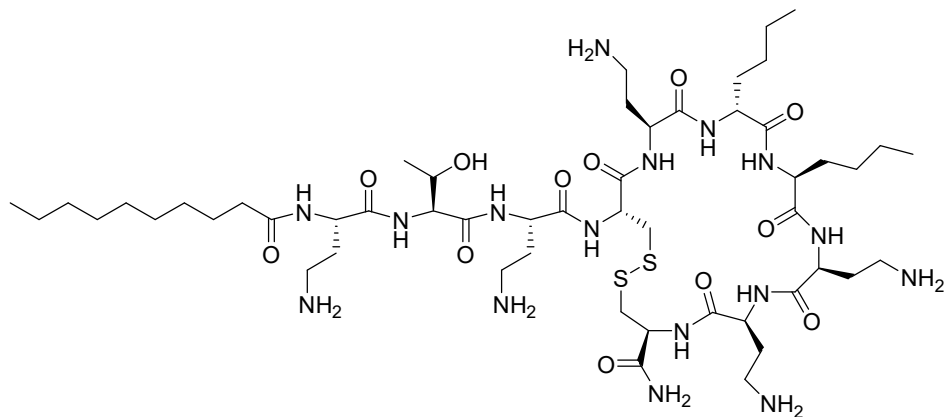
decanoyl-Dab-Thr-Dab-cyclo(S-S) [Cys-Dab-Leu-Leu-Dab-Dab-Cys]

**A4**

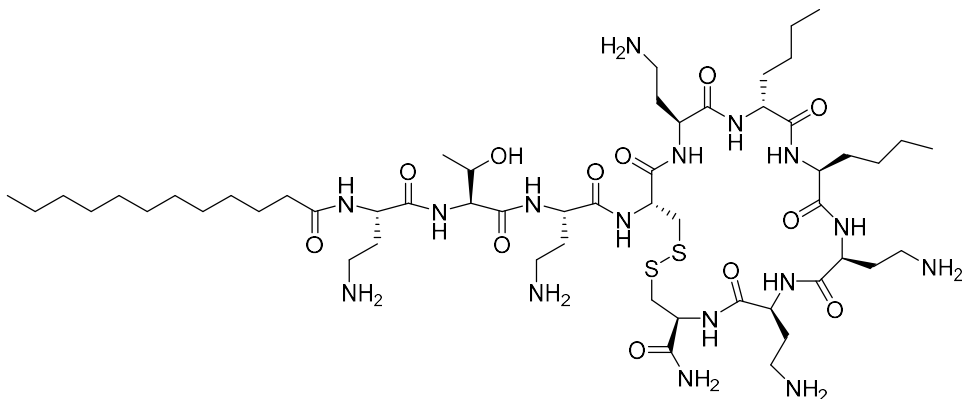
dodecanoyl-Dab-Thr-Dab-cyclo(S-S) [Cys-Dab-Leu-Leu-Dab-Dab-Cys]

**A5**

decanoyl-Dab-Thr-Dab-cyclo(S-S) [Cys-Dab-Nle-Nle-Dab-Dab-Cys]

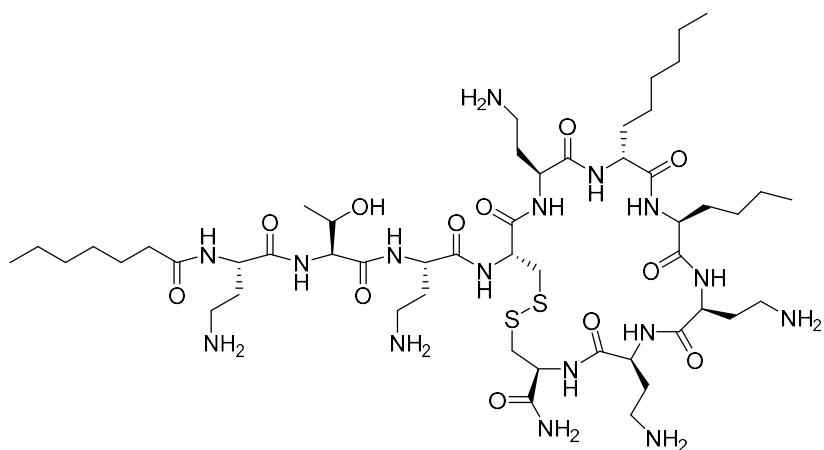
**A6**

dodecanoyl-Dab-Thr-Dab-cyclo(S-S) [Cys-Dab-Nle-Nle-Dab-Dab-Cys]

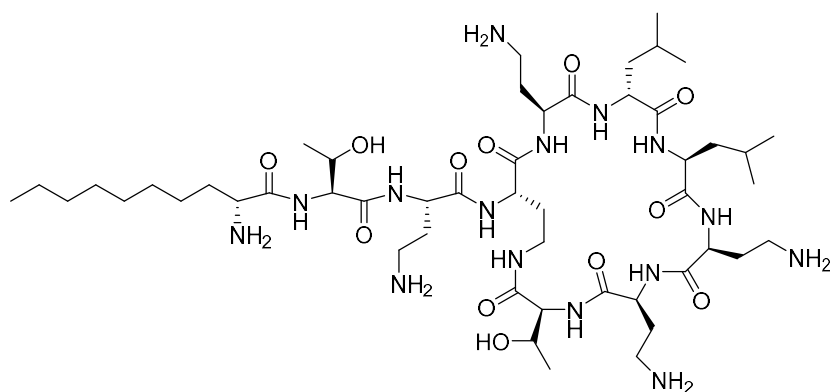


A7

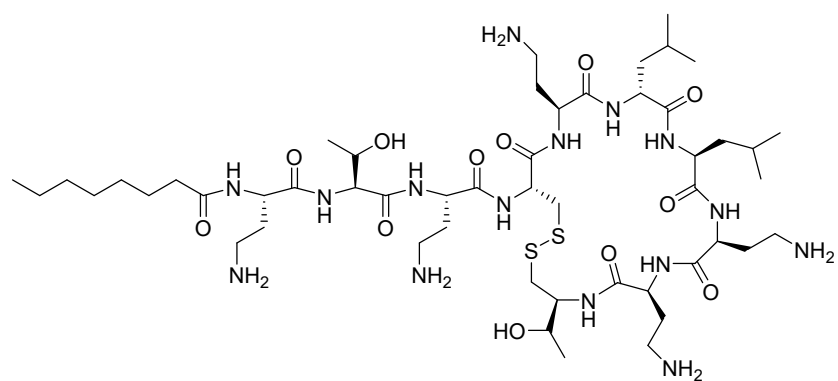
heptanoyl-Dab-Thr-Dab-cyclo(S-S) [Cys-Dab-Aoc-Nle-Dab-Dab-Cys]

**B1**

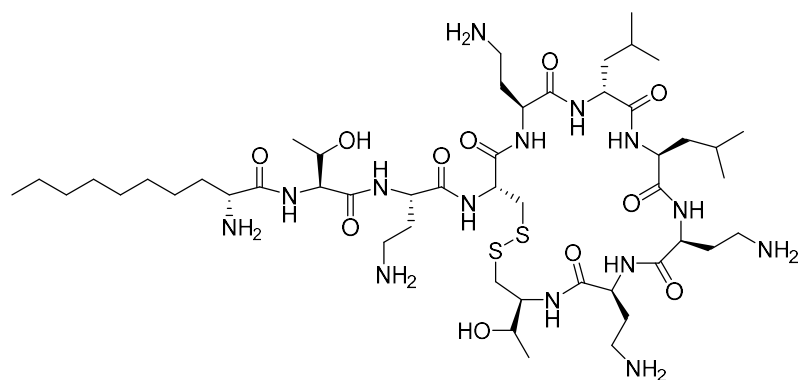
Adec-Thr-Dab-cyclo [Dab-Dab-Leu-Leu-Dab-Dab-Thr]

**B2**

octanoyl-Dab-Thr-Dab-cyclo(S-S) [Cys-Dab-Leu-Leu-Dab-Dab-Ttr]

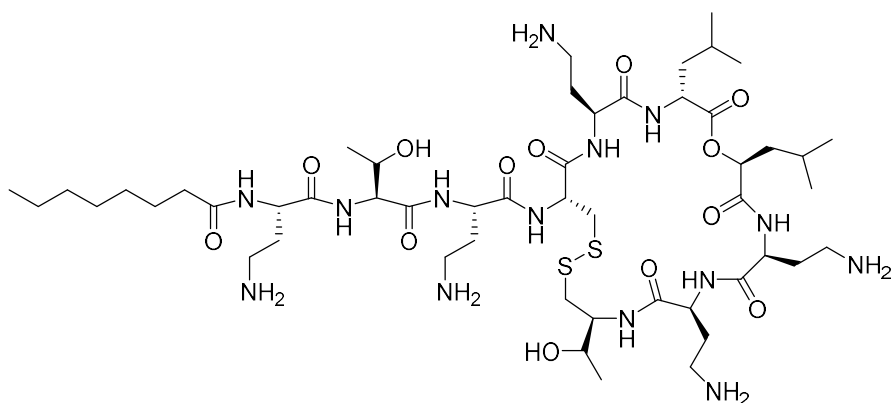
**B3**

Adec-Thr-Dab-cyclo(S-S) [Cys-Dab-Leu-Leu-Dab-Dab-Ttr]

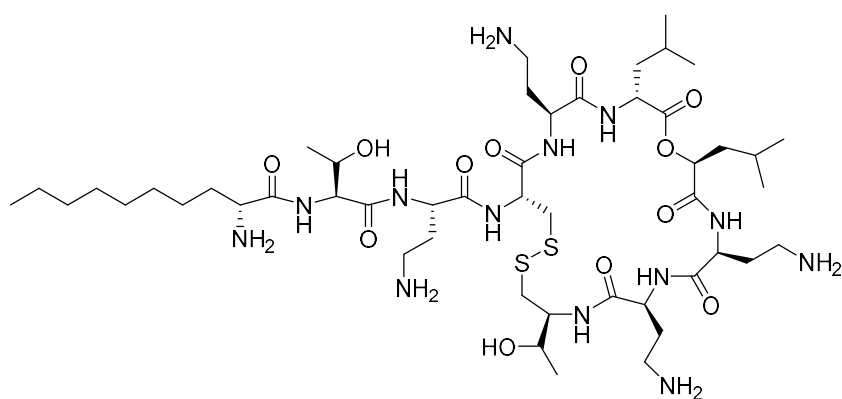


B4

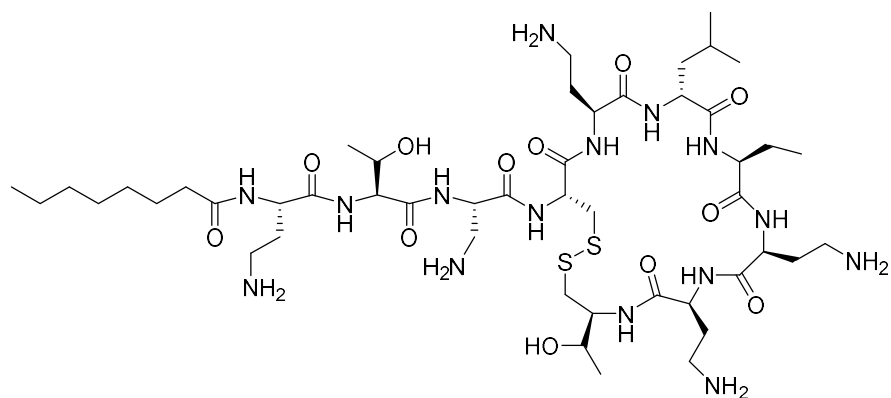
octanoyl-Dab-Thr-Dab-cyclo(S-S) [Cys-Dab-Leu-Leu-Dab-Dab-Ttr]

**B5**

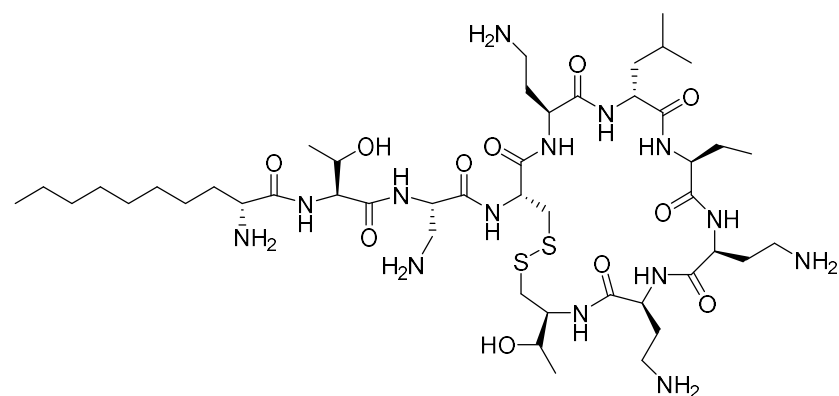
Adec-Thr-Dab-cyclo(S-S) [Cys-Dab-Leu-Leu-Dab-Dab-Ttr]

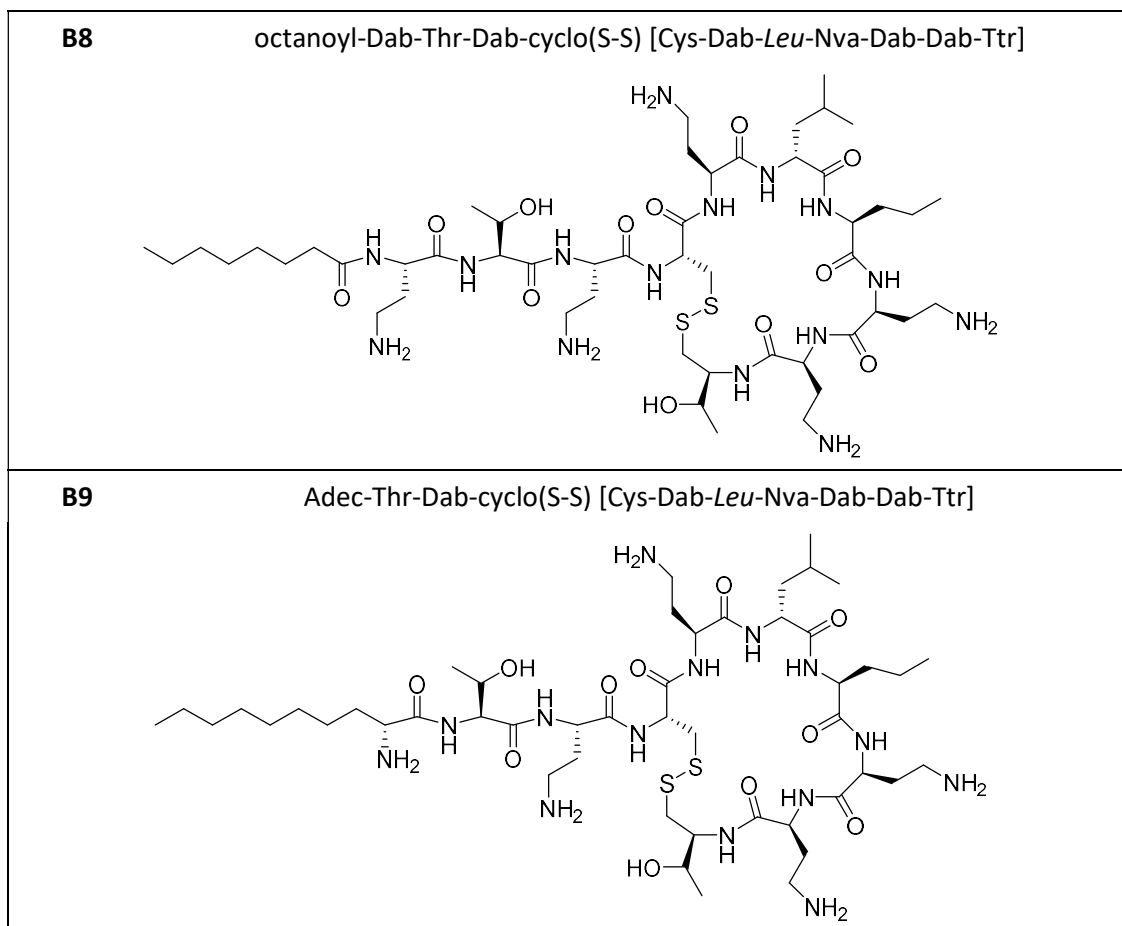
**B6**

octanoyl-Dab-Thr-Dab-cyclo(S-S) [Cys-Dab-Leu-Abu-Dab-Dab-Ttr]

**B7**

Adec-Thr-Dab-cyclo(S-S) [Cys-Dab-Leu-Abu-Dab-Dab-Ttr]





Appendix 7. Structure of the headgroups of the lipids used in this thesis, where R = acyl chain.

Lipid Headgrups	Structure
Phosphatidylcholine PC	
Phosphatidylethanolamine PE	
Phosphatidylglycerol PG	

INDEX

CONTENTS

ABBREVIATIONS AND APPENDICES	I
INDEX	XVII
1. INTRODUCTION	1
1.1. MICROORGANISMS	3
1.2. BACTERIA	4
1.2.1. BACTERIAL STRUCTURE: GRAM-POSITIVE VS GRAM-NEGATIVE	4
1.3. ANTIBIOTICS	8
1.3.1. ANTIBIOTICS CLASSIFIED BY STRUCTURE	9
1.3.2. ANTIBIOTICS CLASSIFIED BY MECHANISM OF ACTION	15
1.3.3. ANTIBIOTICS CLASSIFIED BY EFFECTS ON BACTERIA	17
1.3.4. CURRENT LIMITATIONS OF AVAILABLE ANTIBIOTICS	17
1.4. BACTERIAL RESISTANCE CRISIS	18
1.5. ANTIMICROBIAL PEPTIDES	22
1.5.1. CLASSIFICATION OF AMPS	23
1.6. POLYMYXINS	26
1.6.1. STRUCTURE OF POLYMYXINS	27
1.6.2. MECHANISM OF ACTION OF POLYMYXINS	29
1.6.3. SPECTRUM OF ACTIVITY	31
1.6.4. TOXICITY	32
1.6.5. MECHANISMS OF RESISTANCE TO POLYMYXINS	33
2. OBJECTIVES	35
3. COLISTIN ANALOGUES	39
3.1. ANALOGUES DESIGN AND SYNTHESIS	41
3.1.1. OVERVIEW OF POLYMYXIN ANALOGUES	41
3.1.2. DESIGN OF NEW COLISTIN ANALOGUES	46
3.1.3. CHEMICAL SYNTHESIS OF THE POLYMYXIN ANALOGUES	51
3.1.3.1. Scale-up of the synthesis of colistin analogue #B3	59
3.2. SERIES A	62
3.2.1. IN VITRO ANTIMICROBIAL ACTIVITY	62
3.2.2. HAEMOLYSIS	64
3.2.3. BIOPHYSICAL EVALUATION	66

3.2.3.1. Biological membranes	66
3.2.3.2. Biophysical studies.....	70
3.2.3.3. Lipid monolayers.....	70
3.2.3.4. Liposomes	74
3.2.3.5. Biophysical evaluation of the interaction of colistin analogues with the lipid membrane	78
3.2.3.5.1. Monolayers of Langmuir.....	79
3.2.3.5.2. Aggregation and fusion of vesicles induced by the peptides	81
3.2.3.5.3. FRET experiments to detect membrane fusion.....	84
3.2.3.5.4. Permeabilization of the lipid membrane induced by the peptides	85
3.2.4. TRANSMISSION ELECTRON MICROSCOPY (TEM)	86
3.3. SERIES B.....	89
3.3.1. <i>IN VITRO</i> ANTIMICROBIAL ACTIVITY.....	89
3.2.3. <i>IN VIVO</i> ASSAYS	91
3.2.3.1. Nephrotoxicity	92
3.2.3.1.1. Nephrotoxicity assessment.....	94
3.2.3.2. Pharmacokinetics (PK)	97
3.2.3.2.1. PK assessment.....	98
3.2.3.3. Efficacy	100
3.2.4. DISCUSSION	108
4. CONCLUSIONS.....	117
5. MATERIALS AND METHODS.....	121
5.1. CHEMICAL SYNTHESIS OF COLISTIN ANALOGUES.....	123
5.1.1. SOLVENTS	123
5.1.2. REAGENTS.....	123
5.1.3. INSTRUMENTS	124
5.1.4. METHODS	124
5.1.4.1. Qualitative ninhydrin assay (Kaiser test)	124
5.1.4.2. Solid phase peptide synthesis (SPPS)	125
5.1.4.2.1. Protection of amino acids.....	125
5.1.4.2.2. Initial treatment of resins	127
5.1.4.2.3. Elongation of peptide chain.....	127

5.1.4.2.4. Coupling quantification of the first amino acid	130
5.1.4.2.5. Cleavage, deprotection and cyclization of the peptides	130
5.1.4.3. High performance liquid chromatography (HPLC).....	132
5.1.4.4. Mass spectrometry	133
5.2. IN VITRO BACTERIAL BIOLOGICAL ASSAYS AND HEMOLYTIC ACTIVITY DETERMINATION.....	134
5.2.1. REAGENTS	134
5.2.2. MATERIALS.....	134
5.2.3. INSTRUMENTS	134
5.2.4. METHODS.....	135
5.2.4.1. Minimum Inhibition Concentration (MIC) determination	135
5.2.4.2. Haemolysis determination	135
5.3. DETERMINATION OF THE MECHANISM OF ACTION	137
5.3.1. REAGENTS	137
5.3.2. MATERIALS.....	137
5.3.3. INSTRUMENTS	138
5.3.4. METHODS.....	138
5.3.4.1. Preparation of liposomes.....	138
5.3.4.2. Kinetics of insertion into monolayers	139
5.3.4.3. Aggregation of liposomes measured as light scattering intensity	139
5.3.4.4. Fluorescence assays for lipid mixing.....	140
5.3.4.5. Leakage assay.....	140
5.3.4.6. TEM	141
5.4. IN VIVO ASSAYS	142
5.4.1. REAGENTS	142
5.4.2. MATERIALS.....	142
5.4.3. INSTRUMENTS	142
5.4.4. METHODS.....	143
5.4.4.1. Nephrotoxicity.....	143
5.4.4.2. Pharmacokinetics	144
5.4.4.3. Efficacy	145
5.5. EXPERIMENTAL PART.....	149
6. REFERENCES	153

1. INTRODUCTION

1.1. MICROORGANISMS

From the advent of humanity, microorganisms have been present and remained hidden to our sight until a few centuries ago. It has been reported that in Antiquity lenses were already used for decoration, religious purposes, ignition of fire or even magnification of objects [Sines & Sakellarakis, 1987]. Although it is believed that eyeglasses were invented around 1286 in Italy, it was not until 1590 that the first microscope was created by Hans and Zacharias Janssen [Wollman et al., 2015]. This discovery was the steppingstone that led to the origins of microbiology.

Therefore in 1665 Robert Hooke, an English scientist, using a microscope improved by himself, described in his book *Micrographia* several biological specimens and also introduced the term cell to describe the resemblance of the empty box-like compartments of cork tissue [Gest, 2009].

Shortly after, Antonie van Leeuwenhoek, took the microscope design to new levels and in 1674 managed to observe the first detailed microorganisms, which he named *animalcules*. During the following years Leeuwenhoek continued studying different biological sources and improving his microscopy methods, which he always kept in secret, and described his observations in several letters addressed to the Royal Society of London. Among these communications perhaps the most relevant description is that of the prokaryotes known as bacteria [Lane, 2015].

The relevance of these observations is now indisputable, however at that time it was hard to believe on something that could not be seen by the naked eye, which raised some controversy. This, added to the lack of information of the Leeuwenhoek methods, contributed to the slow progress of microbiology for more than a century.

It was not until 1876 when the first relation between a bacterium and a contagious disease was established. The first bacterial disease ever discovered was anthrax (caused by *Bacillus anthracis*) of cattle and sheep in 1876 [Belvins & Bronze, 2010].

During the following decades, several infectious diseases such as cholera, leprosy, gonorrhoea, typhoid and diphtheria were found to be caused by bacteria, which increased the popular interest in their research [Santer, 2009].

1.2. BACTERIA

Bacteria are prokaryotic, single-celled microorganisms that have a simple internal structure and are in general much smaller than eukaryotic cells. It is believed that not only bacteria were among the first living organisms to live on Earth, but that we owe our existence to them since they spent billions of years releasing the oxygen that was needed for larger life forms to emerge. During all these years, bacteria have evolved progressively and nowadays are incredibly diverse: they can be found almost everywhere and even can survive in extreme environments [Madigan et al., 2002, p22-24].

Bacteria high diversity and its continuous evolution makes it hard to establish a unique bacterial classification, but perhaps one of the most relevant relies on its structure composition based on the presence or absence of an outer lipid-membrane, differentiating thus between Gram-negative and Gram-positive bacteria, respectively [Krieg et al., 2010, p. 304].

1.2.1. BACTERIAL STRUCTURE: GRAM-POSITIVE VS GRAM-NEGATIVE

Although the structure of prokaryotic cells, represented simplified in **Figure 1**, is not unique and can vary, in general terms they are composed of three different regions: the cell envelope (comprising a cell membrane, a cell wall and sometimes a capsule), the appendages and the cytoplasmatic region [Madigan et al., 2002, p56-101].

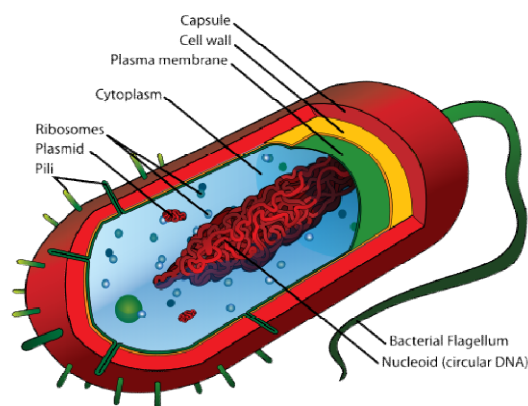


Figure 1. General structure of a prokaryotic cell (bacteria) highlighting the most important regions. Figure taken from Wikimedia.

The intracellular or cytoplasmic region, which contains the aqueous solution called cytoplasm formed by proteins and nutrients, comprises mainly ribosomes (to read gene sequences to synthesize proteins) and chromosomal deoxyribonucleic acid (DNA) that contains the genetic information; however, some specialized groups of bacteria can contain additional complex intracellular structures [Madigan et al., 2002, p171-179; p194-205; Fuerst, 2005].

The cell membrane, also known as cytoplasmic or plasma membrane, is a thin lipid bilayer composed of phospholipids and proteins that encloses the cell cytoplasm and acts as an osmotic or permeability barrier. It is responsible of the transport of ions across the membrane and also has energy generating functions [Madigan et al., 2002, p66-81].

Lying outside the cell membrane there is the cell wall, which is a rigid structure made up of peptidoglycan. The cell wall provides structural integrity to the cell, protecting it from internal turgor pressure and determining its cell shape. The cell wall is relatively porous and permeable for small substrates; however, it is required for the survival of most bacteria [Demchick & Koch, 1996].

In some of these prokaryotes, an external polysaccharide layer named capsule can be found, providing extra protection against external threats, such as white blood cells and other predatory agents, preventing from drying out thanks to its water content, and helping the adhesion of cells to surfaces [Peterson & Baron, 1996, chapter 7].

On some bacteria, an extracellular region formed with structures or appendages, can be found, such as pili or flagella, which allow their mobility, to stick to other surfaces and to interact with other cells [Madigan et al., 2002, p81-89].

Albeit this is the general description of the architecture of prokaryotic cells, there are structural differences between the two big groups of bacteria: Gram-positive and Gram-negative bacteria. While Gram-positive bacteria emulate the previous description with a thicker cell wall, Gram-negative bacteria possess a thinner cell wall surrounded by an additional outer lipid membrane, detailed in **Figure 2** [Madigan et al., 2002, p79-81].

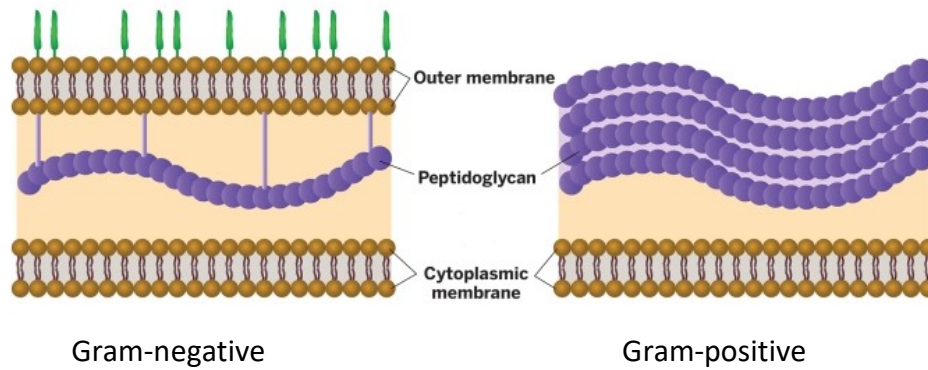


Figure 2. General structure of a prokaryotic cell (bacteria) highlighting the most important regions or formations. Figure taken from Shutterstock.

The nomenclature of Gram-positive or -negative stems from the Gram stain, which is a method of staining used to distinguish and classify bacteria and that was developed by bacteriologist Hans Christian Gram in 1884 [Bartholomew & Mittwer, 1952]. Having a thicker cell wall, Gram-positive bacteria retain efficiently the primary stain, crystal violet, which paints them with a purple color. On the other side, Gram-negative bacteria do not retain the crystal violet and are instead stained by the counterstain, safranin, which grants them a pink color.

The outer lipid membrane is only found in Gram-negative bacteria. Albeit being a lipid bilayer and fulfilling a similar function of limiting permeability, it differentiates from the inner lipid membrane by its composition: aside from phospholipids, it also contains anchored proteins and lipopolysaccharides (LPS) [Madigan et al., 2002, p79-81].

LPS composition differs between bacteria species, but essentially are large molecules composed by a lipid (Lipid A) and a polysaccharide chain (O-specific polysaccharide) linked by covalent bonds through a polysaccharide core (polysaccharide core), as detailed in **Figure 3**. Lipid A functions as an anchor to the outer lipid membrane and both it and the polysaccharide core contain phosphate groups, which confer an overall negative charge to the bacterial surface. The LPS contributes to the structural integrity of bacteria and protects them from chemical insults. Finally, LPS triggers strong immune reaction from animals, sometimes leading to septic shocks; as well as being involved in surface adhesion and interactions with predators. For all these reasons, the outer lipid membrane

greatly differs from the inner lipid membrane or eukaryotic lipid membranes [Madigan et al., 2002, p79-81].

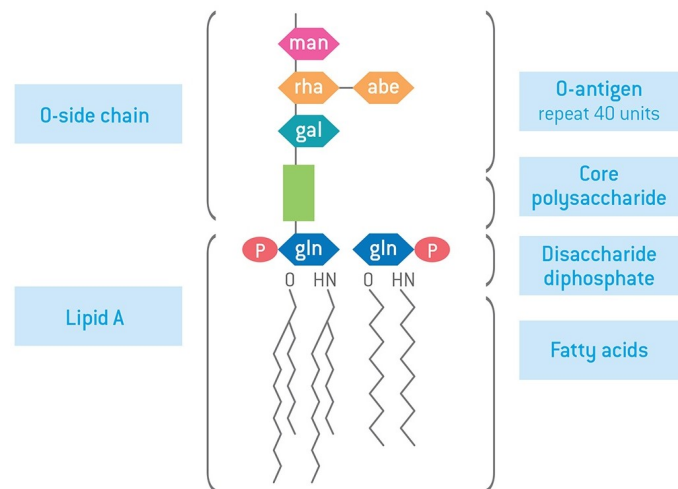


Figure 3. General composition of the LPS membrane of gram-negative bacteria. Figure taken from Lonza website.

The structural differences between the envelopes of Gram-positive and Gram-negative bacteria result in different behavior to the environment and several substances. These differences would also prove critical once the first scientists started identifying compounds which specifically inhibited the growth or killed bacteria: the antibiotics [Madigan et al., 2002, p79-81].

1.3. ANTIBIOTICS

Historical evidence has been found pointing out that in ancient civilizations, like Egypt, Greece, Rome and China, microbial infections were treated using natural sources like herbs, honey, animal feces and mould [Forrest, 1982; Wainwright, 1989].

It was not until the late 1800s when Louis Pasteur and Robert Kock established the relationship between germs and diseases, stating thus that the disease is the visual effect of a cause that can be found and eliminated by a specific treatment. The spread of some diseases led then to the experimentation with possible treatments, especially with arsenic-based compounds; however, the side effects often became worse than the disease [Williams, 2009].

In this context, and during the decade of 1920, the British scientist Alexander Fleming was working in his laboratory at St. Mary Hospital in London when, by accident, discovered a natural substance with antimicrobial activity. In one of his experiments in 1928, Fleming observed that *Staphylococcus aureus* colonies were transparent due to bacterial lysis presumably caused by a mold that was growing in the same Petri dish. That mold species was *Penicillium notatum*, and the bacterial lysis was being caused by a compound produced by it: penicillin [James, 1971]. However, its difficult isolation delayed its availability over more than a decade, and it was not until 1942 that it was effectively used to treat septicemia (blood poisoning). During that period, and following synthetic approaches, J. Klarer and F. Mietzsch, a group of researchers from Bayer, synthesized in 1932 the sulfamidochrysoidine compound, also known as prontosil, which was later effectively tested in mice by G. Domagk against some important antibacterial infections, and effectively used the same year to treat septicemia. Both discoveries, penicillin and prontosil, led to the golden era of antibiotics.

In 1942 Selman Waksman and his collaborators used the term antibiotic describing it as “any substance produced by a microorganism that is antagonistic to the growth of other microorganism in high dilution”. This definition has evolved since then and now an antibiotic (or antibacterial) can be described as a chemical

compound that destroys or inhibits the growth of other microorganisms and is used in the treatment of bacterial infections [Kresge et al., 2004].

Over the following years, further substances from different sources were classified as antibiotics [Coates et al., 2011]. Now, antibiotics can be categorized in several different ways, but the commonest classifications are based on their structure, their mechanism of action and their spectrum of activity. Moreover, antibiotics can be classified based on the route of administration and on their effect over bacteria [Fomnya et al., 2021].

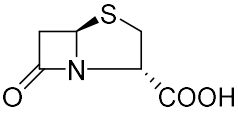
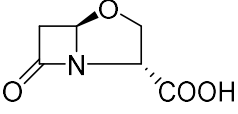
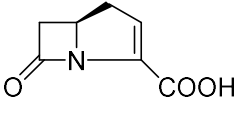
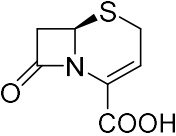
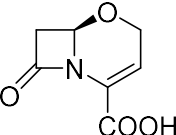
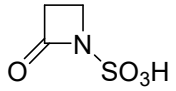
1.3.1. ANTIBIOTICS CLASSIFIED BY STRUCTURE

Antibiotics can be classified in different families depending on their chemical structures. We can distinguish between β -lactams, tetracyclines and glycyliclones, chloramphenicol, aminoglycosides, quinolones, macrolides and ketolides, lincosamides, streptogramins, glycopeptides, sulfonamides, trimethoprim, oxazolidinones, lipopeptides and ansamycins. In the following sections the most common classes will be detailed [Van Hoek et al., 2011; Frank and Tacconelli, 2012; Adzitey, 2015].

➤ β -lactams

This type of antibiotics is the most widely used and contains a β -lactamic ring in their molecular structure. The ring, which is highly reactive, allows them to inhibit the crosslink of peptidoglycan, essential for the synthesis of bacterial cell wall, which results in lysis and cell death. This building block conforms a large class of antibiotics; all of them share the same mechanisms of action but present different spectrum, pharmacokinetics and activity against resistant bacterial strains. Among this family the following classes have been described: penams, clavams, carbapenems, cepheids, oxacepheids and monobactams, detailed in **Table 1** [Mora-Ochomogo & Lohans, 2021; Etebu & Arikekpar, 2016; Van Bambeke et al., 2100; s7].

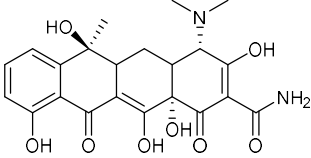
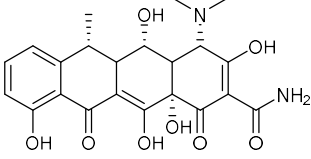
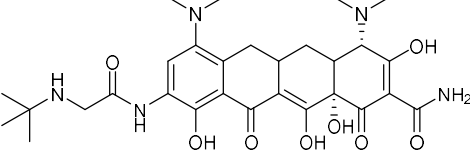
Table 1. Classes of β -lactam antibiotics, with their characteristic structure and some representative examples; it can be observed that all share a common four-piece β -lactam ring [Van Bambeke et al., 2010; s7].

Group	Core structure	Example (of the group)
Penam		Penicilins
Clavam		Clavulanic acid
Carbapenem		Imipenem, meropenem
Cephem		Cephalosporins
Oxacephem		Latamoxef
Monobactam		Aztreonam

➤ Tetracyclines

Tetracyclines are composed of a rigid skeleton of 4 fused rings diversely substituted mainly by hydroxylated hydrophilic groups. Thanks to this structure, tetracyclins are able to interact with the ribosome subunits in charge of transfer ribonucleic acid (tRNA) translation, halting thus the elongation of amino acids to polypeptide chains during protein synthesis in bacteria [Chopra & Roberts, 2001; Etebu & Ariekpar, 2016]. We can differentiate three different generations of this family of antibiotics depending on how they are obtained: First generation (obtained by biosynthesis), Second generation (obtained by semi-synthesis) and Third generation (obtained from total synthesis). Some representative examples of these antibiotics are tetracycline, doxycycline and tigecycline, described in **Table 2** [Fuoco, 2012].

Table 2. Chemical structure of representative examples of different generations of tetracyclines (tetracycline, doxycycline, tigecycline), all sharing the rigid skeleton of four fused rings.

Generation	Example	Structure
First	Tetracycline	
Second	Doxycycline	
Third	Tigecycline	

➤ Quinolones

This family of totally synthetic products was first discovered as nalidixic acid, found as an impurity in the synthesis of quinine. This basic molecule, consisting of two rings, has been modified since then and recent generations can present an added ring that allows them to improve their antimicrobial activity spectrum. We can now distinguish two major groups of compounds, the fluoroquinolones and naphthyridones; some examples are detailed in **Figure 4**.

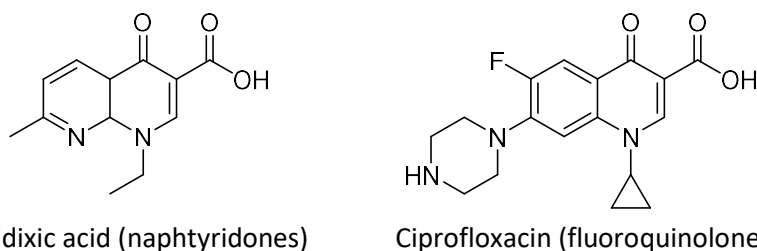


Figure 4. Chemical structure of representative examples of each class of quinolones. Nalidixic acid is an example of naphthyridones, while ciprofloxacin is a representative example of fluoroquinolones.

Most quinolones have a fluorine atom in their structure and are effective against both Gram-negative and Gram-positive bacteria, while also presenting some activity against anaerobic bacteria. The target of quinolones is DNA gyrase (in Gram-negative bacteria) and topoisomerase IV (in Gram-positive bacteria).

In normal conditions these molecules are in charge of cutting the DNA, supercoiling and resealing it; quinolones inhibit the last step which causes the DNA to break down and leads to bacterial death [Pham et al., 2019].

➤ Macrolides

This family includes natural antibiotics and antifungals composed of a large macrocyclic lactone ring (typically 14-, 15- or 16- membered rings) with one or more deoxy sugars attached [Mazzei et al., 1993]. Macrolides bind to bacterial ribosomes, preventing the elongation of amino acid to polypeptide chains during protein synthesis. This class of compounds presents a wider spectrum than penicilins, and also present immunomodulatory and anti-inflammatory effects. Since the first developed macrolide, erythromycin, several derivatives have been obtained with improved bioavailability; **Figure 5** contains some representative examples of this family of antibiotics [Etebu & Arikekpar, 2016].

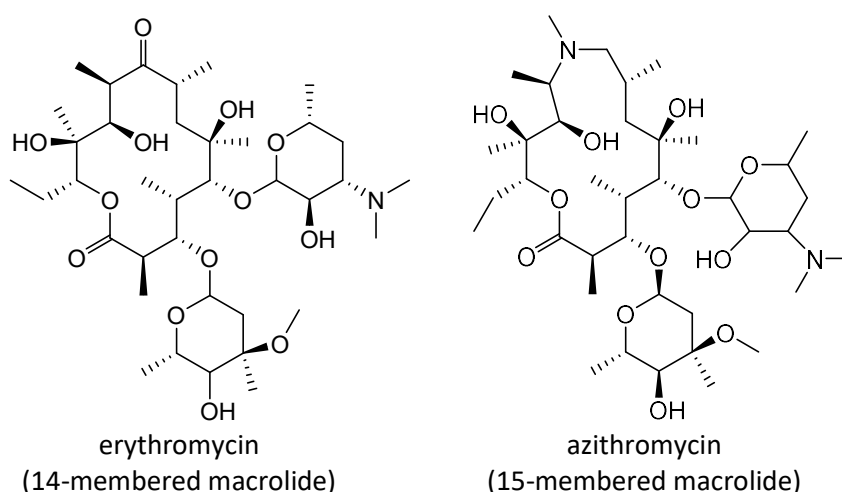


Figure 5. Structure of representative examples of macrolides: erythromycin and azithromycin.

➤ Sulfonamides

Prontosil was the first sulfonamide discovered in 1930s. This discovery opened a new era in medicine, since this large family of compounds was the first drug group that had a wide spectrum of activity against bacterial infections. This type of compounds has in common the sulfonamide functional group, $S(=O)_2-NH_2$, and include not only antibiotics, but also anti-diabetic agents, diuretics, or antivirals. They usually affect bacteria by inhibiting the enzyme dihydropteroate synthase (DHPS), a key step in the bacterial folate synthesis [Henry, 1943].

Although they inhibit both Gram-positive and Gram-negative bacteria, they are carefully administered due to their toxicity and side effects, which can include urinary tract disorders, porphyria, hemolytic anemia and hypersensitive reactions [Choquet-Kastylevsky et al., 2002; Slatore & Tilles, 2004]. **Figure 6** contains some representative examples of sulfonamides, including the first prodrug prontosil.

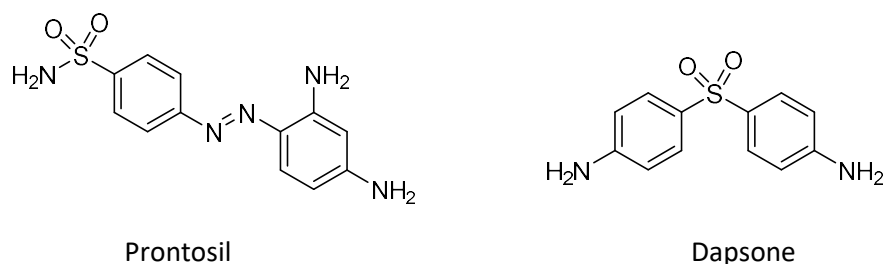


Figure 6. Chemical structure of representative examples of sulfonamides (prontosil and dapsone).

➤ Aminoglycosides

Structurally this family of antibiotics consists usually of 3-amino sugars connected by glycosidic bonds. In 1943 the first compound of this class, streptomycin (**Figure 7**), was isolated. Although streptomycin was highly used due to its broad spectrum of activity against Gram-positive and certain Gram-negative bacteria, it was found to be highly toxic. Over time, natural and semisynthetic derivatives were obtained with improved therapeutic profile, such as gentamicin, tobramycin, amikacin and neomycin [Etebu & Arikekpar, 2016].

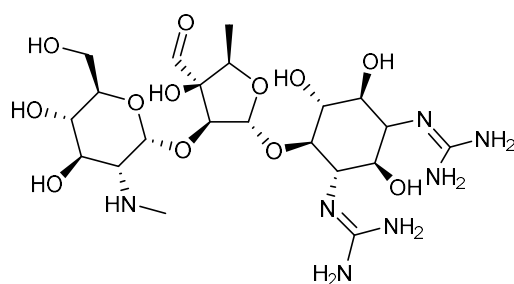


Figure 7. Chemical structure of streptomycin, the first aminoglycoside discovered.

➤ Oxazolidinones

Linezolid (**Figure 8**) was the first member of this group of synthetic antibiotics and its clinical use was approved in 2000. These compounds are characterized by containing 2-oxazolidone in their structure, essential for their antimicrobial effect,

and present a broad spectrum of activity against Gram-positive bacteria. Oxazolidinones target the ribosome region in charge of interaction with the tRNA which causes the block of the elongation of protein synthesis at an earlier step than other antibiotics [Etebu & Arikekpar, 2016].

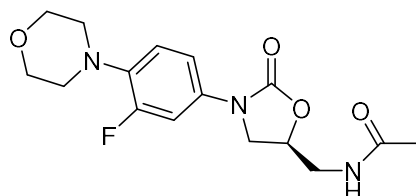


Figure 8. Chemical structure of linezolid, the first oxazolidinones obtained.

➤ Glycopeptides

Obtained originally as natural products, glycopeptides generally consist of a cyclic peptide of 7 amino acids with two sugars attached. The target of glycopeptides is binding to the pentapeptide-ending precursors present at the outer surface of the cytoplasmatic membrane, inhibiting thus the peptidoglycan synthesis of the cell wall. Their large size impedes crossing the outer membrane (OU) of Gram-negative bacteria, limiting their activity only to Gram-positive bacteria. Vancomycin, detailed in **Figure 9**, is a representative example of this family [Etebu & Arikekpar, 2016].

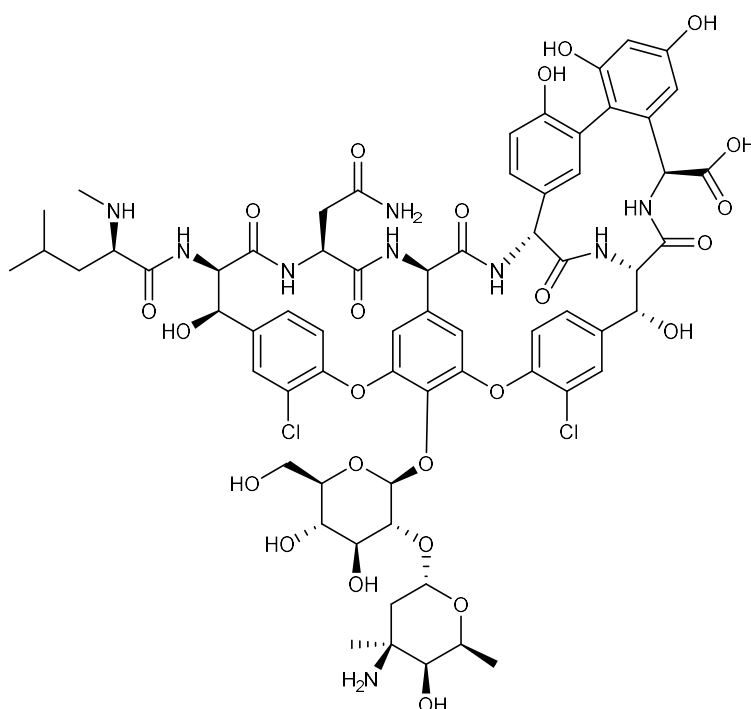


Figure 9. Chemical structure of vancomycin, a representative example of the family of glycopeptides.

1.3.2. ANTIBIOTICS CLASSIFIED BY MECHANISM OF ACTION

All the antibiotics have in common that they target different critical processes of bacterial cell life. However, they can be easily differentiated by the mechanism of action they use to interact with bacteria.

- Inhibition of cell wall synthesis

To specifically target bacteria, one of the best ways is to aim for their main difference in comparison with other cells: the cell wall. Other unicellular beings like *Protozoa* differ from bacteria because they do not possess a cell wall. On the other side, even cells with cell walls like *Archaea*, plants or fungus have a huge difference in composition: *Archaea* walls are made of pseudopeptidoglycan, plants have cellulose walls, fungus have chitin walls, while bacteria have peptidoglycan walls. Therefore, it is not a surprise that the first antibiotic discovered (penicillin) targets specifically the synthesis of the cell wall. Since then, several antibiotics have been described to focus on the cell wall, like the β -lactam family and the glycopeptides [Bush, 2012].

- Breakdown of cell membrane structure of function

While targeting the peptidoglycan cell wall is one of the most specific mechanisms to kill bacteria, this does not mean that less specific mechanisms do not work on them. Therefore, using agents which disrupt the cell membrane such as ionophores is another effective method. These types of antibiotics, such as lipopeptides, are able to form pores in the bacterial cell membrane which have ion specificity. This influx or outflux of ions alters the intracellular cationic environment, which uncouple the cell metabolism and arrests cell growth [Helsel & Franz, 2015].

- Inhibition of the structure and function of nucleic acids

While the previously mentioned antibiotics target the structural parts of the bacterial cell (wall and membranes), there are other classes which act in more subtle ways, by affecting the cell capabilities on biomolecule synthesis. Some antibiotics suppress certain critical proteins in charge of the metabolization of nucleic acids - DNA and ribonucleic acid (RNA): quinolones interfere with topoisomerase II, a key agent in the bacterial DNA replication; and rifampicin blocks

the initiation of RNA synthesis, which is one of the first steps of protein production [Ralph, 1978].

➤ Blockage of key metabolic pathways

As mentioned, the wall, the membrane and the nucleic acids are prime targets for antibiotics due to being essential components of the bacteria cell. Outside of these components, the other essential processes are those in charge of obtaining and using energy: the metabolic pathways. In this context, there are some antibiotics, such as sulfonamides, that mimic the substrate needed for the metabolism of bacteria, like tetrahydrofolate (needed for the synthesis of folic acid). This mimicry means that bacterial enzymes bind to the antibiotic instead of the natural substrate, drastically reducing their efficiency. In the example of sulfonamides, they inhibit their capabilities of synthesizing folic acid, which totally disrupts the production of nucleic acids (DNA and RNA) as well as amino acids [Talaro & Chess, 2008].

➤ Inhibition of protein synthesis

Finally, the last type of antibiotics interferes with protein biosynthesis. For the protein synthesis to happen, two ribosome subunits (30S and 50S subunits) have to be assembled and combined into the 70S ribosome complex, which is the unit in charge of synthesizing protein. The ribosome complex then “reads” the messenger ribonucleic acid (mRNA) and synthesizes a protein following the mRNA sequence. Following this principle, antibiotics which target protein synthesis can act in three different ways [Menninger, 1995]:

- 1) Blocking the formation of the 30S initiation complex between the mRNA and the 30S ribosomal subunit (e.g., tetracyclines);
- 2) Blocking the formation of the 70S ribosome by the 30S and the 50S subunits (e.g., aminoglycosides);
- 3) Impeding the elongation process of assembling amino acids into a polypeptide done by the 50S subunit of the 70S ribosome (e.g., macrolides).

1.3.3. ANTIBIOTICS CLASSIFIED BY EFFECTS ON BACTERIA

As previously mentioned, antibiotics can affect bacteria either by directly killing them (bactericidal) or by inhibiting their growth (bacteriostatic).

Bactericidal antibiotics kill bacteria. The usual mechanism of action for bactericidal antibiotics is inhibiting the cell wall synthesis or disrupting the cell membrane, and this type of antibiotics include the β -lactam family, lipopeptides and quinolones, among others.

Bacteriostatic antibiotics limit the growth of bacteria due to interference with diverse bacterial processes such as protein production, DNA replication, or another cellular metabolism. Therefore, bacteriostatic agents have to work together with the immune system to completely remove the microorganisms from the body. Most antibiotics act as bacteriostatic and notable examples are chloramphenicol or sulfonamides.

Even though this classification seems quite straight-forward, the truth is that most bacteriostatic agents can act as bactericidal at high enough concentrations. Therefore, this distinction is not as useful as it seems [Pankey & Sabath, 2004; Shetty et al., 2010].

1.3.4. CURRENT LIMITATIONS OF AVAILABLE ANTIBIOTICS

As explained, in the last century human kind has discovered and optimized a wide selection of different antibiotics which target bacteria using different mechanisms of action. At first sight, one could think that bacterial infections are a threat from the past, but this is a wrong assumption.

As natural selection guided human beings and similar animals to survive and adapt for millennia, the same happened with bacteria. Therefore, each day, millions of bacteria mutate slightly themselves and, by sheer luck, a handful of them happen to be resistant to a single antibiotic (labelled as antibiotic resistant bacteria). This ability to mutate, as well as the added capability of sharing and accepting genetic material, are the main dangers we currently face when fighting bacteria [Ventola, 2015].

1.4. BACTERIAL RESISTANCE CRISIS

Antibiotic resistance happens when bacteria acquire or develop mechanisms that protect them from the effects of antibiotics. Bacteria that are resistant to antibiotics are much harder to treat because they tolerate low or moderate doses of the antibiotic, requiring higher doses or alternative treatments to control infections. This fact results in several socioeconomic and health issues [Ventola, 2015]:

- Infections take much longer to be successfully treated, posing a more serious risk to the health of patients, and impacting the productivity of companies.
- Treatments using higher concentration of antibiotic mean more potential for adverse effects from the medication, as well as an increased economic cost.
- Bacteria with high resistance to a certain antibiotic usually results in alternative therapeutic agents to be used, which may pose a higher risk to the patient's health.
- Using a new antibiotic in a bacterial infection which is already resistant to a different one may originate a new strain with multi-drug resistance.

As we can see, antibiotics initially started as a novel and effective treatment method for infections but have resulted in an arms race against bacteria. This is apparent in the resistances being developed by bacteria, some of which are summarized in **Table 3** [Reygaert, 2018].

Table 3. Resistance mechanisms evolved by bacteria against the most common families of antibiotics. ABC: ATP Binding Casette family; MATE: Multidrug and Toxic compound Extrusion family; MFS: Major facilitator superfamily; RND: Resistance-Nodulation-cell Division family.

Antibiotic family	Resistance mechanisms
Beta-lactam	Decreased number of porins, lack of outer cell wall, alterations in Penicillin-binding protein, β -lactamases, efflux pumps (RND)
Tetracyclines	Decreased number of porins, ribosomal protection, oxidation or modification of the tetracycline drug, efflux pumps (MFS, RND)
Quinolones	DNA-related enzymes modification, alternative enzymes to the affected ones, acetylation of quinolone drug, efflux pumps (MATE, MFS, RND)
Macrolides	Mutation or methylation of ribosomes, efflux pumps (ABC, MFS, RND)
Sulfonamides	DHPS enzyme with reduced binding, overproduction of resistant DHPS enzyme, efflux pumps (RND)

It is common that not long after the introduction of a new antibiotic in clinical use, resistant bacteria are detected. This fact can be observed in **Table 4**, which details the year of the introduction of a certain antibiotic, and when its resistance was identified.

Table 4. Antibiotics approved or released and the resistant germs identified. Source modified from CDC 2013.

Antibiotic released	Year released	Resistant germ identified	Year identified
Penicillin	1941	Penicillin-resistant <i>Staphylococcus aureus</i>	1942
		Penicillin-resistant <i>Streptococcus pneumoniae</i>	1967
		Penicillinase-producing <i>Neisseria gonorrhoeae</i>	1976
Polymyxins	1947	Polymyxin-resistant <i>Klebsiella pneumoniae</i>	2015
		Polymyxin-resistant <i>Pseudomonas aeruginosa</i>	
		Polymyxin-resistant <i>Acinetobacter baumannii</i>	
Vancomycin	1958	Plasmid-mediated vancomycin-resistant <i>Enterococcus faecium</i>	1988
		Vancomycin-resistant <i>Staphylococcus aureus</i>	2002
Amphotericin B	1959	Amphotericin B-resistant <i>Candida auris</i>	2016
Methicillin	1960	Methicillin-resistant <i>Staphylococcus aureus</i>	1960
Extended-spectrum cephalosporins	1980	Extended-spectrum β -lactamase-producing <i>Escherichia coli</i>	1983
Azithromycin	1980	Azithromycin-resistant <i>Neisseria gonorrhoeae</i>	2011
Imipenem	1985	<i>Klebsiella pneumoniae</i> carbapenemase (KPC)-producing <i>Klebsiella pneumoniae</i>	1996
Ciprofloxacin	1987	Ciprofloxacin-resistant <i>Neisseria gonorrhoeae</i>	2007
Fluconazole	1990	Fluconazole-resistant <i>Candida</i>	1988
Caspofungin	2001	Caspofungin-resistant <i>Candida</i>	2004
Daptomycin	2003	Daptomycin-resistant methicillin-resistant <i>Staphylococcus aureus</i>	2004
Ceftazidime-acibactam	2015	Ceftazidime-avibactam-resistant KPC-producing <i>Klebsiella pneumoniae</i>	2015

This situation turns out to be critical, if we examine the number of new antibiotics developed during the last decades: as shown in **Figure 10**, it has been decreasing considerably over time. For Gram-negative bacteria this situation is even worse, considering that the last newly introduced antibiotic family for clinical use was nearly in 1970.

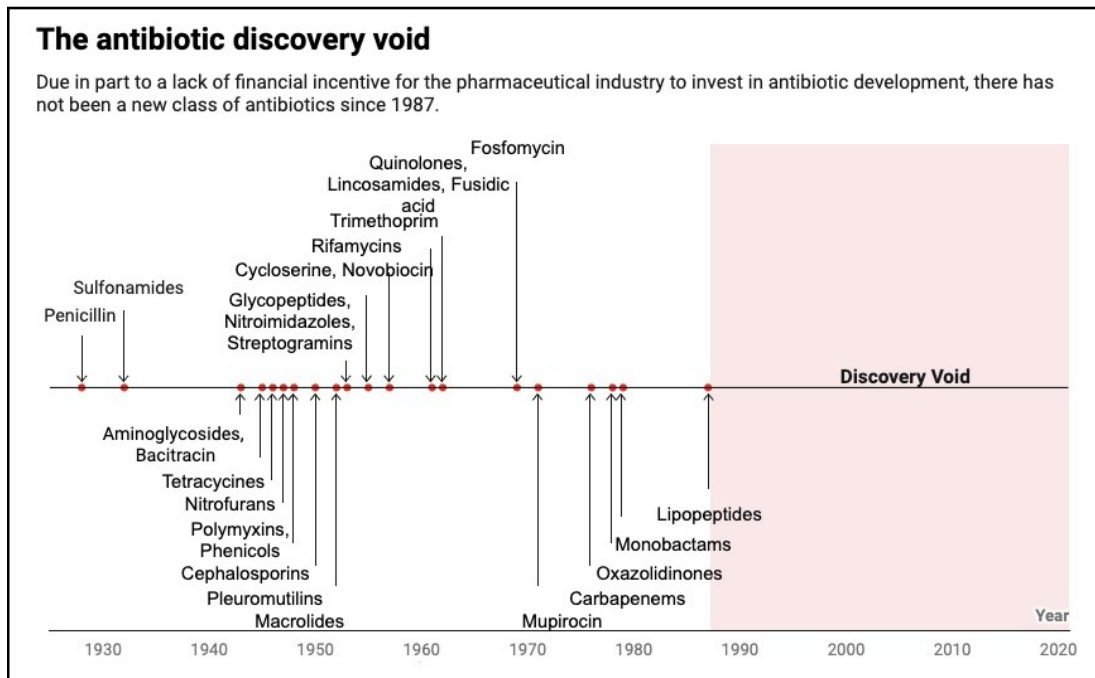


Figure 10. Timeline of antibiotic discovery during the last century, including the discovery void since late 80s. Figure taken from ReAct Group website.

Since the 1980s no new classes of antibiotics have been discovered, and the last approved antibiotics that reached the market were variations of drugs already existing. One of the reasons of this situation is that typically discovery and development of an effective new antibiotic can take between 10-15 years and around 1.5 billion of dollars, whereas the estimated profit is roughly 46 million of dollars per year. This economic gap, combined with the lack of incentives to develop new antibiotics and the regulatory obstacles before a new drug is approved, has forced many pharmaceutical companies to leave the antibiotic field since it is considered non-profitable. Furthermore, if the economic burden was not enough, no one can guarantee that bacteria would not develop resistance to it.

In order to fight this antimicrobial crisis, some first steps were taken such as preventing infections in the first place, improving antibiotic use to slow the development of resistance and stopping the spread of resistance when it does

develop. This antimicrobial resistance crisis was a global priority until Covid-19 pandemic appeared [CDC website]. However, since then, not only were efforts focused on combating Covid-19, but also the direct effects of the viral pandemic had a negative impact on all the progress that had been made in the bacterial resistance crisis since patients were treated with antibiotics despite not needing them, and hospitals experienced staffing shortages that hindered the implementation of infection control practices and monitoring antibiotic-resistant germs.

In this context of antibiotic resistance crisis, together with the difficulties implied in developing novel synthetic antibiotics, many research groups suggest taking a step back towards compounds naturally produced by other organisms and think on potential ways to improve them by reducing their toxicity towards human beings but conserving their antibiotic properties. Examples of these antibiotics are the antimicrobial peptides (AMPs), such as polymixin B and colistin. Albeit showing great efficacy against bacteria, their toxicity limits their use in humans. However, due to their peptide nature, they can be modified in several ways to potentially improve their antimicrobial profile [Cassir et al., 2014].

1.5. ANTIMICROBIAL PEPTIDES

Antimicrobial peptides, also known as host defense peptides, are some of the most ancient examples of innate immune response in life. They are produced both by unicellular organisms, which use them to compete for nutrients against other organisms, while also being part of the immune system of multicellular creatures. Therefore, they were the first weapons in the biological arms race which have been evolving for millions of years [Ageitos et al., 2017].

The first AMPs discovered followed closely the discovery of penicillin, as in the 1930s a research group extracted an antimicrobial compound from a strain of *Bacillus* which could protect mice from pneumococci infection and was named gramicidin [Dubos, 1939]. This was followed by the discoveries of tyrocidine, purothionin and polymyxins during the 1940s, from other *Bacillus*, plant *Triticumaestivum* and *Paenibacillus polymyxa*, respectively [Dubos & Hotchkiss, 1941; Balls et al., 1942; Benedict & Langlykke, 1947]. The main disadvantage of these antimicrobial compounds was that they exhibited some toxicity in humans, although they could be avoided if they were administered topically, like gramicidin.

These first discoveries had in common that they were identified in organisms totally different from animals: bacteria, plants, and fungus, which led the researchers to think that the AMPs were not present in animals. However, this changed when in 1956 a group reported the discovery of phagocytin, the first animal-originated AMP, or how it is known nowadays: defensin [Hirsch, 1956]. This discovery was the trigger for several research lines for the discovery of new animal AMPs which lacked the characteristic toxicity to humans of bacterial, plant or fungus AMPs. Therefore, in a short span of time, bombinin was purified from epithelia, and lactoferrin from cow milk. Finally, AMPs were also identified in human leukocytes [Groves et al., 1965; Zeya & Spitznagel, 1963].

Several important works followed, including not only vertebrates. For example, in the 1980s two different laboratories were researching the immune system of insects: due to their characteristic lack of lymphocytes, researchers postulated that insects possessed a different immune system to those of vertebrates. By different approaches, the research groups purified peptides from the hemolymph of

Hyalophora cecropia and *Sarcophaga peregrina*, respectively, and described their bactericidal activity [Steiner et al., 1981; Okada & Natori, 1983].

Most AMPs share some features: they have small size and present cationic and hydrophobic sequences. However, what makes them that interesting as potential treatment against bacteria is that they often affect bacteria by non-specific mechanisms, which enables them to circumvent most of the existing antibiotic resistances.

1.5.1. CLASSIFICATION OF AMPS

AMPs have such a great diversity, that it is difficult to classify them. There are several different approaches to do it, one of them is according to their mechanism of action [Huan et al., 2020]:

- Membrane targeting mechanisms
 - Toroidal pore model

AMPs embedded perpendicularly into the cell membrane accumulate and then bend to form a ring hole with a diameter of 1-2 nm, compromising the membrane barrier. Examples of this model include magainin 2 or lacticin Q [Omardien et al., 2018].

- Barrel-stave model

AMPs aggregate, penetrating the cell membrane in the form of multimers, and form channels that result in cytoplasmic outflow. This cytoplasmic outflow can result in cell membrane collapse and cell death. Examples of this model include alamethicin and protegrin-1 [Lipkin & Lazaridis, 2015].

- Carpet-like model

AMPs following this approach are arranged parallel to the cell membrane, and when a certain concentration is reached, they disrupt the bilayer lipid membrane, generally forming micelles. Therefore, these AMPs perform a detergent-like effect that destroys the membrane. AMPs with this approach include cathelicidin LL-37, and most AMPs with β -sheet structure [Shenkarev et al., 2011; Corrêa et al., 2019].

➤ Non-membrane targeting mechanisms

▪ Inhibition of protein biosynthesis

These AMPs affect transcription (RNA synthesis from DNA), translation (protein synthesis from RNA), and assembly into functional peptides (protein folding) by interfering with enzymes and effector molecules involved. Examples of such are the Tur1A, which inhibits transition to extension phase of protein synthesis in *Escherichia coli*; and Bac7, which targets ribosomes to inhibit protein translation [Mardirossian et al., 2014; 2018].

▪ Inhibition of nucleic acid biosynthesis

AMPs using this mechanism of action affect key enzymes of the nucleic acid biosynthesis pathways, or degrade nucleic acid molecules. As an example, indolicidin inhibits the DNA topoisomerase I enzyme [Subbalakshmi & Sitaram, 1998].

▪ Inhibition of protease activity

Protease activity is involved in several metabolic and infection activities. Therefore, AMPs which follow this approach, such as histatin 5 or indolicidin, are capable of halting the metabolism and viability of bacteria [Le et al., 2017].

▪ Inhibition of cell division

These AMPs inhibit cell division by either inhibiting DNA replication, DNA damage response, arresting the cell cycle, or causing the failure of chromosome separation. MciZ is an example of this approach, as it is an AMP which inhibits bacterial cell division and Z-ring formation [Yadavalli et al., 2016; Cruz et al., 2020].

As shown in **Table 5**, there is a wide array of alternative AMPs with proven efficacy against bacterial diseases. Amongst them, we can highlight the polymyxins, a family of AMPs which initially was believed to follow the carpet-like model and that had notable relevance between 1947 and 70s before safer antibiotics had been identified. Due to the current issues with antibiotic resistance in bacteria, there is a renewed interest in polymyxin research [Landman et al., 2008].

Table 5. Main targets and mechanisms of action for AMPs, along with an example for each and the affected bacteria by the example [Gottschalk et al., 2013; Huan et al., 2020; Ouardien et al., 2018; Lipkin & Lazardis, 2015; Corrêa et al., 2019; Mardirossian et al., 2018; Kragol et al., 2001; Subbalakshmi & Sitaram, 1998; He et al., 2017; Li L. et al., 2016; Imura et al., 2008; Mukhopadhyay et al., 2004; Turaman, 2021; Selsted et al., 1991; Su et al., 2009; Yadavalli et al., 2016].

Target	Mecanism of action	Example	Main susceptible bacteria
Membrane	Toroidal pore model	Magainin-2	<i>Bacillus megaterium</i>
Membrane	Barrel-Stave model	Protegrin-1	<i>Pseudomonas</i> species
Membrane	Carpet-like model	Cathelicidin LL-37	Wide spectrum
Protein Biosynthesis	Transcription inhibition	Microcin J25	Gram-negative
Protein Biosynthesis	Translation inhibition	Tur1A	<i>Escherichia coli</i>
Protein Biosynthesis	Protein folding inhibition	Pyrrhocoricin	<i>Escherichia coli</i>
Nucleic Acid Biosynthesis	Enzyme inhibition	Indolicidin	Gram-negative
Nucleic Acid Biosynthesis	Nucleic acid degradation	TFP 1-1TC24	<i>Staphylococcus aureus</i>
Protease Activity	Protease inhibition	Indolicidin	Gram-negative
Cell Division	DNA replication inhibition	LP5	<i>Staphylococcus aureus</i>
Cell Division	DNA damage response inhibition	WRWYCR peptide	<i>Salmonella</i> species
Cell Division	Cell cycle arrest	APP	<i>Candida albicans</i>
Cell Division	Chromosome separation disruption	C18G	<i>Escherichia coli</i>

1.6. POLYMYXINS

The discovery of penicillin and later implementation of the process to mass produce it generated a wide interest in the search of more antibiotics from natural sources during the first half of the 20th century. In this context, two independent groups recognized the antibiotic properties of compounds produced by *Bacillus aerosporus* Greer and *Bacillus polymyxa* in 1947. Unbeknownst to them, they had both discovered the first members of the polymyxin family [Ainsworth et al., 1947].

Polymyxins were widely used for the treatment of a wide variety of Gram-negative bacteria during most of the mid-20th century, even though they exhibited some neuro- and nephrotoxic behavior. Polymyxins were used for the treatment of relevant bacteria such as *Escherichia coli*, *Klebsiella species*, *Enterobacter species*, or *Pseudomonas aeruginosa*. However, they ran out of favor around the 70s, as researchers found alternative antibiotic compounds with less side effects and better pharmacologic profiles [Landman et al., 2008].

Several years after that change of paradigm, we find ourselves in a much different situation. Following the wide, and sometimes not fully justified, use of antibiotics for the treatment of doubtful infections, including not only human but veterinary and agricultural use, some bacteria have developed resistance to the most widespread antibiotics. This means that specific strains from common bacteria such as *Escherichia coli* or *Staphylococcus aureus* are resistant to numerous antibiotics. This fact makes such strains lethal to immunocompromised or sensitive population.

For this reason, for the last years there has been renewed interest in polymyxins. As more and more antibiotics are unsuccessful against multi-drug resistant bacteria (also nicknamed as “superbugs”), physicians start using polymyxins as last-line therapeutic agent for patients in critical status, despite their potential toxicity [Velkov et al., 2013].

1.6.1. STRUCTURE OF POLYMYXINS

Polymyxins are compounds produced naturally by *Paenibacillus polymyxa* discovered originally in 1947. Polymyxins are lipodecapeptides - which means that they are a peptide formed by ten amino acids, with a fatty acyl chain. These peptides are structurally interesting because they are cyclic, and they contain five residues of a positively charged amino acid: L-2,4-diaminobutyric acid (Dab). The fatty acyl chain can be of different lengths [Rabanal & Cajal, 2017]. Within the heterogeneous mixture that conforms the polymyxins family, up to 30 slightly different structures, detailed in **Table 6**, can be found.

Table 6. Structure of naturally occurring polymyxins. AA: amino acid.

Polymyxin	Fatty acyl tail	AA ³	AA ⁶	AA ⁷	AA ¹⁰
B1	(S)-6-Methyloctanoyl		D-Phe	Leu	
B1-Ile	(S)-6-Methyloctanoyl		D-Phe	Ile	
B2	6-Methyheptanoyl		D-Phe	Leu	
B3	Octanoyl		D-Phe	Leu	
B4	Heptanoyl		D-Phe	Leu	
B5	Nonanoyl		D-Phe	Leu	
B6	3-Hydroxy-6-methyloctanoyl		D-Phe	Leu	
E1	(S)-6-Methyloctanoyl		D-Leu	Leu	
E2	6-Methyheptanoyl		D-Leu	Leu	
E3	Octanoyl		D-Leu	Leu	
E4	Heptanoyl		D-Leu	Leu	
E7	7-Methyloctanoyl		D-Leu	Leu	
E1-Ile (circulin A)	D-Leu Ile		D-Leu	Ile	
E1-Val	(S)-6-Methyloctanoyl		D-Leu	Val	
E1-Nva	(S)-6-Methyloctanoyl		D-Leu	Nva	
E2-Val	6-Methyheptanoyl		D-Leu	Val	
E2-Ile	6-Methyheptanoyl		D-Leu	Ile	
E8-Ile	7-Methylnonanoyl		D-Leu	Ile	
A1	6-Methyloctanoyl	D-Dab	D-Leu	Thr	Thr
A2	6-Methylheptanoyl	D-Dab	D-Leu	Thr	Thr
C1	6-Methyloctanoyl	Dab	Phe	Thr	Thr
C2	6-Methylheptanoyl	Dab	Phe	Thr	Thr
D1	6-Methyloctanoyl	D-Ser	D-Leu	Thr	Thr

D2	6-Methylheptanoyl	D-Ser	D-Leu	Thr	Thr
F1	6-Methyloctanoyl	(Dab 5, Thr, Leu 2, Ser, Ile)			
F2	6-Methylheptanoyl	(Dab 5, Thr, Leu 2, Ser, Ile)			
M1	6-Methyloctanoyl	Dab	D-Leu	Thr	Thr
M2	6-Methylheptanoyl	Dab	D-Leu	Thr	Thr
S1	6-Methyloctanoyl	D-Ser	D-Phe	Thr	Thr
T1	6-Methyloctanoyl	Dab	D-Phe	Leu	Leu
T2	6-Methylheptanoyl	Dab	D-Phe	Leu	Leu
PMB1	6-Methyloctanoyl	D-Dab	D-Phe	Thr	Thr
PMB2	6-Methylheptanoyl	D-Dab	D-Phe	Thr	Thr
P1	6-Methyloctanoyl	D-Dab	D-Phe	Thr	Thr
P2	6-Methylheptanoyl	D-Dab	D-Phe	Thr	Thr

Perhaps among all the polymyxin compounds, the most common ones are Polymyxin B and Polymyxin E (also known as Colistin). **Figure 11** describes structurally an example of each of these polymyxins: polymyxin B1 and E1.

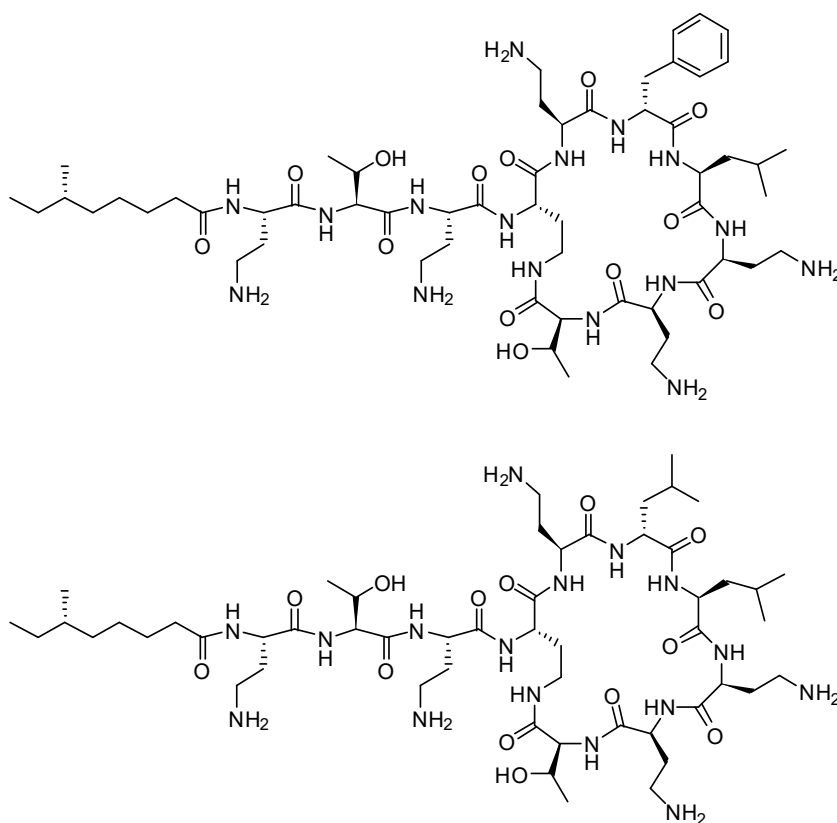


Figure 11. Structure of representative polymyxins: polymyxin B1 (top) and polymyxin E1 (bottom).

1.6.2. MECHANISM OF ACTION OF POLYMYXINS

As already highlighted, polymyxins are selective against Gram-negative bacteria. This selectivity is due to the fact that their first molecular target is LPS, which is the main component of the outer membrane of Gram-negative bacteria. Gram-negative bacteria are typically resistant to several of the new molecules being tested as antibiotic, as their envelope, consisting of two separate membranes, exhibits very low permeability. However, the presence of LPS in that outer membrane, which is the responsible for its tight packing, rigidity, and low permeability, also allows for the polymyxins to interact [Zgurskaya et al., 2015].

LPS is composed of three domains: lipid A, a central core oligosaccharide, and an O-antigen chain, as detailed in **Figure 3**. Polymyxins mainly target the lipid A, which is also responsible for the outer membrane tight packing. Furthermore, bacteria which are sensitive to polymyxin also exhibit several anionic charges in their LPS, which trigger strong electrostatic interactions with the polycationic polymyxins [Nikaido, 2003; Raetz & Whitfield, 2002].

The activity of polymyxins starts when the divalent cations Ca^{2+} and Mg^{2+} , which are in charge of membrane stabilization, are competitively displaced from the LPS layer by the cationic residues of polymyxin. The lack of the divalent cations causes destabilization of the LPS layer, which allows the insertion of the hydrophobic acyl chain of the antibiotic into the membrane, parallel to the hydrophobic domain of lipid A (**Figure 12**). The insertion of polymyxins causes an expansion of the LPS monolayer that results in disruption of the outer membrane permeability barrier, which facilitates the entrance of polymyxin into the periplasmic space via self-promoted uptake [Hancock, 1997; 1998]. It has been demonstrated that the N-terminal fatty acyl chain is needed for this step [Vaara & Vaara, 1983].

Once the polymyxin molecules have crossed the outer membrane, they have to interact with the inner membrane (IM) to kill the bacteria. Several research lines have focused on the effect of polymyxins on inner membranes. On one side, a high enough concentration of the peptide can affect the permeation of the inner membrane. However, on the other side, the minimal inhibitory concentration of

polymyxins is much lower than the required to affect the permeation of the inner membrane. Therefore, the bactericidal effect cannot be explained by an unspecific lytic or detergent effect [Hancock & Chapple, 1999; Zhang et al., 2000; Mortensen et al. 2009].

It has been described a more likely mechanism of action which involves the formation of contacts between the outer and inner membranes of Gram-negative bacteria, which has also been observed in other antimicrobial peptides such as cecropins [Oh et al., 1998; Yu et al., 2015; Oh et al., 1998]. According to this model, once in the periplasmic space, stoichiometric amounts of polymyxin form contacts between the two enclosed phospholipid interfaces (outer membrane and inner membrane), promoting a fast and selective exchange of anionic phospholipids (**Figure 12**). These changes in membrane composition trigger an osmotic imbalance that leads to bacterial stasis and cell death. Biophysical studies using model membranes have proven that polymyxin and colistin induce the apposition of anionic vesicles and the formation of vesicle-vesicle contacts at concentrations around the minimum inhibitory concentration (MIC) [Oh et al., 2000; Cajal et al. 1996]. This model is also supported by studies using sublethal concentrations of polymyxin B in growing *Escherichia coli*. This concentration of polymyxin causes the bacteria to transcribe the *osmY* gene without leakage of solutes and protons [Oh et al. 1998; 2000]. As the *osmY* expression is also induced by hyperosmotic stress, the interpretation is that polymyxin forms functional contacts in the periplasmic space between the inner layer of the outer membrane and the outer layer of the inner membrane and promotes the exchange of phospholipids, altering thus their composition and causing an osmotic imbalance [Gonzalez-Perez et al., 2021]. Similar findings supporting this model have been done in *Acinetobacter Baumannii* [Henry et al., 2015].

Finally, other mechanisms of antimicrobial activity for polymyxins involving intracellular targets are still studied [Velkov et al., 2013; Rhouma et al., 2016]. As an example, the entry of polymyxin into the cytoplasm of Gram-negative bacteria has been demonstrated by scanning confocal microscopy. In those experiments, the polymyxins initially accumulate in the outer membrane of

Klebsiella pneumoniae, gradually penetrating the outer membrane and finally accessing the inner membrane at concentrations close to five times the MIC. While polymyxins may have a role when inside the bacterial cell as shown in the experiments, it is still not clear whether these are just complimentary to the previously described osmotic stress. Therefore, further research is needed in order to fully understand the mechanism of action of polymyxin peptides [Yu et al., 2015].

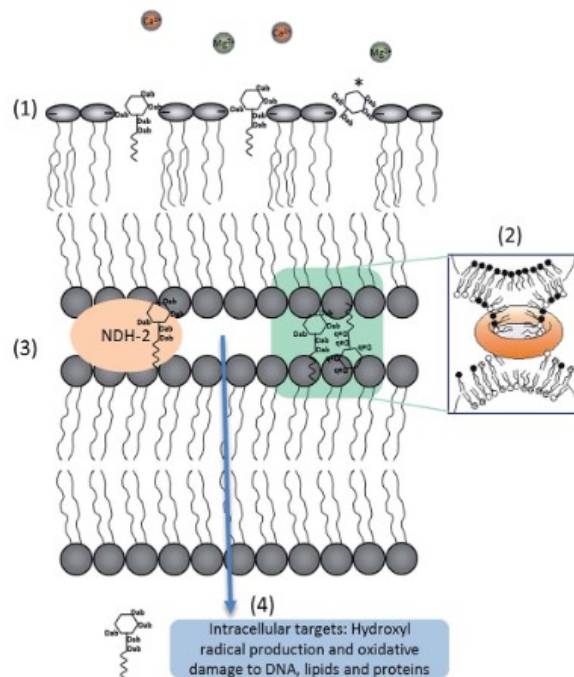


Figure 12. Representation of the putative mechanism of action of polymyxin on Gram-negative bacteria. (1) Displacement of Ca²⁺ and Mg²⁺ and binding to lipid A; (2) self-promoted uptake to the periplasmic space and formation of OM-IM contacts and lipid exchange; (3) inhibition of respiratory enzyme type II reduced nicotinamide adenine dinucleotide (NADH)-quinone oxidoreductase; (4) entry into the cytoplasm and access to intracellular targets. *Polymyxin B nonapeptide activity is limited to step (1). Figure taken from Rabanal & Cajal, 2017.

1.6.3. SPECTRUM OF ACTIVITY

Due to the mechanism of action exhibited by polymyxins, their spectrum of activity is mainly on Gram-negative bacteria. As previously mentioned, Gram-positive bacteria exhibit a thick cell wall, and they lack both LPS and external or outer membrane. As the main targets for insertion of polymyxins into the membrane are not present, this explains the lack of activity.

The efficiency of the interaction between polymyxins and LPS has been noticed several times; for this reason, nonapeptide polymyxin analogues have been

administered as a synergistic compound combined with other drugs to ease their entry into Gram-negative bacteria. An example of this kind of compounds is SPR741, detailed in **Figure 13** [Corbett et al., 2017].

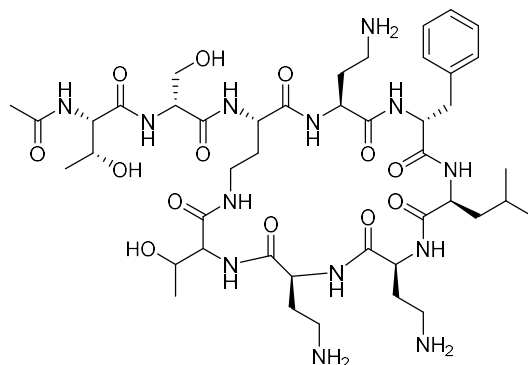


Figure 13. Structure of SPR741, a nonapeptide polymyxin analogue used in combination with other antibiotics to improve their antimicrobial activity against Gram-negative bacteria. Figure taken from Corbett, 2017.

1.6.4. TOXICITY

As previously mentioned, polymyxins were extensively used during the mid-20th century, as they were active towards very prevalent bacteria and the means for their mass-production were rapidly optimized. However, during the 70s different toxic effects were attributed to polymyxin treatment.

Polymyxins mainly target the cytoplasmatic membrane of Gram-negative bacteria. However, the fact that they exhibit positive charges and a fatty acyl chain means that they have some minor affinity towards eukaryotic membranes. This is especially apparent when high doses of polymyxin are used in a critical situation. In this context, polymyxins trigger side-effects in systems where membranes and ion permeability are the most important: the excretory and the nervous systems.

Toxicity in the excretory system is mainly focused on the kidneys and the renal function (nephrotoxicity). On the other side, neurotoxicity typically includes paraesthesia (abnormal sensation of the skin), respiratory apnoea (interruption in normal breathing), and neuromuscular blockade. For this reason, polymyxins have an important role in non-systemic administration (topical and inhalation) that evade the effects over those systems.

The toxicity of the members of the polymyxin family has resulted in the use of only two members nowadays: polymyxin B (referred as polymyxin) and polymyxin E (or colistin). Finally, while recent research has pointed that these side effects of polymyxins are less prevalent than initially considered, modern standards on drug safety force the development of polymyxins with better pharmacologic profile, if they are to be used widely [Falagas & Kasiakou, 2006].

1.6.5. MECHANISMS OF RESISTANCE TO POLYMYXINS

As previously discussed, the use of polymyxins has increased for the last 15 years due to the emergence of multi-drug resistant bacteria. Like any arms race, though, bacteria have already been evolving to overcome polymyxins antibiotic activity.

Resistance to polymyxins typically arises from chromosomal mutations. These mutations modify the composition of LPS and Lipid A in the bacterial outer membrane under certain conditions. As an example, one of these mutations result in a decline of anionic charges of LPS when Fe^{3+} concentration is high, which lowers the affinity of polymyxins, and therefore their antibiotic effect. Other mutations modify the LPS composition in a similar way, but changing the stimulus needed (e.g., chlorhexidine exposure, also polycationic).

A different mechanism of resistance is shown in some strains of *Acinetobacter baumannii* which makes them lose their LPS. Lack of LPS in those strains cause resistance to polymyxins instead of bacterial death, because the bacterial cell is not affected due to expression of transporters that act as rescue mechanisms.

As a summary, the progressive evolution of bacteria to present resistance to polymyxins forces the research of new polymyxin analogues to avoid the new resistances [Li et al., 2019].

2. OBJECTIVES

Resistance to most or all commonly used antibiotics by some bacteria is an increasingly important public health concern. Given that there is a percentage of the population that would be helpless against these strains (sensitive and immunocompromised persons), there is a huge need to identify new antibiotics that circumvent the resistances attained by these bacteria strains.

Therefore, the main objectives of this work were the following:

- Design, synthesis, purification and characterization of polymyxin E (colistin) analogues to increase its activity and/or lower its toxicity to obtain a better pharmacological profile, while simplifying the synthesis steps of these analogues for upscaling purposes.
- Study of the biophysical activity of the synthesized analogues using different membrane models to correlate their antimicrobial activity and their biophysical behavior.
- *In vitro* study of the biologic activity of the synthesized analogues by measuring the antimicrobial activity and their cytotoxicity.
- Evaluation of the most promising analogues in animal models to assess their nephrotoxicity, pharmacokinetics, and efficacy.

3. COLISTIN ANALOGUES

3.1. ANALOGUES DESIGN AND SYNTHESIS

3.1.1. OVERVIEW OF POLYMYXIN ANALOGUES

As previously discussed, polymyxins are natural compounds that exhibit a great antimicrobial activity. While some bacteria strains resistant to polymyxins have already been identified, such resistance is not yet as common as for other antibiotic families, which makes them drugs of last resort [Ledger et al., 2022]. Multi-drug resistant bacteria are even more fearsome due to the fact that no new antibiotic families to treat them have been developed in the last decades. As a result to the emergence of these drug-resistant bacteria, several countries have approved the use of polymyxins as a last resort treatment, such as the commercially available colistin methanesulfonate (CMS). However, during the current crisis situation, healthcare professionals demand for new, more effective, antibiotics [Wertheim et al., 2013; Rabanal & Cajal, 2017; Zhang et al., 2020].

Due to the critical situation, many research groups are studying different modifications of the polymyxin peptide. While polymyxins are naturally produced by Gram-positive bacteria such as *Paenibacillus polymyxa*, they can also be synthesized chemically. Therefore, when synthesizing the different modified analogues, two different methods are typically available: using the polymyxin gathered from natural sources and modifying it directly; or a total chemical synthesis, which is usually performed via solid phase. While the first one is much cheaper, starting from the complete molecule limits the possibilities of modifications that can be done to the peptide. On the other side, complete synthesis allows a much wider array of modifications [Rabanal & Cajal, 2017].

Since 1970, and in the last couple of decades, polymyxin and colistin analogues have been developed with improved microbiological, pharmacological, and toxicological profiles [Velkov et al., 2010].

Within the next pages, an overview of the main modifications is shown, classified in changes on the N-terminal of the molecule (both fatty acyl chain and the linear tripeptide), changes to the cycle, and general changes. For better comprehension, **Figure 14** details the most relevant regions and residues of polymyxin structure.

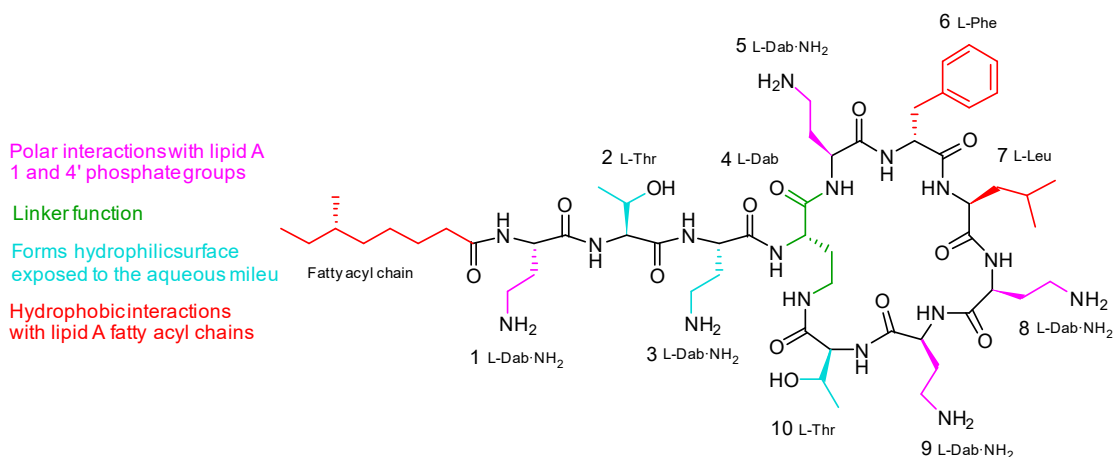


Figure 14. Color coded schematic diagram summarizing the key contacts involved in complex formation between Polymyxin B and the lipid A component of LPS. FA = N-terminal fatty acyl chain.

A) Modifications on the N-terminus

On the N-terminus, polymyxin and colistin have the fatty acyl chain, which is the region responsible of the insertion into the LPS bacterial membrane, whose model was characterized several years ago [Pristovsek & Kidric, 1999; 2004; Cajal et al., 1996]. Furthermore, we can also notice that the three amino acids closest to the acyl chain of the lipopeptide are not part of the cycle (Dab¹-Thr²-Dab³) and are involved in the hydrogen bonds necessary for the correct folding of the components binding to LPS. Given the importance of this N-terminal region in the insertion of the polymyxin molecule, several research groups have studied it and published their work on different modification strategies.

For the acyl chain, long before the interaction model with LPS had been described, early works had already identified that it was a necessary region for the antimicrobial activity of polymyxins. By generating analogues lacking the acyl chain, it was demonstrated that the resulting molecules were still able to bind to LPS, but missed any antimicrobial activity [Vaara & Vaara, 1983]. However, other studies of conjugated administration of acyl-less polymyxin analogues with other hydrophobic antibiotics showed that the peptides retain a certain disruptive effect on the membrane, as they allowed the antibiotics to penetrate the bacteria, thus avoiding the resistances from Gram-negative bacteria [Vaara, 1992; Tsubery et al., 2005].

Examples of modifications to the fatty acid region include its substitution by other chemical groups (aromatic urea, pyrene, piperazine or piperidine rings) with

promising results both at the *in vitro* and *in vivo* levels [Quale et al., 2012; Brown et al., 2014; 2015; 2015; Wiederhold et al., 2015; Boakes et al., 2015]. Furthermore, there are also research lines focusing on the optimal length of the acyl chain, which points towards 7-9 carbon acyl chains being the best candidates [Okimura, et al., 2007; O'Dowd et al., 2007].

On the other side, the effects of deletions or substitutions in the linear tripeptide have also been studied and it has been demonstrated that the deletion of more than one or their substitution by alanine severely hinders the antimicrobial activity of the peptide, if not inactivating it completely [Sakura et al., 2004; Vaara et al., 2008]. Between the three amino acids, it was found that the Thr² was the most important one, as its substitution affected the antimicrobial activity the most [Kanazawa et al., 2009]. Finally, the substitution of one or several of the amino acids of the tripeptide by neutral or hydrophobic amino acids caused a decrease in activity while the inclusion of a negatively charged residue, such as Glu, generated an inactive compound. This would be consistent with the electrostatic repulsion with the negatively charged phosphate groups of lipid A in the interaction model [Vaara et al., 2008; Katsuma et al., 2009].

Examples of modification to the linear tripeptide include the Pfizer 5x analogue, which has a substitution of residue 3 by a 2,3-diaminopropionic acid (Dap), resulting in promising *in vitro* results. Unfortunately, the toxicological profile *in vivo* allowed no therapeutic window, so it had to be discontinued [Magee et al., 2013]. Other teams decided to carry more profound modifications, such as substituting the whole N-terminus (fatty-acyl and tripeptide) by a lipopeptide, such as the octanoyl-Thr-DSer segment in NAB739 by the Northern antibiotics group, with mostly positive results in comparison with polymyxin [Vaara et al., 2010].

Finally, a notable mention is needed for the MicuRx group, as they were able to replicate the activity of polymyxin with analogues that had an ester in the acyl chain. While functionally the analogues worked similar to the polymyxin, the ester bond was rapidly hydrolyzed once filtered by the tubular cells in the kidney due to the reducing environment [Brown et al., 2015; Hobbs, 1996]. As the main cause of

nephrotoxicity by polymyxins is their accumulation at the kidneys, the ester group could be a nice addition to reduce it in other peptides.

B) Modifications of the cyclic peptide ring

The characteristic peptide ring of polymyxins is formed by 7 amino acids with two highly hydrophobic residues in positions 6 and 7 whose function is to insert themselves into the bacterial outer membrane, via hydrophobic interactions with the fatty acyl chains of lipid A. Moreover, the main difference between polymyxin and colistin is located here, as D-Phe⁶ for polymyxin is instead a D-Leu⁶ in colistin.

There has been attempts to modify the hydrophobic segment, either the residue 6 for Trp, Ala, or Phe; or the residue 7 for Trp. While these analogues largely maintained their functionality, the simultaneous change of both residues 6 and 7 resulted in inactive peptides. Therefore, while the hydrophobic segment can be altered, it has to retain the hydrophobicity at least partially [Kanazawa et al., 2009].

An example of analogues synthesized following this strategy includes the Monash University FADDI analogues, which had residues 6 and 7 changed by new hydrophobic residues such as octylglycine or biphenylalanine. Some of such analogues showed a significant improvement of *in vitro* efficacy against polymyxin resistant strains, as the new residues were able to avoid bacteria resistances. In contrast, the efficacy against polymyxin sensitive bacteria was lower. However, efficacy tests with *in vivo* models showed optimistic results [Velkov et al., 2014]. Similar attempts had previously been made with other mimics of the residues 6 and 7, such as δ -aminovaleric acid or 4-phenyl-4-carboxymethylpiperidine, but those had resulted in inactive compounds [De Visser et al., 2003].

The interaction model of the polymyxin-LPS complex also shows that the size of the ring is a must for the electrostatic and hydrophobic contact points with LPS. This explains why most of the analogues synthesized with alterations in the ring size resulted in minimal to no activity. As an example, the addition of a Dab residue, which enlarges the ring, resulted in peptides with very minor activity. In the same manner, analogues with smaller rings also see their permeabilizing activity greatly reduced [Vogler & Studer 1966; Vogler et al., 1961; Tsubery 2000; 2000; 2000].

C) General modifications

While the N-terminus and the cycle are the main regions of the polymyxin lipopeptide, there are some modifications that transcend such differentiation. Great examples are the charged residues. There are 5 positive lateral chains in the polymyxin molecule in the form of 5 Dab (L-2,4-diaminobutyric acid) residues in positions 1, 3, 4, 8, and 9. As previously mentioned, these positive charges interact with the negative residues in LPS and blocking all of them results in a compound with no activity [Barnett et al., 1964]. Other teams tried to substitute the Dab residues with basic amino acids, such as Arg or His, which did not affect the binding with LPS [Porro et al., 1993; 1993; 1995; 1996]. However, analogues that had the Dab side chains substituted for less cationic alternatives, showed an increased activity against Gram-positive bacteria [Weinstein et al., 1998; Witzke & Heding, 1976]. Finally, additional experiments also demonstrated that the Dab residues inside the cycle (residues 5, 8, and 9) were more relevant for the antimicrobial activity than the N-terminal residues, as their substitution for Ala or 2-aminobutyric acid reduced the activity of the molecule [Kanazawa et al., 2009; Vaara et al., 2008].

Furthermore, there are plenty of polymyxin B analogues through the literature. Linear polymyxins have been synthesized with the aim of decreasing the toxicity of the molecule but resulted in mostly inactive compounds [Rustici et al., 1993; Vaara, 1991]. Other groups tried to covalently conjugate polymyxin B (PxB) molecules to neutralize the septic effect of LPS, which once again proved fruitless [Griffin & Judice, 2002].

Finally, several research groups changed their approach and developed antibiotics by mimicking the physicochemical properties of polymyxins using cyclic amphipathic peptides formed by alternate cations (Lys) and non-polar (Val or Phe) residues, based on the structure of PxB. This last approach proved effective in developing very active compounds with promising perspectives [Freder et al., 2004].

3.1.2. DESIGN OF NEW COLISTIN ANALOGUES

As previously mentioned, the main goal for this thesis was to develop new colistin (PxE) analogues in hope for obtaining new antimicrobials with similar or higher activity against Gram-negative bacteria to that of polymyxin or colistin. To be successful, these new colistin analogues should exhibit less toxicological effects than the polymyxin family.

As one of the main objectives is that the analogues are meant to be easily escalated to industrial mass production, we added a few minor modifications to the structure of colistin during the synthesis of the analogues.

During this project, the following modifications were applied:

Modification of the fatty acyl chain

The (S)-6-methyloctanoic acid of colistin was substituted by linear fatty acids without any stereocenter, which are much more commercially available. Specifically, hexanoic, octanoic, decanoic and dodecanoic acids were used. As previously explained, several fatty acid modifications have been historically tested, which resulted in the identification of 7 to 9 carbons being the sweet spot for the fatty acid length in polymyxins. However, previous tests had been performed based around the polymyxin basis, not the colistin one [Rabanal et al., 2015]. Even though they are very similar structurally, there is a difference in residue 6, which is a Phe in polymyxin and Leu in colistin. This modification may have implications on the molecule's interaction with the LPS, as both the residues 6 and 7, as well as the fatty acyl chain are involved in the interaction with the bacterial outer membrane. Therefore, new peptides were developed with different fatty acyl chain lengths while keeping the skeleton of the colistin as a basis.

Moreover, the (S)-6-methyloctanoic acid was alternatively substituted by (S)-2-aminodecanoic acid (DAdec) in order to maintain the amino residue of the acyl chain of polymyxins while simplifying the synthesis of the analogues, since the coupling of the Dab residue would not be needed and the synthesis process would be shortened.

Introduction of metabolically labile functionality

The amide bond between the residues 6 and 7 was substituted by an ester bond in order to facilitate the metabolisation of the analogues, since it has been previously demonstrated that an ester bond used to link the fatty acyl chain with the cyclic part eases the decomposition of the compound [Gordeev et al., 2016; Gordev, 2018].

Modifications of the hydrophobic regions of amino acids 6 and 7

As mentioned, the main difference between colistin and polymyxin is Leu⁶. We have already mentioned how other teams approached the hydrophobic region by substituting either of the amino acids or even permutating the segment. In our case the Leu⁶ was substituted with different amino acids in order to shorten, lengthen or redistribute the lateral side chain of this residue in order to study its effect regarding antimicrobial activity.

Introduction of disulfide bridge for cycle formation

The amide bond in the cycle between Dab⁴ and Thr¹⁰ was substituted by a disulfide bond between two Cys residues or a Cys and thiolate threonine (Ttr) placed in the same positions, simplifying the chemical synthesis of the analogues while maintaining the size of the cycle, which is crucial for preserving the antimicrobial activity.

Several natural antimicrobial peptides have been described with disulfide bridges, such as ranalexin and esculetin. Moreover, there are currently several drugs in clinical use that are composed of cycles formed with disulfide bridges, such as terlipressin, setmelanotide or vasopressin. For this reason, an increase of the toxicity when introducing the disulfide bridge in the analogues was not expected.

Modification of the lateral chain of residue Thr¹⁰

Related to the previous modification, the replacement of Thr¹⁰ with Cys for the disulfide bridge formation directly implied having a lateral carboxylic acid instead of the natural lateral chain of the Thr. In order to avoid the negative charge of the carboxylic acid, it was replaced by a carboxamide, obtained with the use of a Rink amide Linker. This carboxamide was expected to maintain the hydrogen bonding that intervenes in the interaction of polymyxin with Lipid A.

Despite all the previous modifications, our strategy was to maintain the basic structure and characteristics of colistin, which are key for its activity. Modifications performed within this thesis resulted in two different series, series A and series B, detailed below. The sequences, numeration and the molecular weight of all the analogues synthesized are specified in **Table 7**.

Table 7. Summary of all the peptides synthesized and tested during the present thesis, as well as control PxB and PxE. The peptide sequence and molecular weight (MW) are also included. D-amino acids are denoted in italics, whereas amino acids linked by an ester bond are denoted underlined.

#	Sequence	MW mg·mmol ⁻¹
PxE	(S)-6-methyl-octanoyl-Dab-Thr-Dab-cyclo-[Dab-Dab- <i>Leu</i> -Leu-Dab-Dab-Thr]	1168.77
PxB	(S)-6-methyl-octanoyl-Dab-Thr-Dab-cyclo-[Dab-Dab- <i>Phe</i> -Leu-Dab-Dab-Thr]	1202.75
A1	hexanoyl-Dab-Thr-Dab- cyclo(S-S)-[Cys-Dab- <i>Leu</i> -Leu-Dab-Dab-Cys]	1146.64
A2	octanoyl-Dab-Thr-Dab- cyclo(S-S)-[Cys-Dab- <i>Leu</i> -Leu-Dab-Dab-Cys]	1174.67
A3	decanoyl-Dab-Thr-Dab- cyclo(S-S)-[Cys-Dab- <i>Leu</i> -Leu-Dab-Dab-Cys]	1202.70
A4	dodecanoyl-Dab-Thr-Dab- cyclo(S-S)-[Cys-Dab- <i>Leu</i> -Leu-Dab-Dab-Cys]	1230.73
A5	decanoyl-Dab-Thr-Dab- cyclo(S-S)-[Cys-Dab- <i>Nle</i> -Nle-Dab-Dab-Cys]	1202.70
A6	dodecanoyl-Dab-Thr-Dab- cyclo(S-S)-[Cys-Dab- <i>Nle</i> -Nle-Dab-Dab-Cys]	1230.73
A7	heptanoyl-Dab-Thr-Dab- cyclo(S-S)-[Cys-Dab- <i>Aoc</i> -Nle-Dab-Dab-Cys]	1146.64
B1	Adec-Thr-Dab- cyclo-[Dab-Dab- <i>Leu</i> -Leu-Dab-Dab-Thr]	1097.73
B2	octanoyl-Dab-Thr-Dab- cyclo(S-S)-[Cys-Dab- <i>Leu</i> -Leu-Dab-Dab-Ttr]	1175.69
B3	Adec-Thr-Dab- cyclo(S-S)-[Cys-Dab- <i>Leu</i> -Leu-Dab-Dab-Ttr]	1118.67
B4	octanoyl-Dab-Thr-Dab-cyclo(S-S)-[Cys-Dab- <i>Leu</i> - <u>Leu</u> -Dab-Dab-Ttr]	1176.67
B5	Adec-Thr-Dab-cyclo(S-S)-[Cys-Dab- <i>Leu</i> - <u>Leu</u> -Dab-Dab-Ttr]	1119.65
B6	octanoyl-Dab-Thr-Dap-cyclo(S-S)-[Cys-Dab- <i>Leu</i> -Abu-Dab-Dab-Ttr]	1133.64
B7	Adec-Thr-Dap-cyclo(S-S)-[Cys-Dab- <i>Leu</i> -Abu-Dab-Dab-Ttr]	1076.62
B8	octanoyl -Dab-Thr-Dab-cyclo(S-S)-[Cys-Dab- <i>Leu</i> -Nva-Dab-Dab-Ttr]	1161.67
B9	Adec-Thr-Dab-cyclo(S-S)-[Cys-Dab- <i>Leu</i> -Nva-Dab-Dab-Ttr]	1104.65

Series A

In the first series of peptides synthesized (series A), we aimed to investigate the effect of the length of the fatty acyl chain in the peptide without changing the colistin basic skeleton (#A1-4) or performing some conservative changes in residues 6 and 7 (#A5-7).

The length of the fatty acyl chain of colistin is 8 carbons (plus the ramification of the 6-methyl), for that reason, the lengths assayed consisted in 6, 8, 10, or 12 carbons (#A1-4, respectively). The use of commercially available molecules such as hexanoyl or octanoyl would support the potential industrial scale up of the process.

Furthermore, in the first series of peptides, we also tested some combinations of fatty acyl chains with modifications in residues 6 and 7 - the hydrophobic region of the ring. Previous studies from our group had already identified that including Nle instead of Leu in positions 6 and 7 of the colistin cyclic ring improved the pharmacological profile of the molecule. Therefore, modifications suggested included the change of DLeu⁶-Leu⁷ to DNle⁶-Nle⁷, in combination with a 10-carbon (#A5) or 12-carbon (#A6) fatty acid chain. As both the fatty acyl chains and the hydrophobic residues of the ring are the main actors interacting with the Lipid A, it makes sense to modify them with the same strategy in mind. In this case, we are extending the fatty acyl chain from the historically tested optimal length (7-9 carbons) while also substituting the ramified leucine by norleucine, which is longer but maintains the hydrophobicity.

As the last modification in the first series of peptides, we substituted the DLeu⁶-Leu⁷ of colistin by DAoc⁶-Nle⁷, while also using a slightly shorter fatty acyl chain as heptanoyl (#A7). This last analogue was a promising peptide which had already been developed at our research team and that we needed more results about.

Taking into consideration that the amide bond needed for the cyclization of the ring is challenging from the synthetic point of view, the natural Thr¹⁰ of polymyxins was substituted with a DCys, allowing the cyclization by a disulfide bridge between both Cys, a much simpler procedure. However, in order to avoid the presence of the negative charge of the resultant carboxylic acid, a Rink Linker was used, obtaining thus a carboxamide, which maintained the hydrogen binding need for the interaction with Lipid A.

Series B

The second series of peptides synthesized (series B) further elaborated on the results from series A regarding fatty acyl chain and tried to simplify the N-terminal

hydrophobic chain in parallel to the substitution of hydrophobic residues in positions 6 and 7 with new alternatives.

The first apparent difference between Series A and B is the fact that Series B analogues were synthesized using a different strategy. Series A were synthesized using benzhydrylamine hydrochloride resin (BHA) functionalized with Fmoc-Rink linker, whilst series B were synthesized on 2-chlorotrityl chloride resin (2-CTC). The 2-CTC resin requires a cleavage step which is significantly less acidic than the needed for Rink-BHA. As a result, we postulate that the yield of the synthesis of the analogues will be significantly higher due to lower acid-related degradation.

In order to simplify the cyclization of the peptides by disulfide bridge, as explained previously, a thiol-modified threonine was used, maintaining this way the lateral side chain of the natural Thr¹⁰ in colistin. Due to this, although #B1 is shown having a regular Thr instead of the usual Cys as the first amino acid, the rest of the analogues (#B2-9) had a thiothreonine (Ttr) to allow for an easier cyclization reaction via a disulphur bond with Cys⁴.

As we will see in the following sections, the 8-carbon fatty acyl chain analogues tested in series A (#A2) showed promising results, so the bulk of series B peptides were based around the octanoyl fatty acyl chain. However, a potential simplification that is tested in this series is substituting the octanoyl + Dab¹ domain by a DAdec. DAdec is a fatty acyl chain that contains an amino group that allows us to only do one step of coupling instead of the two required ones for octanoyl and Dab. This would allow us to increase the yield of the peptide synthesis. To compare whether there are significant changes between the octanoyl-Dab and the DAdec approaches, most of the analogues for Series B are listed with the only difference being the N-terminus (e.g., #B2 and #B3; #B4 and #B5, etc).

A total of 3 different modifications were tested in Leu⁷ of the hydrophobic dipeptide of the ring. The first modification was the use of leucic acid instead of a leucine (#B4 and #B5), allowing the incorporation of an ester bond which replaced the regular amide bond between amino acids. We hypothesized that this ester bond could be easier to hydrolyze during the kidney metabolization of the peptide. Therefore, this could result in an easier urine excretion and lower nephrotoxicity.

The second modification was changing the Leu⁷ for Abu (L-2-Aminobutanoic acid) (#B6 and #B7). This amino acid, Abu, is shorter than Leu, which could be relevant in the interaction with lipid molecules modifying the hydrophobicity, which could result in better toxicity profile.

The third and final modification was substituting the Leu⁷ for Nva (norvaline) (#B8 and #B9). Similar to Abu, Nva is also shorter than Leu, and it resembles a linear version of valine. Following the same approach, we wanted to test whether these analogues showed less toxicity than the colistin they are based on.

3.1.3. CHEMICAL SYNTHESIS OF THE POLYMYXIN ANALOGUES

Analogues were manually synthesized following standard Fmoc/^tBu procedures. Two different resins were used: BHA for the analogues of series A, whereas for the synthesis of the analogues of series B 2-CTC resin was used. When using the resin BHA, a reference amino acid was used (usually Fmoc-Ala-OH), to reduce steric and electronic problems, and carboxamide as the C-terminal side of the peptide was obtained instead of the carboxylic acid by using an Fmoc-Rink amide linker. Additionally, this Rink amide linker facilitates the cleavage of the peptide with 95% of trifluoroacetic acid (TFA). On the contrary, the 2-CTC resin is very acid labile, thus, the cleavage is achieved with lower concentrations of TFA.

Series A

For the synthesis of the analogues from series A, the following amino acids with the specified protecting groups were used: Fmoc-Cys(Trt)-OH, Fmoc-DCys(Trt)-OH, Fmoc-Dab(Boc)-OH, Fmoc-Leu-OH, Fmoc-Nle-OH, Fmoc-DAoc-OH, Fmoc-Thr(^tBu)-OH. Right after the removal of the Fmoc group of the last coupled amino acid, different fatty acids were used for the chain elongation: specifically, hexanoic, octanoic, decanoic and dodecanoic acids.

The coupling of the different amino acids was performed using diisopropylcarbodiimide (DIPCDI) as activating agent and hydroxybenzotriazole (HOBt) as additive to minimize racemisation. In each case, 3 eq. of all the previous reagents were added directly to the resin and left to react with occasional stirring for 1 hour in dimethyl formamide (DMF) in order to conduct the coupling.

Right after a successful coupling, the Fmoc group was deprotected using 20% of piperidine in DMF, allowing this way the incorporation of a new amino acid after washing with DMF. This procedure was continuously repeated until the sequence was completed, being the last addition the fatty acid, which was coupled like a regular amino acid but using 5 eq. of all the reagents instead. In all the cases where the coupling was not complete, half of the quantities of all the reagents were used to repeat the step, but the reaction was left to react for 30 minutes instead.

The peptides were cleaved from the resin with a treatment of an acydolitic reagent composed of TFA/TES/H₂O (95:3:2, v/v) for 1 hour. The filtrate was evaporated using N₂ stream, and the obtained product was precipitated with cold anhydrous diethyl ether.

The crude peptide was cyclized in aqueous medium at a concentration of 1.5 mg·mL⁻¹ and adding a 3% of dimethyl sulfoxide (DMSO) to the solution that allowed the disulfide bond formation. The mixture was continuously stirred at room temperature and left to react at least 48 hours; the cyclization was monitored by high-performanceliquid chromatography (HPLC) analysis (example shown in **Figure 15**). Once the cyclization was complete, the mixture was lyophilized.

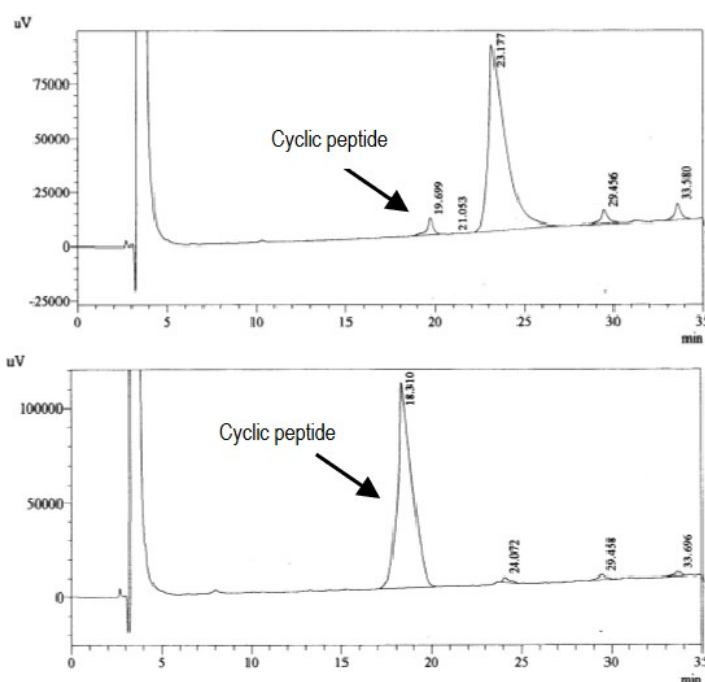


Figure 15. Monitoring by analytical HPLC of the reaction of cyclization in solution using DMSO/H₂O (3:97, v/v). Elution conditions of 20% to 35% B in 30 min, solvent A: 0.045% TFA and B: 0.036% TFA in ACN.

The obtained crude peptides were purified by semi-preparative HPLC trying to obtain the highest purity (>99%); the purified peptides were finally characterized by analytical HPLC and mass spectrometry.

An example of the synthetic route followed in this peptide series is shown in **Figure 16**.

Series B

For the synthesis of the analogues from series B, the following amino acids with the specified protecting groups were used: Fmoc-Cys(Trt)-OH, Fmoc-Dab(Boc)-OH, Fmoc-Leu, Fmoc-Thr(tBu)-OH, Fmoc-Ttr(tBu)-OH, Fmoc-Abu-OH, Fmoc-Nva-OH, Boc-2-D-Adec-OH, Fmoc-Dab(Mtt)-OH; for the ester-containing peptides, leucic acid was used. Right after the removal of the Fmoc group of the last coupled amino acid, different fatty acids were used for the chain elongation: specifically octanoic and Boc-2-D-Adec-OH acids.

Mostly, the coupling of the amino acids was performed exactly as described in Series A, with minor differences detailed below.

The coupling of leucic acid was performed using 2 eq. of the hydroxyacid, 4 eq. of HOBt and 4 eq. of DIPCDI. The leucic acid lacks the Fmoc group, thus its deprotection was not needed and an amino acid was coupled directly by the formation of the symmetric anhydride for its activation. The generation of the symmetric anhydride was accomplished by dissolving 6 eq. of the amino acid in DMF and adding 3 eq. of DIPCDI; the mixture was left to react for 30 minutes under stirring. The symmetric anhydride was then added directly to the resin, together with 0.1 eq. of 4-dimethylaminopyridine (DMAP), used as catalyst; the reaction was left for 1 hour. If the coupling was not complete, monitored by the ninhydrin test, the whole process was repeated using half of the quantities of all reagents and diminishing the reaction time to 30 minutes.

For the cleavage of peptides, the same protocol as described in Series A was applied, with also minor differences detailed below.

For the peptide that contained the Fmoc-Dab(Mtt)-OH amino acid and Fmoc-Thr(Trt)-OH in positions 4 and 10, respectively, and thus, the cyclization needed to be conducted by the formation of a lactamic bond, the cleavage and partial deprotection was performed by using a solution of HFIP/TFE/TES/DCM (20:10:5:65, v/v), also for 1 hour. The filtrate was evaporated under N₂ stream, and the peptide crude was precipitated with cold Milli-Q water. Then the peptide crude was lyophilized, and cyclization was carried out by using HATU, HOAt and diisopropylethylamine (DIEA). Specifically, cyclization was performed by dissolving

the peptide crude in DMF at a peptide concentration of $2.5 \text{ mg}\cdot\text{mL}^{-1}$, and adding HATU/HOAt/DIPEA (2:2:4 eq); the mixture was left to react for 45 minutes. Once cyclization was complete, the peptide was precipitated using cold Milli-Q water. The peptide crude was treated with an acydolytic mixture composed of DCM/TFA/TES/H₂O (50:45:3:2, v/v) and left to react for 45 minutes. The mixture was then evaporated under N₂ stream, the crude peptide was precipitated with cold diethyl ether, and finally the crude peptide was lyophilized. This synthetic route, represented in **Figure 17**, was applied only for the synthesis of #B1 analogue, whereas the rest of the Series B was synthesized using Fmoc-Cys(Trt)-OH and Fmoc-Ttr(^tBu)-OH in positions 4 and 10 respectively, and applying same cleavage and cyclization conditions than Series A (synthetic route detailed in **Figure 18**).

An example of the cyclization monitoring is shown in **Figure 19**.

Purification and characterization of peptides was carried out exactly as described in Series A.

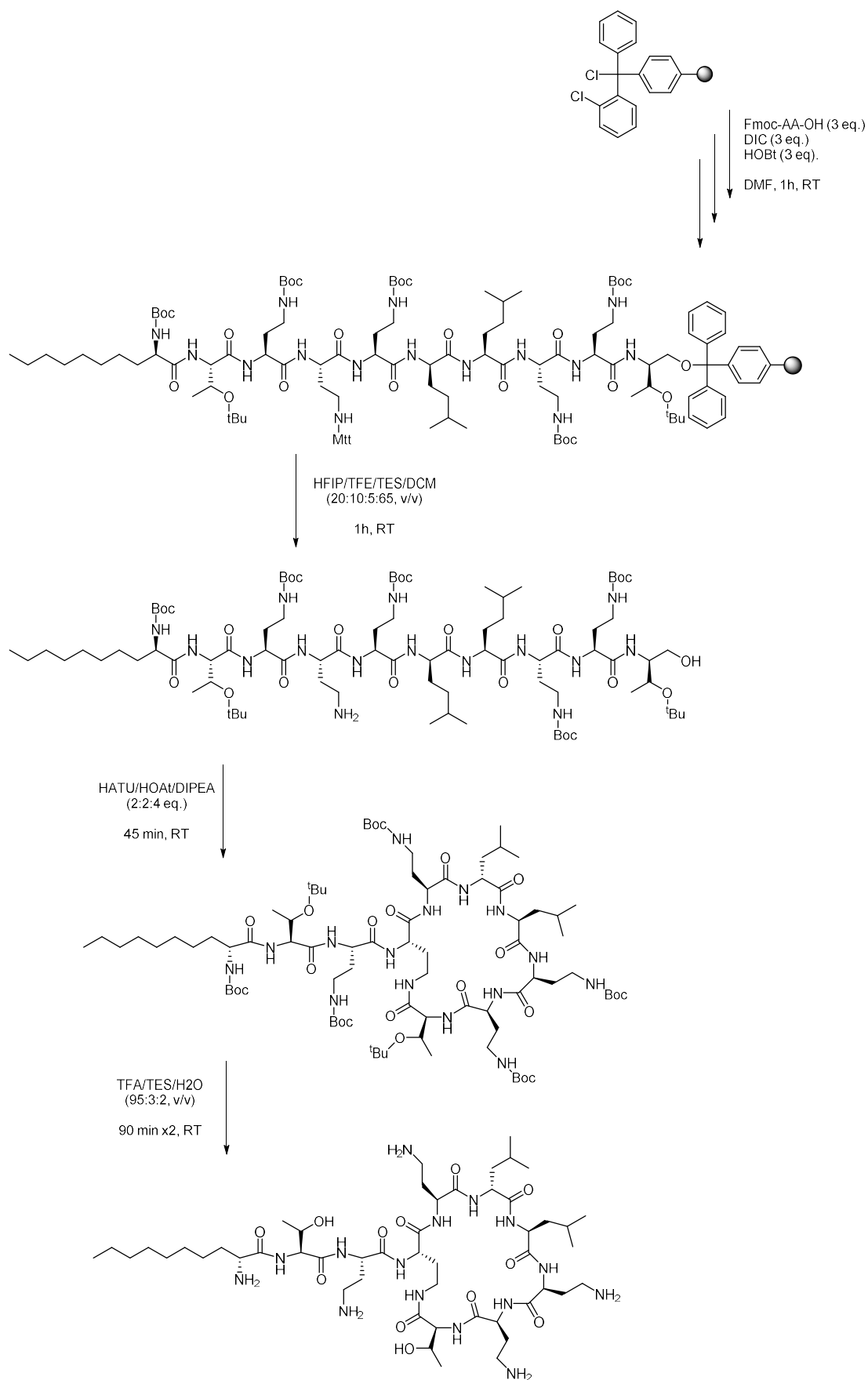


Figure 17. General scheme of the synthetic strategy followed for the colistin analogues from series B. In this example, synthetic route for analogue #B1 is represented.

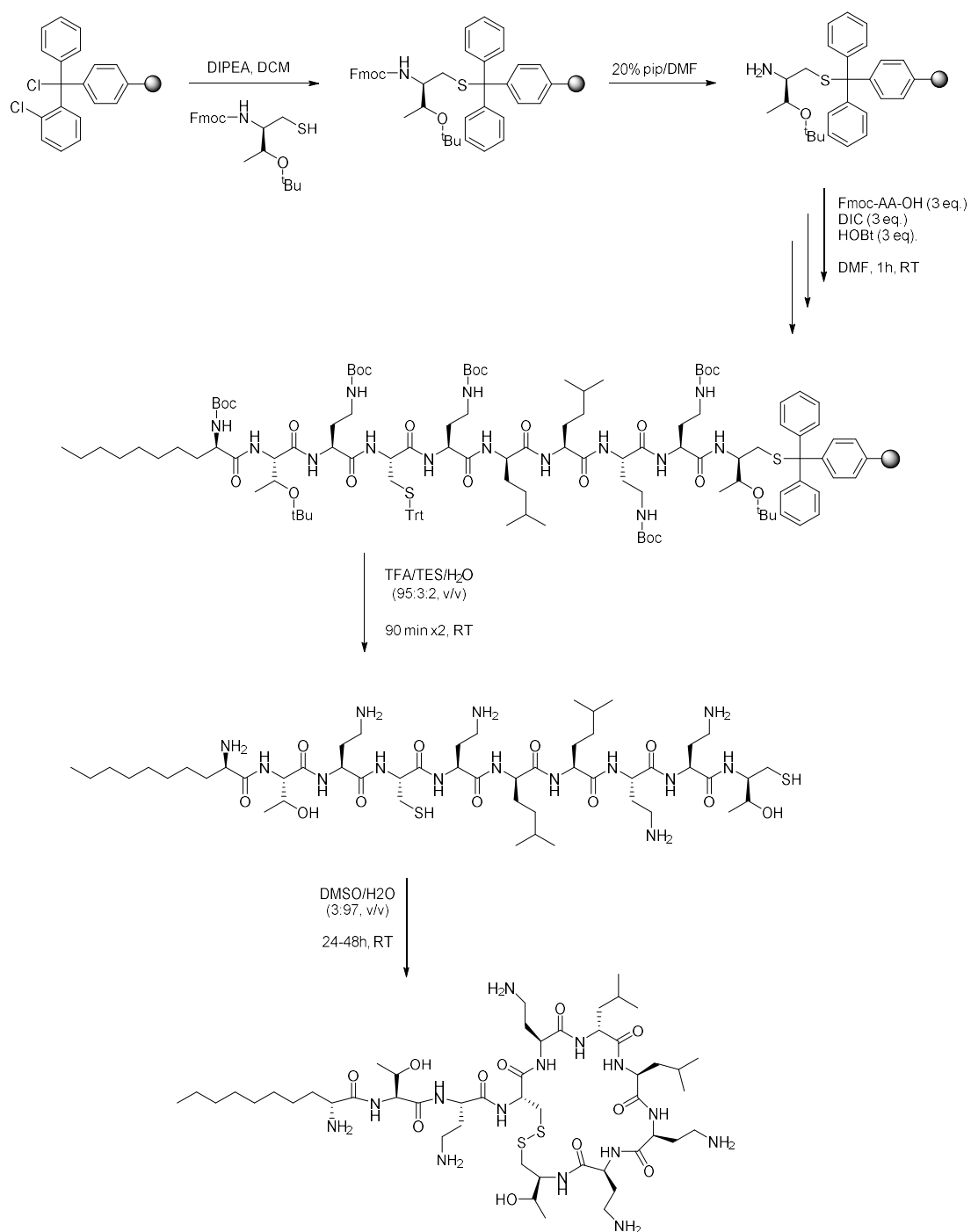


Figure 18. General scheme of the synthetic strategy followed for the colistin analogues from series B. In this example, synthetic route for analogue #B3 is represented.

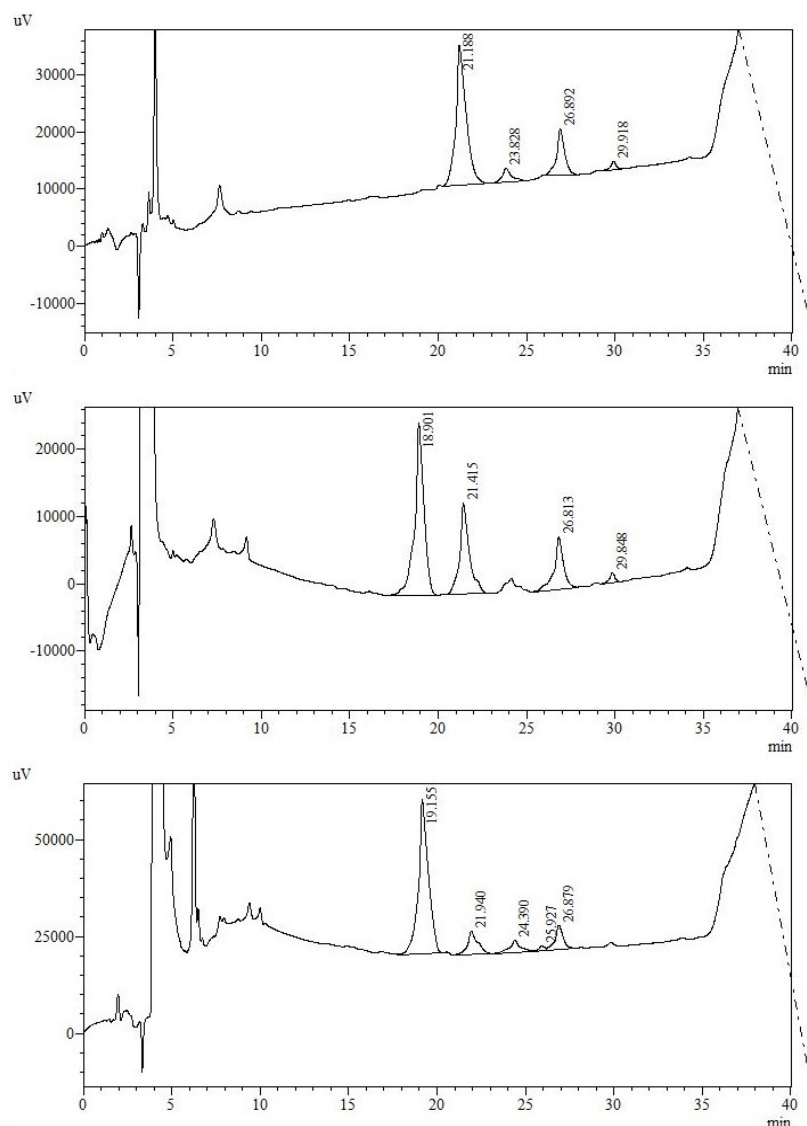


Figure 19. Monitoring by analytical HPLC of the reaction of cyclization in solution of peptide #B9 using DMSO/H₂O (3:97, v/v). Elution conditions of 20% to 35% B in 30 min, solvent A: 0.045% TFA and B: 0.036% TFA in ACN.

3.1.3.1. Scale-up of the synthesis of colistin analogue #B3

Among all the colistin analogues studied by *in vitro* and *in vivo* assays (which will be presented in the following sections), analogue #B3 was the peptide which we obtained the most promising results with (see section 3.3.1. and 3.2.3. for obtained MIC values and results for *in vivo* assays, respectively). For this reason, its scale-up process was performed using higher amounts of resin (1000 mg) and using the following different coupling reagents:

- 1) DIC/HOBt
- 2) HATU/HOBt/DIEA
- 3) DIC/K-Oxyma

Table 8. Summary of the details of the synthesis of the analogue B3 for the different coupling conditions used.

Coupling reagents	Initial resin weight / loading (mg / mg·mmol ⁻¹)	Crude peptide weight (mg)	Crude purity (%)	Synthesis yield (%)	Pure peptide weight (mg)	Final yield (%)
DIC/HOBt	131 0.5	145	86	82	85.9	49
DIC/HOBt	1000 0.5	659	45	78	287	34
HATU/HOBt/DIEA	1000 0.5	620	38	73	205	24
DIC/K-Oxyma	1000 0.5	560	40	67	253	30

Table 8 summarizes the details of the different synthesis performed for the #B3 colistin analogue. It can be observed that lab-scale (130 mg of initial resin) was significantly more efficient than bigger-scale synthesis (1000 mg of resin), applying same conditions of coupling and cleavage. Although the synthesis yield was similar (82% vs 78%), the crude peptide obtained using bigger amounts of resin was significantly worse, since the crude purity highly decreased from 86% to 45%, as shown in **Figure 20**.

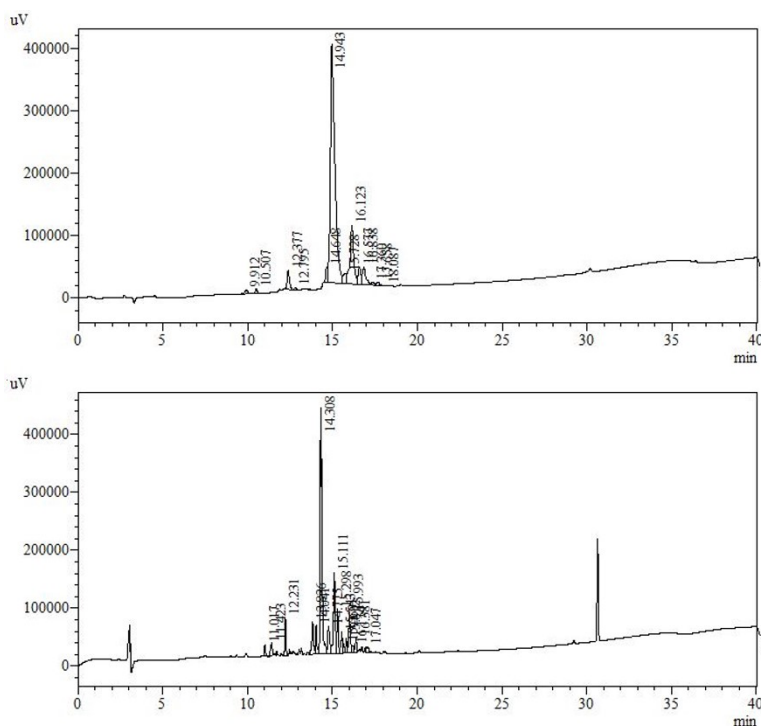


Figure 20. HPLC profile of #B3 crude peptide, synthesized with DIC/HOBt using 131 mg of initial resin (top) and 1000 mg of initial resin (bottom). Elution conditions of 5% to 95% B in 30 min, solvent A: 0.045% TFA and B: 0.036% TFA in ACN.

Mass spectrometry analysis of the linear #B3 peptide, obtained right after the cleavage, and from the synthesis performed using DIC/HOBt, revealed that the most relevant impurity identified was the *tert*-butylated product found at 1177.8 [M+H]⁺ (theoretical mass 1176.75), taking into consideration that linear #B3 analogue was identified at 1121.7 [M+H]⁺ (theoretical mass 1120.68).

Since this observation was encountered in both, lab-scale and large-scale synthesis, we decided to replace DIC/HOBt coupling conditions for HATU/HOBt/DIEA with the hope of obtaining a better crude profile. Unfortunately, not only the crude peptide was slightly worse, but the synthesis yield obtained was also, although similar, minor to the one obtained with the initial conditions.

Although HOBt is effective to minimize racemisation and it has been extensively used during the last decades, it was demonstrated in 2005 that this compound and its derivatives present explosive properties [Wehrstedt et al., 2005], thus, these compounds were regrouped under the “Class 1 explosive category” and their transportation became strictly regulated. This situation made evident the need to find alternative efficient additives for SPPS, which was a big challenge considering that additives based on other compounds such as *p*-nitrophenol (HONp), *N*-hydroxysuccinimide (HOSu) or pentafluorophenol (HOPfp), are less efficient than HOBt, since active esters of ONp, OSu or OPfp are less reactive than benzotriazole esters [Klose et al., 1999; El-Faham, 2000]. Since we were trying to scale-up the synthesis of #B3 analogue, the limitations of HOBt were considered and the use of K-oxyma combined with DIC was proposed in hope of obtaining also better results in the synthesis than the previous conditions (DIC/HOBt, HATU/HOBt/DIEA). Unfortunately, the use of K-oxyme combined with DIC did not render better results, and although the crude purity was similar than the ones obtained in the large-scale synthesis, this coupling conditions led to the worst synthesis yield of the conditions assays, 67%, compared to the best large-scale synthesis yield of 78%.

In view of the obtained results, further studies should be performed in order to optimize this synthesis, and since three different conditions of coupling reagents were studied with similar results, changing the resin could be an alternative approach.

3.2. SERIES A

3.2.1. IN VITRO ANTIMICROBIAL ACTIVITY

To find out which of the synthesized peptides showed better activity, we needed to assess comparatively the antibacterial effects of each one. The easiest way to measure it is the determination of the minimum inhibitory concentration. The MIC is the lowest concentration at which an antimicrobial compound inhibits the visible growth of a microorganism after culture it overnight (18-20 hours). It is usually determined by using a standard broth dilution assay [Wiegand 2008].

The microorganisms used, obtained from American Type Culture Collection (ATCC), were the following:

- *Escherichia coli* (*E. coli*): Gram-negative bacteria (ATCC 25922)
- *Pseudomonas aeruginosa* (*P. aeruginosa*): Gram-negative bacteria (ATCC 27853)
- *Acinetobacter baumannii* (*A. baumannii*): Gram-negative bacteria (ATCC19606)
- *Staphylococcus aureus* (*S. aureus*): Gram-positive bacteria (ATCC 25923)

The rationale behind this selection of bacteria is that *E. coli*, *P. aeruginosa*, and *A.baumannii* are the most prevalent Gram-negative bacteria causing nosocomial (contracted at the hospital) diseases. Being the most prevalent in hospitals, they are some of the bacteria which accumulate more antibiotic resistances. On the other side, *S. aureus* was used as a Gram-positive bacteria control, since it is the main reference for multi-resistant bacteria, which makes it a very relevant bacterium to be studied.

In order to determine the MIC of a peptide for a given bacteria strain, the bacteria strain is incubated in liquid media with different concentrations of the applicable peptide. After 18-20 hours, the cultures are checked and the MIC is taken as the lowest concentration at which bacterial growth is not observed (i.e., cloudiness of the culture). Therefore, the lower the MIC of a peptide, the more sensible is the bacteria to it.

Table 8 details the results of the MIC assays for the series A analogues obtained using *E. coli*, *P. aeruginosa*, *A. baumannii* and *S. aureus* after incubating 18h.

Each determination was done by triplicate and using bacteria in the pre-exponential phase.

Table 8. MIC values in $\mu\text{g}\cdot\text{mL}^{-1}$ for peptides in Series A using *E. coli*, *P. aeruginosa*, *A. baumannii* and *S. aureus*.

Code	<i>E. coli</i>	<i>P. aeruginosa</i>	<i>A. baumannii</i>	<i>S. aureus</i>
PxE	0.5	2	2	>32
A1	>32	>32	>32	>32
A2	32	8	>32	>32
A3	8	4	>32	16
A4	16	8	>32	8
A5	16	4	>32	32
A6	8	8	>32	8
A7	16	8	>32	>32

We can appreciate that the short fatty acyl chains of #A1 and #A2 (6 and 8 carbons, respectively) greatly reduces the antimicrobial activity of the analogues, as their MIC is mostly undetectable in the concentrations used. In the same manner, the long fatty acyl chain of #A4 (12 carbons) also reduces the antimicrobial activity in Gram-negative *E. coli* and *P. aeruginosa*, while we can see an improvement for *S. aureus*, probably due to the different envelope composition. As Gram-positive bacteria possess a thicker cell wall, it could be the case that the longer fatty acid destabilizes it in some way. As a summary, the optimal length of the fatty acyl chain from the conditions assayed is 10 carbons for Gram-negative bacteria, while 12 carbons seem to be more effective towards *S. aureus*.

On the other side, substitution of Leu by Nle does not seem to bring any significant improvement. The comparison between #A3/#A5 and #A4/#A6 show similar, if not lower, antimicrobial activity for all bacteria when adding the Nle residue. The effect of substituting the Leu in 6th position by a DAoc, however, results in a minor improvement in the antimicrobial activity for *E. coli* and *P. aeruginosa*.

Finally, none of the peptide analogues presented in series A show any kind of antimicrobial activity against *A. baumannii* at the concentrations assayed.

3.2.2. HAEMOLYSIS

Haemolysis is defined as the breakage of erythrocytes (also known as red blood cells), which results in the release of their contents to the surrounding liquid [Beris & Picard, 2015]. Haemolysis is caused by the exposure of the erythrocytes to, amongst other compounds, toxic agents, such as lead, haemolysins, or polycationic AMPs, such as polymyxins [Zhu et al., 2021; Beris & Picard, 2015].

Any AMP under development needs to show low or no toxicity towards mammalian cells and be selective to kill the target bacteria. Haemolysis represents the most commonly employed initial toxicity assessment due to its simplicity, reproducibility, and the information it provides. The erythrocyte is often employed as model of mammalian cell membranes, as its membranes have been studied and characterized - they are composed of varying concentrations of PC, SP, PS, PI and PE in an uneven distribution. Specifically, erythrocytes exhibit high concentrations of PE and PC in their outer leaflet, which is the cause for the neutral charge in their membrane. This neutral charge greatly differentiates it from the anionic bacterial cell, and makes the erythrocyte membrane a representative model for eukariotic cells [Greco et al., 2020; Virtanen et al., 1998; Dodge & Philips, 1967].

This assay aims to measure the haemolysis caused by polymyxin analogues and use that data as a model of mammal toxicity. Therefore, this assay allows us to extrapolate which peptides are the least toxic.

For all the reasons explained above, to be a candidate for its use in humans, antibacterial compounds should not only have a low MIC value (high efficacy) but also keep their haemolytic activity at a minimum (hence, low toxicity) in order to not be considered harmful. Therefore, after the MIC values, the haemolytic effect of analogues was measured by triplicate.

The basis behind the haemolysis assay consists of the following: the peptides are incubated with erythrocytes isolated from animal blood (generally rabbit) with a serial 2-fold dilution assay [Strandberg et al., 2007], using citrate phosphate dextrose-stabilized blood. After an incubation time, samples were then centrifuged and the absorbance of the supernatant containing haemoglobin was measured. Percentage of haemolysis was calculated relative to 100% lysis by 1% Triton X-100.

All peptide analogues of the Series A were assayed for haemolysis, with the results shown in **Figure 21**. It can be observed how the peptides with 6 or 8 carbons in the fatty acyl chain (PxE, #A1 and #A2) show a lower haemolysis percentage in comparison to the rest of the peptides. Moreover, when increasing the length of the fatty acyl chain to 12 carbons (#A4 and #A6), the haemolysis is significantly higher, for example at a concentration of $77 \mu\text{mol}\cdot\text{L}^{-1}$, #A6 presents a high increase of haemolysis, inducing almost 50% of lysis. The 10-carbon analogues (#A3 and #A5) are less haemolytic than the 12-carbon ones, and at $77 \mu\text{mol}\cdot\text{L}^{-1}$ the haemolysis is around 12% but are still more haemolytic than those with shorter fatty acyl chains, where the % of haemolysis at the same concentration is around 6%.

On a side note, the substitution of Leu by Nle did increase the haemolytic effect of analogues (comparing #A6 with #A4, and #A5 with #A3), although the differences are not as relevant as those seen when changing the length of the fatty acyl chain.

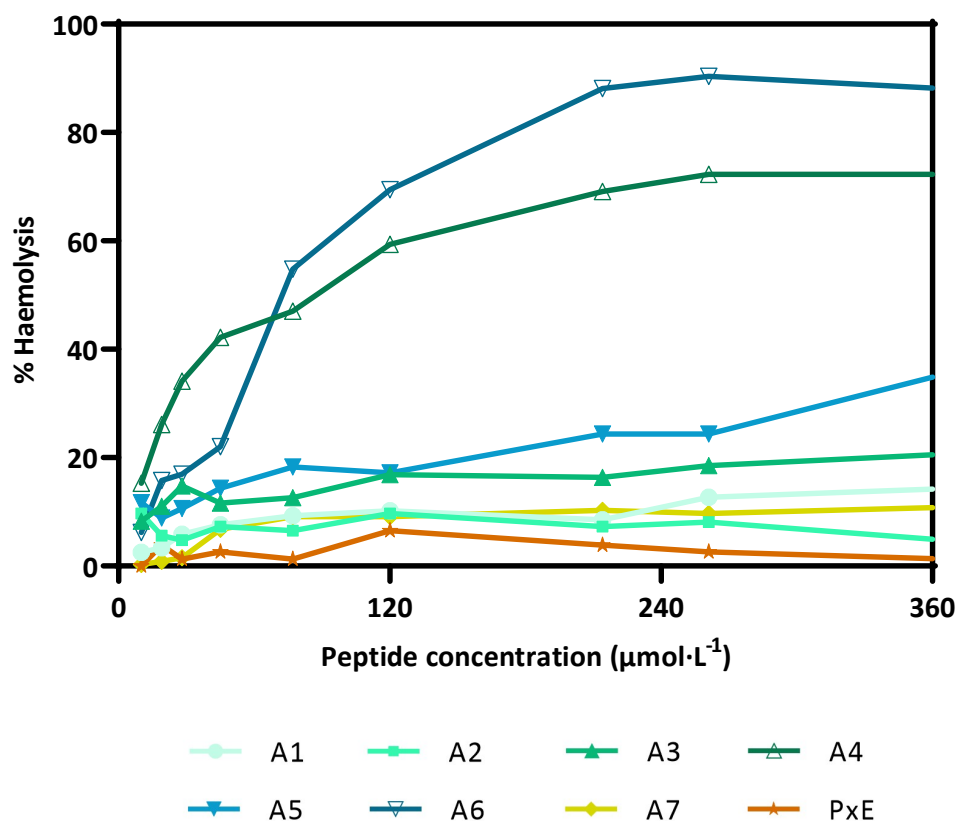


Figure 21. Percentage of haemolysis using different peptide concentrations.

3.2.3. BIOPHYSICAL EVALUATION

3.2.3.1. Biological membranes

The determination of the molecular mechanisms underlying drug-membrane interaction is of critical significance in the pharmacological field. Once a drug is administered, it moves into the bloodstream and is transported to the action site. Before the drug can perform its therapeutic effect, it might need to cross several biomembranes, such as gastrointestinal membranes, the walls of blood capillaries or even the blood-brain barrier. Moreover, the interaction of the drug with biomembranes can alter their physical properties such as their structure, viscosity, surface charge, order, dynamics, fluidity, mobility and lipid conformation, which directly affects the normal function of biomembranes by modifying their cell shape, membrane permeability and function of membrane proteins. The interaction of the drug with biomembranes not only can modify its physicochemical properties, but its bioavailability and pharmacological effect. On the other side, drug interactions with biomembranes can also lead to adverse effects, such as drug resistance or even toxicity [Andrade et al., 2021; Li et al., 2017]. For all these reasons, the study of the biophysical properties of the interaction between drugs and biomembranes is crucial for the drug development.

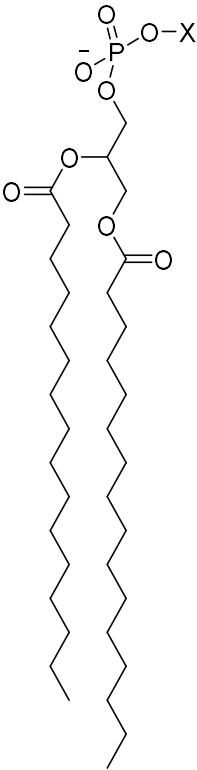
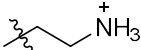
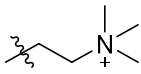
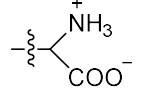
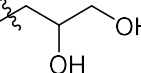
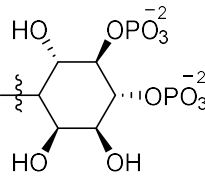
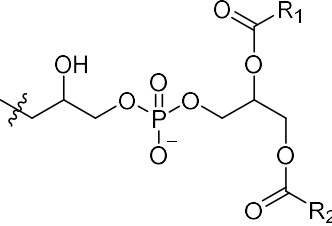
One of the first approaches to identify effective drug candidates is to apply computational models to reduce time and resources during drug development. However, these models are not perfect, and they are not able to properly simulate the conditions of biological membranes. Due the high complexity of biomembranes, the drug-membrane interaction is not easy to characterize; for this reason, several membrane models have been developed during the last decades in order to understand the mechanism of action of drugs [Peetla et al., 2009]. For this reason, and taking into consideration that the lipid bilayer is one of the most important parts of biological membranes, it is not surprising that several models have been developed to emulate it [Andrade et al., 2021].

Lipid bilayers are structures composed of several amphiphilic lipid molecules that are bound through hydrophobic interactions thanks to the fatty acyl chains and electrostatic interactions between the polar groups. These bilayers separate

intracellular and extracellular environments, being thus the key for cell compartmentalization and responsible of their homeostasis. Moreover, they control the transport and communication between inter or intracellular compartments and several catalytic reactions depend on its presence.

In 1972, Singer and Nicholson proposed the first model of the membrane structure: a fluid mosaic composed of a bilayer of phospholipids. Within the plane of this mosaic, globular proteins were embedded and could freely circulate [Singer & Nicholson, 1972]. During the following decades, this model was expanded and nowadays it is well described that the two layers of the membrane are asymmetric on the lipid composition, and it also varies between different regions or domains [Escriba, 2006]. It is also known the existence of microdomains within the lipid membrane that are enriched in cholesterol (Chol) and tightly packed sphingolipids (SP) that reduce its fluidity [Silvius, 2005].

Table 9. Basic phospholipid structure and common head groups. The lipid characteristic and the resultant net charge at physiological pH are specified.

Basic phospholipid structure	Headgroup (X)	Phospholipid/Characteristic/Net charge (at pH 7)		
		PE	zwitterionic	0
		PC	zwitterionic	0
		PS	anionic	-1
		PG	anionic	-1
		PI	anionic	-5
		CL	anionic	-2

Membranes are conformed of amphipathic lipids that consist of a hydrophobic region, typically composed of fatty acids and a glycerol moiety, and a polar region composed of a phosphate group and a polar head group. Depending on their chemical structure, membrane lipids can be classified as glycerophospholipids, sphingolipids, and sterols [Peetla, et al., 2009]. Moreover, glycerophospholipids, or phospholipids, can be conformed of different hydrophilic head groups: phosphatidylethanolamine (PE), phosphatidylcholine (PC), phosphatidylserine (PS), phosphatidylglycerol (PG), phosphatidylinositol 4,5-bisphosphate (PI) and cardiolipin (CL), detailed in **Table 9**.

There are also different types of sphingolipids depending on the presence or absence of a phosphate group, named phosphosphingolipids and glycosphingolipids, respectively; however, the most common group of sphingolipids in membranes is perhaps sphingomyelin (SM). On the other hand, sterols are molecules derived from cholesterol, which is the most common one. Both lipids, sphingomyelin and cholesterol, are detailed in **Figure 22**.

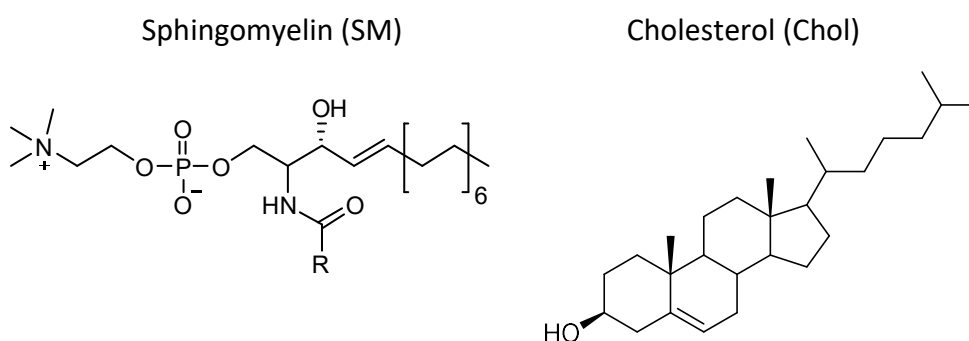


Figure 22.Structure of sphingomyelin (left) and cholesterol (right).

Depending on the type of cell, the composition of the lipid membrane can differ a lot. On one side, the outer leaflet of bacterial cells is conformed mainly of negatively charged phospholipids such as CL or PG, depending on if cells are from Gram-negative or Gram-positive bacteria, whereas the outer membrane of mammalian cells is composed of neutral lipids such as Chol, PC and SM [Beining et al., 1975; Morein et al., 1996; Salvioli et al., 1978]. Additionally, Gram-negative bacteria generally have higher amounts of PE than Gram-positive bacteria. Moreover, bacterial membranes possess a highly asymmetric lipid charge distribution, which results in a high transmembrane potential. The electrical

potential is necessary for several energy-dependent catalytic or transport processes. Therefore, bacterial membranes tend to fall in one of two major membrane archetypes: Gram-positive and Gram-negative. Gram-negative bacteria have an outer membrane which is rich in PG, LPS and divalent cations such as calcium and magnesium that act binding together the LPS molecules, followed by a 2 nm thick peptidoglycan wall that protects the inner, cytoplasmic membrane. On the contrary, Gram-positive bacteria do not possess an outer membrane, but a 20-40 nm thick peptidoglycan wall that is directly surrounding the cytoplasmic membrane, as detailed in **Figure 23**. Additionally, some examples of lipid composition of different cells are detailed in **Table 10**.

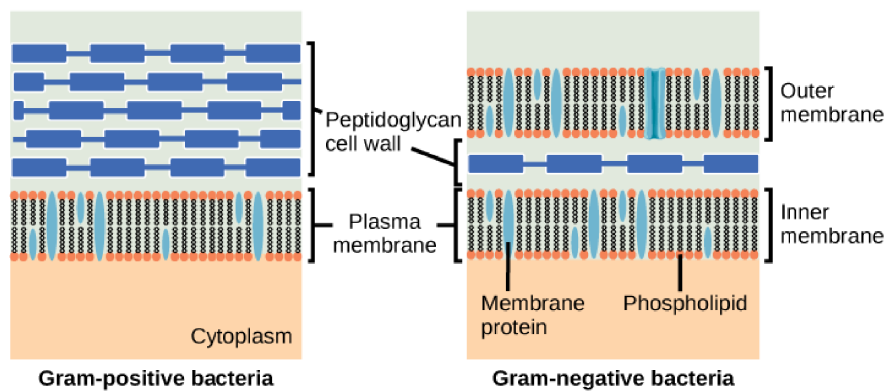


Figure 23. Structural differences between Gram-positive and Gram-negative bacteria. Image taken from <https://simbac.gatech.edu/>.

Table 10. Differences in lipid composition between representative cells of Gram-negative (*P. aeruginosa*) and Gram-positive (*Bacillus subtilis*) bacteria, and eukaryote cell (human fibroblasts) [Malanovic & Lohner, 2016]. For Gram-negative bacteria, the inner and outer membranes are very similar in composition, mainly zwitterionic phospholipids such as PE that vary between species, except for the outer layer of the outer membrane, which is composed mainly of LPS. Gram-positive bacteria favour the negatively charged PG [Nikaido & Nakae, 1980].

Lipid	Gram-negative cell (<i>P. aeruginosa</i>)	Gram-positive cell (<i>Bacillus subtilis</i>)	Eukaryote cell (human fibroblasts)
PG	21%	70%	
PE	60%	12%	32%
CL	11%	4%	
PS			6%
PI			3%
PC			44%
SM			14%

The differences between bacterial and mammalian cells allow the selectivity of cationic antimicrobial agents and are key for the discovery of new drugs. In order to mimic the characteristics of membranes detailed previously, different models such as lipid monolayers, supported lipid bilayers, micelles and liposomes can be used to study the mechanism of lipid-peptide interaction by using different techniques. In general, these models are quick to prepare, economical and reproducible, which allows for fast biophysical assays [Andrade et al., 2020].

3.2.3.2. Biophysical studies

As the mechanism of action of polymyxins is based upon the interaction with the bacterial membrane [Zasloff, 2002], the study of said interaction is relevant to foresee their activity. However, the study of membranes of living cells in the laboratory setting can be difficult, mainly due to the composition and asymmetry. For this reason, synthetic membrane models, whose composition can be defined, were used. Specifically, we emulated different membrane compositions by using lipid monolayers and liposomes. As it will be described, the molecules that will be used to form the membrane models are lipopolysaccharide (LPS), and the phospholipids: phosphatidilcholine (PC), phosphatidylethanolamine (PE) and phosphatidylglycerol (PG). Since the majority of phospholipids found in cell membranes are asymmetrical regarding the fatty acyl chains, usually with one saturated and the other with one or more unsaturations, we will use palmitoyl (saturated 16:0) and oleoyl (unsaturated 18:1). Therefore, the nomenclature of the phospholipids will be POPC, POPE and POPG (structures in **appendix 7**).

3.2.3.3. Lipid monolayers

One of the most accepted models to characterize drug-lipid membrane interactions is the Langmuir lipid monolayer, also known as lipid monolayer. Is a simply, precise method that allows mimicking one single leaflet of a bilayer membrane while setting a specific lipid composition, pH, temperature and surface pressure to emulate biological conditions [Brockman, 1999].

Basically, this technique consists in forming lipid monolayers by extending amphiphilic lipids in the air/water interface of an aqueous solution and compressing

them to reach a certain surface pressure, typically $30 \text{ mN}\cdot\text{m}^{-1}$, which is the surface pressure equivalent to a biological membrane, and then monitoring the surface pressure changes while adding the study compound in the aqueous subphase. Although this model is based on the formation of a thin layer of only one molecule of thickness, and thus only can represent half of a cellular membrane, it presents an important advantage in front of more complex models: the lipid composition of the monolayer formed can be exactly established, as well as its packing level, determined by the surface pressure. Thus, the alteration of the composition and the superficial pressure of the lipid monolayers allow obtaining information on the drug-lipid interactions and also between the drug and other relevant components, as well as the conformation of the studied molecules. Adding amphipathic molecules to an air-water interface will cause a surface pressure increase, and further surface pressure increases will be observed when one of the lipopeptide antibiotics that are injected into the subphase inserts into the lipid molecules or disturbs the packaging of the pre-stabilized lipid monolayers [Brockman, 1999].

Depending on how the formation of monolayers takes place, it can be distinguished between Gibbs adsorption monolayers, and extension or Langmuir monolayers [Gaines, 1966].

➤ Gibbs adsorption monolayers

Gibbs monolayers are obtained when adding amphipathic molecules and these are partly soluble in one of the phases separated by the interface. The solubility of the compound in the solution will establish a dynamic equilibrium between surfactants in the bulk solution and in the interface, forming a monolayer, with a continuous exchange between them.

A clear example is when introducing phospholipids into water: their polar region will face inwards to the solution, while the non-polar face will point outwards to the air, causing a decrease of the superficial tension of the solvent.

➤ Extension of Langmuir monolayers

Langmuir monolayers are insoluble monolayers obtained when depositing amphipathic molecules directly at the interface of a polar solution. This deposition can be carried out either in solid form or dissolved in a volatile solvent. In this case while the nonpolar region of the molecule is insoluble in the aqueous solvent, the polar domain regulates its orientation in respect to the subphase, as well as its extension. The low solubility of the surfactant allows a high degree of self-organization through the monolayer, which can remain in a stable state for several hours.

Antimicrobial peptides are usually amphipathic, which means that they have superficial activity. Furthermore, as their biological activity requires that they interact with the interface of membranes, the monolayer model is a great candidate for studying both the biological and physicochemical characteristics. This is due to the fact that the experiments conducted in the air/water interface provide information about the flexibility and superficial activity of the molecules [Zhang et al., 2001; Tian et al., 2006; Ambroggio et al., 2004].

The interaction between the colistin analogues with bacterial membranes was characterized using Langmuir monolayers by measuring the kinetic of penetration at constant area. The surface pressure was measured using the Wilhelmy method: introducing a platinum plate (also named Wilhelmy plate) in the subphase that is attached at the same time to an electrobalance that measures the force that the liquid exerts on the plate (**Figure 24**).

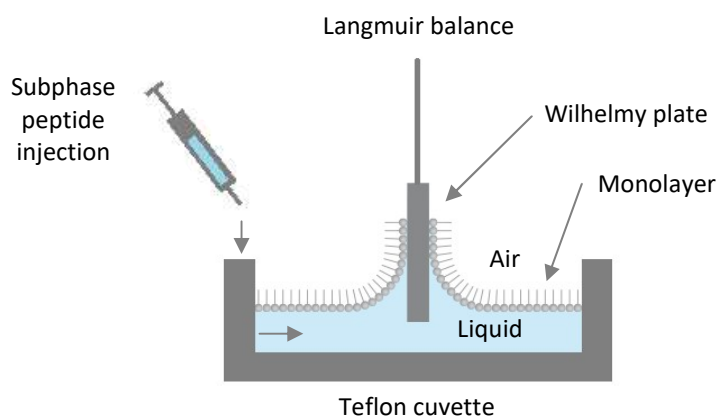


Figure 24. General schema of the assay used to measure superficial pressure while adding colistin analogues to Langmuir monolayers of different composition.

It has to be considered that the plate experiences gravitational forces, the surface tension towards the water and the counteraction force of floatability displacing the plate upwards from the water. By knowing the dimensions of the plate and having the balance calibrated, the force detected at the plate can be converted to surface tension units ($\text{mN}\cdot\text{m}^{-1}$).

This assay was carried out by extending a Langmuir monolayer by depositing a solution of lipid, dissolved in an organic volatile solvent, over the surface of an aqueous solution. The lipid monolayer was set to a certain surface pressure by depositing small drops of the lipid solution with a microsyringe, until the desired pressure was reached and stabilized for 15 minutes allowing for solvent evaporation. Then the peptide solution was added into the subphase through a side hole to avoid disturbing the lipid monolayer, allowing its interaction with the molecules that conformed the Langmuir monolayer. As mentioned before, a pressure increase was observed when the addition of the peptide caused its insertion into the lipid monolayer or it disturbed its packing, and thus, being proof that the peptide interacted with that particular monolayer and was inserted at some level between the phospholipid molecules.

By monitoring the magnitude of the effect (change in surface pressure) as a function of time for the different peptides, and using different lipids to form the monolayer, the degree of interaction between the peptide and the monolayer was extrapolated, taking into consideration that the area of the monolayer remained constant during all the time. For this reason, these studies are also known as kinetics of penetration at constant area.

One of the main advantages of the lipid membrane model is that despite its simplicity, it allows to correlate directly the thermodynamics between the monolayers and the bilayer membranes; however, these lipid monolayers only emulate the outer leaflet of cellular membranes, and lipid monolayers are also less stable than lipid bilayers [Lucio et al., 2010]. The limitations of this lipid monolayer 2D model can be outcomed by using 3D models such as liposomes, since they mimic bilayers instead of lipid monolayers [Andrade et al., 2021].

3.2.3.4. Liposomes

Liposomes are spherical lipid vesicles that enclose an internal aqueous medium and that were first described in 1964 [Bangham & Horne, 1964] as artificially prepared closed vesicles measuring between 20 nm to some micrometres. Obtaining liposomes is simple, since their formation is based on the hydrophobic interactions that take place between the aqueous solution and the lipid molecules. They can be formed by either one or more lipid bilayers, which are usually phospholipids, oriented concentrically around the aqueous compartment. Since phospholipids are amphipathic molecules, they spontaneously self-organize in bilayers in contact with water. These bilayers are formed with the polar regions of phospholipids oriented towards the aqueous solution, while the hydrophobic regions face the interior of the bilayer, avoiding contact with aqueous solution (thermodynamically stable) (**Figure 25**) [Szoka & Papahadjopoulos, 1980; Lasic, 1988].

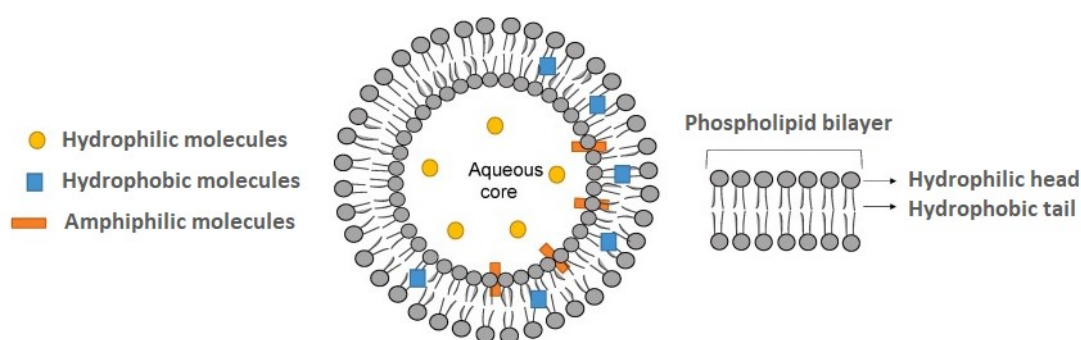


Figure 25. Representation of a unilamellar liposome. Figure modified from Guimarães et al., 2021.

Liposomes not only are widely used as model membranes, mimicking the lipid composition of any biological membrane, but they are also used as drug delivery systems due their ability to compartmentalise and separate the internal aqueous medium from the external environment [Agmo Hernández et al., 2011; Matos et al., 2012]. This peculiar morphology allows them to be used as diagnostic and therapeutic tools by containing markers or drugs, and also permits studying the mechanism of action of certain substances. Furthermore, it has been reported, that using liposomes as a carrier for a drug reduces its toxicity and also allows to

improve its bioavailability to particular target cells. This wide array of applications of liposomes resulted in a high interest for studying their physicochemical properties during the last decades.

In the case of liposome as membrane models, typically they are obtained with identical composition on both leaflets of the bilayer, which is not representative of the biological membranes. However, it is also possible to obtain liposomes with asymmetric leaflet composition, although the procedure has some limitations and is more complex than obtaining regular liposomes [Doktorova et al., 2018; Takaoka et al., 2018; Redelmeier et al., 1990].

Liposomes can be classified according to their size and the number of lipid bilayers, as detailed in **Figure 26** [Vance & Vance 1996; Laouini et al., 2012; Li et al., 2017]:

➤ Unilamellar vesicles

They are formed by just one lamella and can present the following types:

▪ Small unilamellar vesicles (SUVs)

Liposomes with small size ranging from 20 to 100 nm in diameter. As they are much smaller than LUVs, they also have a higher membrane curvature and are less stable.

▪ Large unilamellar vesicles (LUVs)

These vesicles range in size from 50 to 500 nm in diameter. They are very interesting because they exhibit a surface pressure similar to biological membranes ($30\text{-}32\text{ mN}\cdot\text{m}^{-1}$) and the lipid distribution between internal and external face is roughly 1:1. As such, they are the most well-known membrane model in both the physical, chemical, and mechanistic properties. Finally, their intra-vesicular volume is large enough to encapsulate water-soluble substances

▪ Giant unilamellar vesicles (GUVs)

These vesicles range in size from 1 μm to 100 μm in diameter, and are used as eukaryotic cell models.

➤ Multilamellar vesicles (MLVs)

These liposomes are formed by various concentric lamellae (usually ranging from 7 to 19) which are separated by large aqueous spaces. They have a wide array of sizes, as they can be from 100 to 1000 nm in diameter, obtained in heterogeneous populations.

➤ Multivesicular vesicles (MVs)

Vesicles which contain other closely packed non-concentric vesicles.

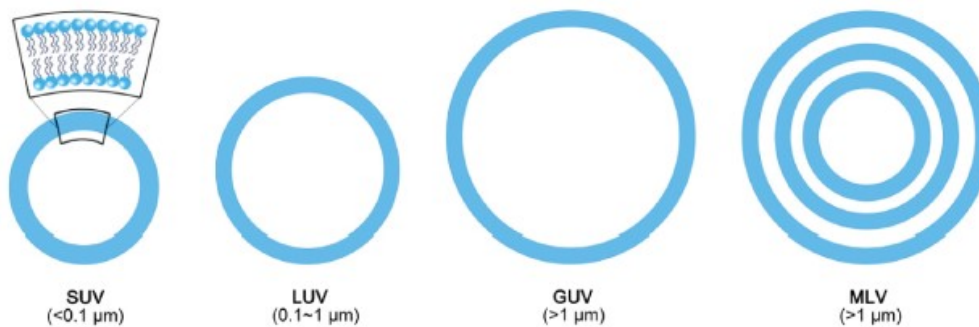


Figure 26. Schematic representation of the most commonly used liposomes, including small unilamellar vesicles (SUV), large unilamellar vesicles (LUV), giant unilamellar vesicle (GUV) and multilamellar vesicle (MLV). Figure taken from Li et al., 2017.

Obtaining liposomes is a simple procedure based on the hydrophobic interactions between an aqueous solution and lipid molecules. Typically, an organic solvent is used to dissolve the lipid molecules, which is evaporated under an inert gas stream, since the exposition of the lipid to O_2 might cause lipid oxidation. The thin lipid film obtained after the solvent evaporation can be rehydrated with an aqueous solution, which will allow the spontaneously self-assemble of the lipid film into liposomes. The buffer used for the resuspension of the lipid film can be of different characteristics depending on the needs or the desired application, such as pH or the presence or absence of counter ions [Routledge et al., 2019].

The preparation of liposomes can be summarized as follows: 1) drying down of lipids from organic solvents; 2) dispersion of the lipid in the aqueous solution and mechanical agitation; 3) purification of the liposomes obtained; and 4) characterization of the final product (size, distribution, lamellarity and/or lipid concentration) [Lasic, 1988; Mozafari, 2005]. During the last decades, different specific processes have been developed to obtain liposomes, such as extrusion [Olson, 1979], sonication [Gregoriadis, 1984], electroformation [Angelova

&Dimitrov, 1986], swelling [Needham & Evans, 1988] or reverse-phase evaporation [Szoka & Papahadjopoulos, 1978]. Each of these techniques has specific advantages and disadvantages and will allow the obtention of specific size liposomes. Rehydration of liposomes will form a heterogenous mixture of liposomes of different size. If the swelling technique is applied, GUVs will be obtained; however, this procedure is time consuming, and the use of electrodes (electroformation) can be applied to speed the process. On the other hand, the use of sonic force (sonication) or mechanical force (extrusion) can be applied to obtain smaller liposomes. In particular, when applying the extrusion technique by passing the liposome through filters of the different sizes, LUVs and SUVs can be obtained [Routledge et al., 2019]. It has to be taken into consideration that the size of the liposome will determine its curvature of the bilayer, influencing thus the ability of some proteins to bind and will affect lipid packaging. For this reason, the selection of a specific type of liposome has to be evaluated to match the desired application.

As mentioned, liposomes are valuable model membranes because they allow studying the basics of interesting processes that involve biological membranes. Liposome model membranes can be used to study the efficacy of drugs by determining their partition coefficient, measuring thus the amount of drug that is able to penetrate into the lipid membrane [Peetla et al., 2009]. Moreover, liposomes can be used to determine the amount of drug transported into cells, as well as their mechanism of transport [Baciu et al., 2006]. Another application of liposomes is studying the mechanism of toxicity of some drugs, specifically at known toxic *in vivo* concentrations [Gruszecki et al., 2003].

For the studying of the properties of peptide-lipid interactions when using liposomes, such as the ones detailed previously, several techniques can be applied; these techniques are specified in **Figure 27**.

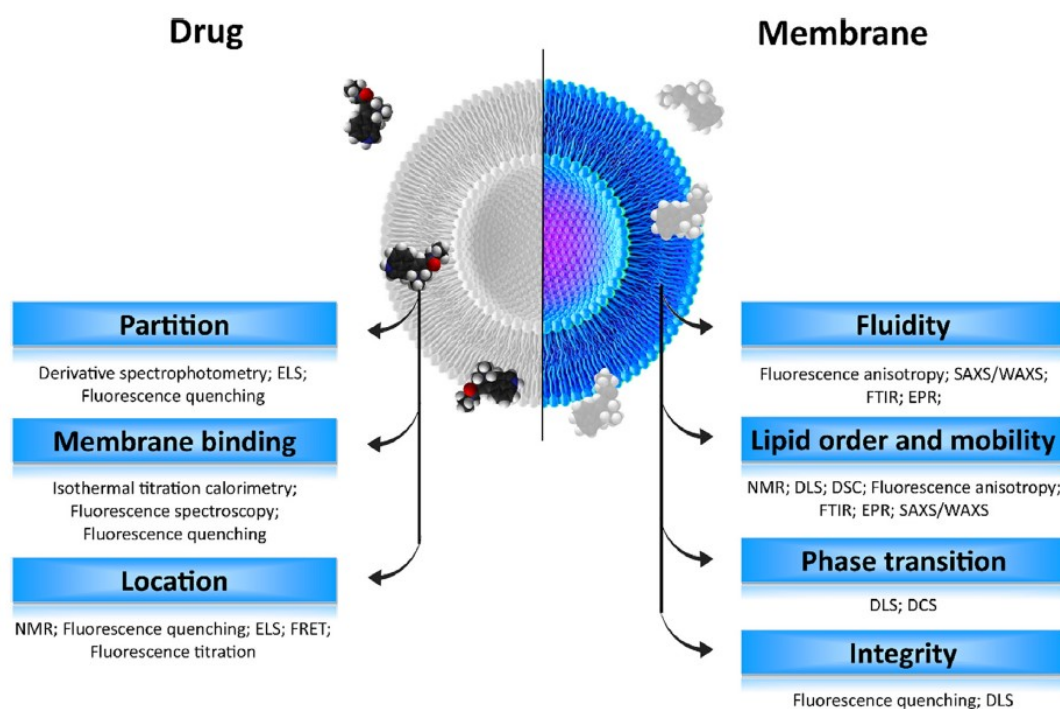


Figure 27. Most studied biophysical parameters, and respective techniques applied to liposomes as *in vitro* membrane models. DLS: Dynamic light scattering; DSC: Differential scanning calorimetry; ELS: Electrophoretic light scattering; EPR: Electron paramagnetic resonance; FRET: Fluorescence resonance energy transfer; FTIR: Fourier-transform infrared spectroscopy; NMR: Nuclear magnetic resonance; SAXS: Small angles X-ray scattering; WAXS: Wide angle X-ray scattering. Figure taken from Andrade et al., 2021.

3.2.3.5. Biophysical evaluation of the interaction of colistin analogues with the lipid membrane

Biophysical evaluation of the membrane interaction of the antimicrobial peptides was carried out by using monolayers and liposomes of different physiologically relevant compositions.

Composition of monolayers and liposomes was selected depending on the membranes they mimic:

- POPG was used to emulate Gram-positive cytoplasmic membrane.
- POPE/POPG (6:4) was used to emulate Gram-negative cytoplasmic membrane.
- LPS was used to emulate the external envelope of Gram-negative bacteria.
- POPC was used to emulate the membrane of eukaryotic cells.

Specifically, Langmuir monolayers at the air/water interface were used to study the kinetics of insertion of the different colistin analogues depending on the lipid compositions.

On the other side, unilamellar liposomes were prepared via extrusion method and used to characterize the interaction between synthesized colistin analogues with the lipid membranes by applying mainly fluorescence-based techniques. Specifically, the biophysical techniques carried out included light scattering determination, Förster resonance energy transfer assays, and peptide-induced leakage of aqueous vesicle contents.

The details of each assay are explained in the following sections, together with the obtained results.

3.2.3.5.1. Monolayers of Langmuir

Monolayers of Langmuir were obtained by depositing the amphipathic lipids on the surface of an aqueous solution, obtaining a superficial film or monolayer at the air/water interface. Since the lipid is insoluble in the aqueous subphase (which is polar), this determines the orientation of the molecule with the polar headgroups in contact with the solvent and the acyl chains oriented to the air phase, away from the solvent. Briefly, monolayers of POPG, POPE/POPG (6:4), POPC and LPS were formed by applying small drops of the lipid stock solutions in chloroform on an aqueous subphase until achieving a surface pressure of $32 \text{ mN}\cdot\text{m}^{-1}$, as described in **section 5.3.4.2.**, in order to emulate the turgency of a cell membrane. Once the monolayer pressure was stable, the peptides were injected into the subphase from a stock solution in water, and the increase of surface pressure was monitored over time. Obtained results for each peptide and lipid composition are shown in **Figure 28**, whereas **Table 11** details values obtained 25 minutes after peptide injection.

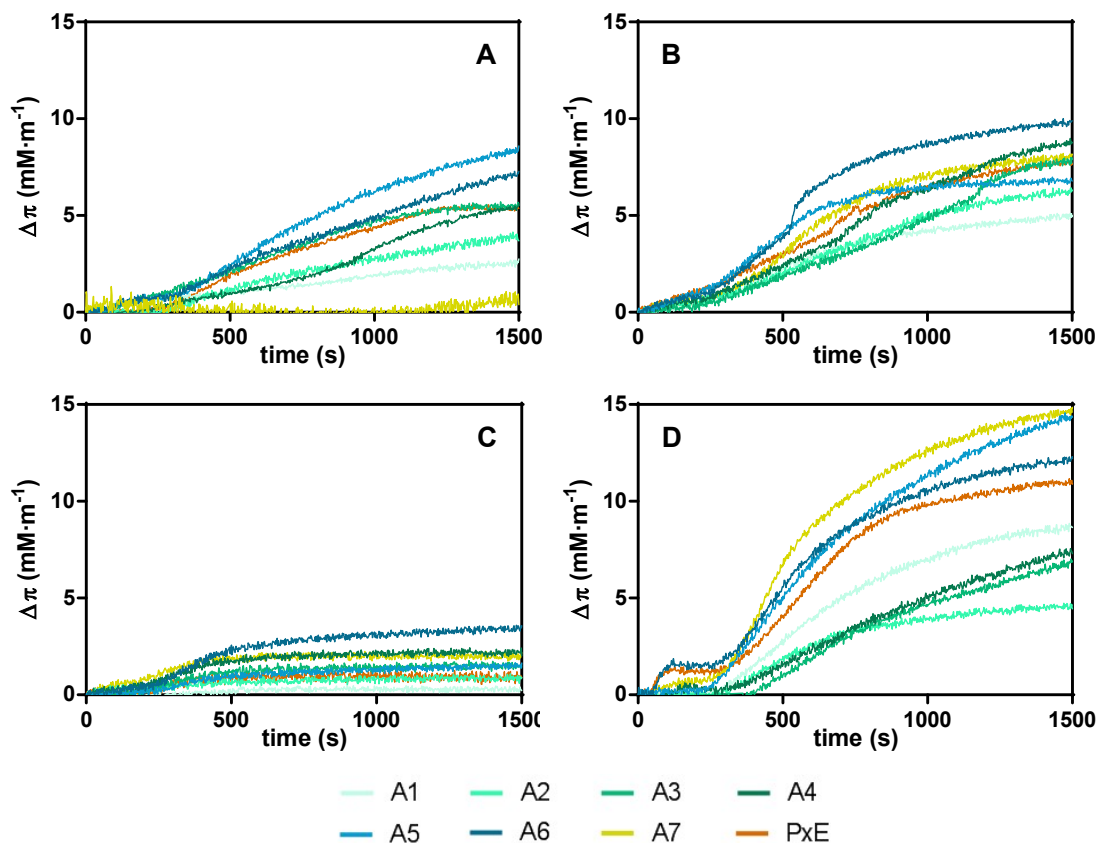


Figure 28. Variation in surface pressure ($\Delta\pi$) of the monolayers of different composition: A) POPG, B) POPE/POPG (6:4), C) POPC, D) LPS, as a function of time after injection of colistin and colistin analogues. Initial surface pressure $32 \text{ mN}\cdot\text{m}^{-1}$. Peptide concentration in the subphase $0.48 \text{ }\mu\text{M}$.

Table 11. Increase in surface pressure ($\Delta\pi/\text{mN}\cdot\text{m}^{-1}$) upon penetration of the antimicrobial lipopeptides into monolayers at an initial pressure of $32 \text{ mN}\cdot\text{m}^{-1}$ and measured 25 minutes after peptide injection.

Composition	Compound							
	A1	A2	A3	A4	A5	A6	A7	PxE
POPC	0.4	0.8	1.3	2.2	1.5	3.5	2.1	0.8
POPG	2.4	4.0	5.6	5.5	8.6	7.3	0.8	5.3
POPE/POPG	5.0	6.4	7.9	9.1	6.8	9.8	8.2	7.9
LPS	8.8	4.6	7.1	7.6	14.7	12.4	14.8	11.1

It can be observed that all the studied peptides present a high affinity for the LPS monolayer, which in fact is a must-have quality for the mechanism of action on bacteria, since it is well known that polymyxins must bind to LPS as a necessary first step for antimicrobial activity. Furthermore, all peptides also insert into monolayers of POPE/POPG, a model of Gram-negative inner membrane, which is also a target for natural polymyxins. In general, the longer the peptide acyl chain, the higher the

surface pressure increase, indicating that not only the electrostatic interaction is important for binding, but also the length of the fatty acid facilitates the insertion of the lipopeptide into the monolayer, parallel to the phospholipid acyl chains.

On the other side, results with monolayers of POPG, a mimic of Gram-positive membrane, show increases in surface pressure that are comparable to the mixed PE/PG monolayer, indicating that the electrostatic interaction between the positively charged peptides and the anionic phospholipids are mostly responsible for the interaction.

Finally, there are very low levels of insertion of the peptides into POPC monolayers, a model of eukaryote membrane, albeit this is slightly higher for long fatty acyl chain peptides. These results indicate low affinity to bind this particular membrane model, and are consistent with the low levels of haemolysis induced by the peptides at similar concentrations, as previously discussed.

3.2.3.5.2. Aggregation and fusion of vesicles induced by the peptides

It is well known that natural polymyxins, both PxB and PxE, bind to anionic vesicles and induce the formation of small clusters where peptide-mediated vesicle-vesicle contacts are formed [Cajal et al., 1995]. To determine if the synthetic analogues have also this way of action, two experiments were conducted, one based on the changes in the intensity of scattered light to detect changes in particle size, and another based on the fluorescence resonance energy transfer (FRET) between two probes located in different populations of vesicles.

The 90° light-scattering assay gives information on the induction of aggregation of vesicles upon addition of the peptides. If the peptides provoke the formation of contacts or the aggregation between vesicles, this will result in an increase on the size of the particles, which can be measured as an increase in light scattering [Zimmerberg et al., 1993]. On the other side, detecting a decrease in light scattering tends to point towards the peptide acting as a detergent, lysing the vesicles with the formation of smaller sized particles such as micelles. In this experiment, vesicles of different lipid compositions were used.

The peptides were added in small aliquots from a stock solution in water to a suspension of vesicles in 10 mM Tris buffer pH 7.4, and the changes in turbidity at 360 nm were recorded as a function of time.

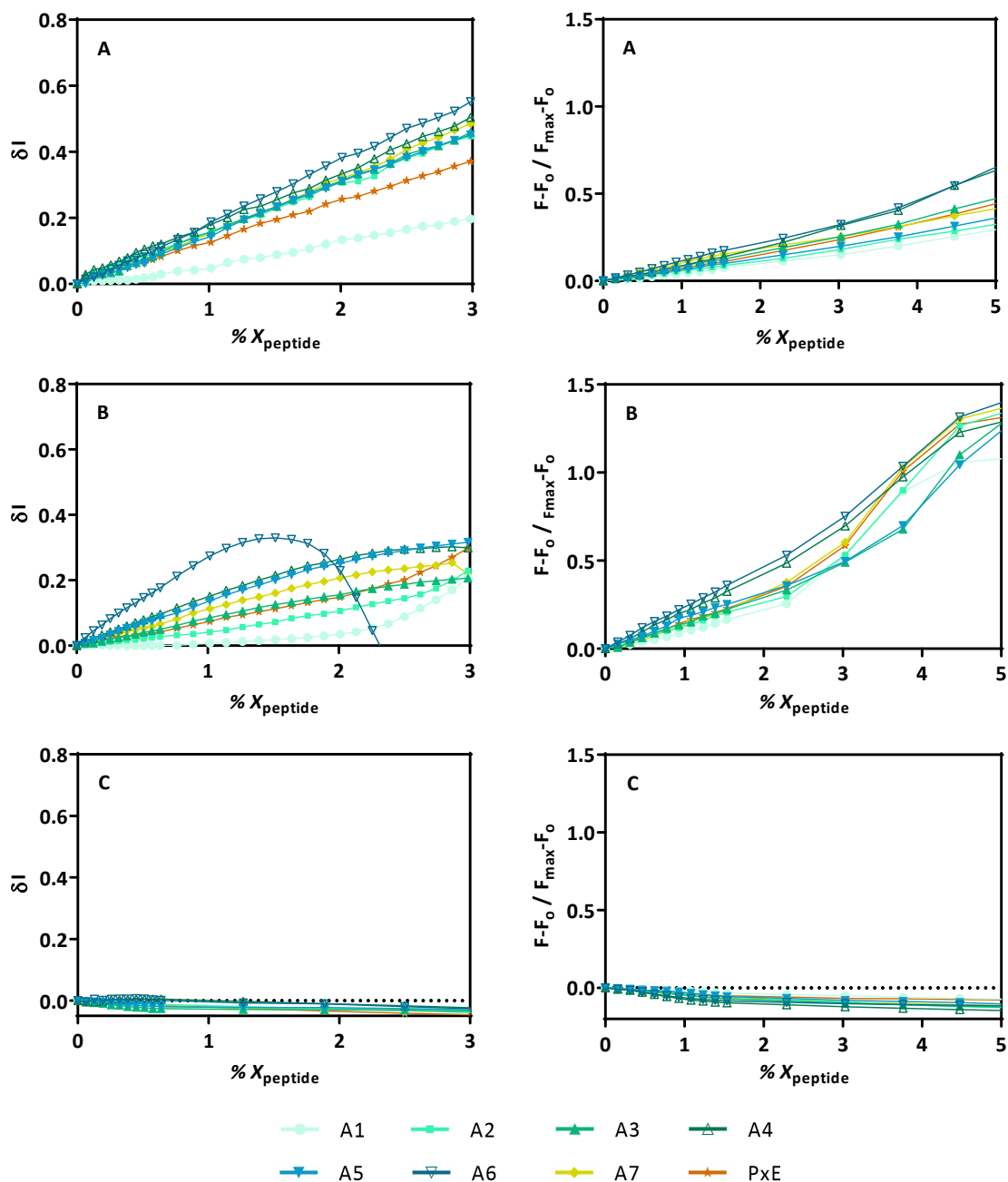


Figure 29. Effect of colistin and colistin analogues on the intensity of scattered light (left column) and FRET assay (right column) with liposomes of A) POPG, B) POPE/POPG and C) POPC, with the different peptides #A1-#A7, using PxE as control.

Results are shown in **Figure 29** (left column), and clearly indicate that all of the colistin analogues as well as the parent peptide cause a concentration-dependent increase in particle size, consistent with the induction of aggregation, on anionic vesicles, both POPG and mixed PE/PG. The peptides showing more increase in

scattering, indicating a bigger particle size, are those with the longest fatty acyl chain, #A4 and #A6 (12 carbons), with slightly more effect when having the Nle residues instead of the Leu (#A6). These results also rule out a possible detergent or lytic effect on the anionic vesicles. At high peptide concentrations on the membrane, the aggregates formed are so large that they precipitate in the cuvette, as one can see with the naked eye as a white precipitate. This is the reason that in some cases a decrease in scattering signal is seen, but this is not relevant since it only happens at peptide concentrations well above the MIC.

Finally, none of the peptides induced aggregation of the POPC vesicles, modelling eukaryotic membranes, even at high peptide concentration, up to 3 mol%.

Fluorescence resonance energy transfer experiments were designed to determine peptide-induced vesicle-vesicle aggregates and lipid mixing, due to hemifusion. This method is based on the non-radiative transfer of the excited state energy from NBD-PE (donor probe covalently coupled to the phospholipid) to Rh-PE (acceptor probe, also covalently coupled to PE). Both probes have a Förster distance of 5 nm, so when they are incorporated at 0.6% in separate vesicle populations and mixed in a 1:1 proportion, no FRET signal is detected because the distance is too big for FRET to take place. Then, successive aliquots of peptide were added from a stock solution in water, and changes in the intensity of emission of acceptor fluorescence are monitored over time upon donor excitation. Any increase in this signal will indicate that NBD and Rh are in close proximity on the membrane, allowing for FRET to take place.

Results shown in **Figure 29** (right column) are consistent with the scattering changes: on anionic PG and PE/PG vesicles, all the colistin analogues induced a concentration-dependent increase in FRET, indicating the formation of clusters of vesicles and possibly the exchange of phospholipids between those vesicles due to the formation of peptide-mediated vesicle-vesicle contacts, as it is described for polymyxins. The effect is seen from very low concentrations of peptide on the membrane, and the increase in fluorescence is almost linear up to ≈ 2 mol% of peptide. Above this concentration, FRET increases more significantly, however the

signal after each peptide addition is not stable, and fluorescence emission increased with time, an event that is attributed to unspecific fusion of membranes.

As expected, none of the analogues had any effect on zwitterionic POPC vesicles, even at high concentrations.

3.2.3.5.3. FRET experiments to detect membrane fusion

In another experimental design, we performed a FRET assay with liposomes co-labelled with NBD-PE as a donor molecule, and Rh-PE as acceptor. In this case, co-labelled vesicles had a very efficient FRET, due to the fact that both donor and acceptor are in the same membrane. The experiment consists in mixing these vesicles with a 100-fold excess of unlabelled vesicles of the same lipid composition. Before peptide addition, no change in FRET signal is detected since labelled and unlabelled vesicles do not interact. Once the different peptide analogues are added to the vesicle mixture, one can see a clear decrease in the intensity of rhodamine fluorescence emission (**Figure 30**), clearly indicating that vesicles are not only aggregated, but that lipids are being exchanged between vesicles, allowing surface dilution of the probes and thus a decrease in FRET.

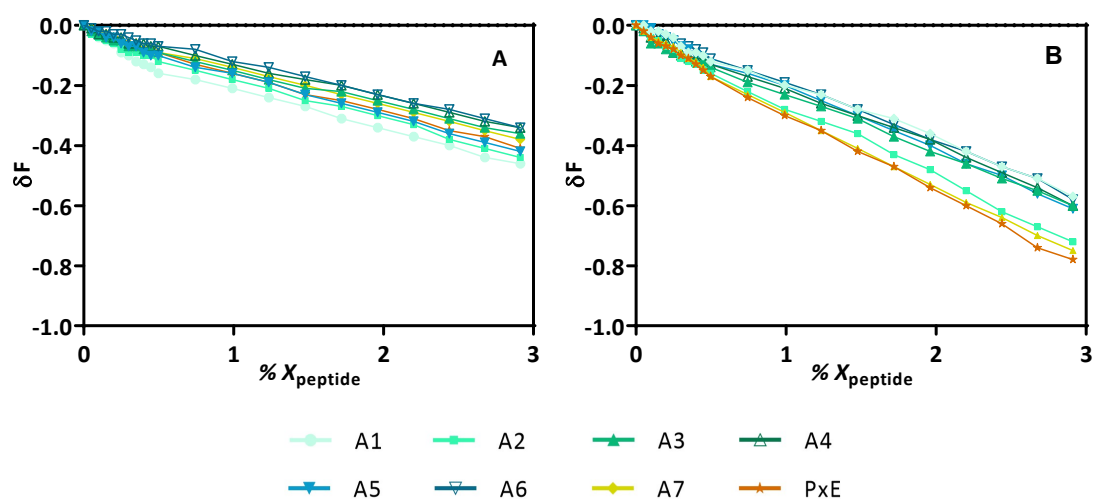


Figure 30. FRET Fusion assay with liposomes made of a) POPG and b) POPE/POPG, when adding the peptides.

Fusion is observed in both POPG and POPE/POPG vesicles, however in the Gram-negative membrane model (POPE/POPG) the amount of fusion for the same peptide concentration is higher than in the Gram-positive one (POPG), which is consistent with the results obtained in the previous assays. When comparing

between the different analogues, however, only remarkable differences were observed at the POPE/POPG model, as peptides PxE, #A7, and #A2 showed more fusion potential than other analogues. No relevant differences were observed in neither of the rest of peptides on POPE/POPG membranes, nor generally in POPG membranes.

3.2.3.5.4. Permeabilization of the lipid membrane induced by the peptides

Many AMPs are described to permeabilize lipid membranes, causing the leakage of aqueous contents. This can be due to a detergent effect, causing the loss of bilayer structure and lysis, due to the formation of channels or pores, or even by transient destabilization of the membrane if the peptide simply translocates the lipid bilayer and enters the cell. One first approach to determine if a peptide can cause leakage is to use liposomes of the desired composition encapsulating fluorescent probes.

In our case, the leakage assay is based on the use of synthetic liposomes encapsulating a fluorophore and a quencher of fluorescence. After the liposomes are exposed to a sufficiently high concentration of specific peptides, their membranes are partially disrupted, which provokes a leakage of the compounds to the external medium. This event triggers the dilution of fluorophore and quencher, which can be measured as an increase in fluorescence of the sample or % leakage [Wimley, 2015].

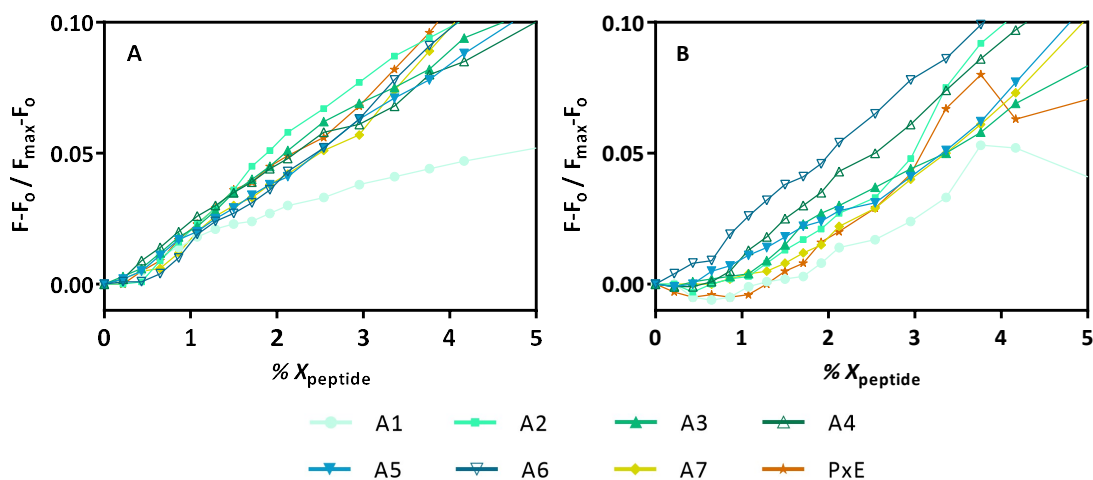


Figure 31. Graphic representation of the leakage of the dye ANTS coencapsulated with DPX in liposomes of: A) POPG, and B) POPE/POPG, as a function of peptide mole fraction.

This assay was carried out co-encapsulating ANTS (as fluorophore) and DPX (as quencher) probes into vesicles of different lipid composition, and measuring the fluorescence variation induced by the titration of peptides.

As shown in **Figure 31**, all peptides induce a concentration-dependent leakage from both POPG and POPE/POPG vesicles (models of Gram-positive and Gram-negative bacteria, respectively).

In the case of POPG vesicles, #A1, the peptide with the shorter fatty acyl chain induced significantly less leakage than the ones with longer acyl chains; however, no differences were observed between them, which induced a similar level of leakage than colistin.

In the case of POPE/POPG vesicles, peptides with longer fatty acyl chains generally induced a higher degree of permeabilization.

It is important to notice that in all the peptides, leakage is almost inexistent at low mole fractions, for example below 0.5 mol% in POPG, but more importantly below 1 mol% in POPE/POPG vesicles. This is also the case with colistin, and indicates that at this low concentration of the peptide in the membrane, leakage is not relevant.

Comparing both lipid compositions, it has to be pointed out that #A6 analogue, one of the analogues with the longest fatty acyl chain (12 carbons), presents more specificity for POPE/POPG than for POPG, which is consistent with the polymyxins activity, presenting more affinity towards Gram-negative models.

3.2.4. TRANSMISSION ELECTRON MICROSCOPY (TEM)

Transmission electron microscopy (also known as TEM) is a microscopy technique that consists in a beam of electrons that is transmitted through a sample to form an image. This sample is usually a section of very thin thickness (thinner than 100 nm or a suspension). The beam of electrons forms an image after interacting while being transmitted across the sample, which is amplified afterwards. The image is focused onto an imaging device, like a fluorescent screen, a layer of photographic film, or a sensor [Franken et al., 2020].

Due to using electrons instead of photons, which have a much shorter wavelength, the TEM technique allows us to visualize images at a much higher resolution than microscopes which are based on light. Therefore, TEM allows us to capture small structures or formations, such as single columns of atoms [Franken et al., 2020].

As already mentioned, polymyxins mainly target the cytoplasmic membrane of bacteria. For this reason, perhaps one of the most interesting assays to conduct in this case is the transmission electron microscopy. On contrast to the light microscopy, the electronic one allows us to appreciate the effects of antibiotics in the subcellular level. In this case, TEM lets us qualitatively observe the effects of the diverse peptide analogues on the cytoplasmic membrane.

For the assay, only the #A2 and #A3 peptides were used, which were the most effective that had not shown high levels of haemolysis (which is used as a first cytotoxicity indicator). As our objective was to appreciate the effects of the peptides on the membrane, we opted for not using exactly the MIC value, but 2/3 or it. The rationale is that using exactly the MIC may impair the cytoplasmic membrane far too much, which would make comparing the different conditions impossible.

As for the bacteria strains used, only *E. coli*, *P. aeruginosa*, and *S. aureus* were included; *A. baumannii* was dropped because in the MIC assays none of the peptides could inhibit its growth at any concentration.

Representative TEM images of bacteria taken after incubation with synthesized colistin analogues are detailed in **Figure 32**.

It can be observed that under control conditions (images a, b, and c), bacteria present a normal morphology with no damage to structures and membranes. However, once we treated *E. coli* and *P. aeruginosa* with the #A2 peptide at 2/3 MIC values, ($21 \mu\text{g}\cdot\text{mL}^{-1}$ and $5 \mu\text{g}\cdot\text{mL}^{-1}$ respectively), both bacteria showed important alterations in their membranes. In both cases, blebs of membrane protrusions are formed, and in some cases breakage of the outer membrane is clearly seen, with leakage of intracellular contents, which can be observed as little vesicles around the bacteria.

For *S. aureus* we used the #A3 peptide, but even though at high concentration there was inhibition of its growth in the MIC assays, this inhibition either is too small to be observed at 2/3 MICvalue ($11 \mu\text{g}\cdot\text{mL}^{-1}$) or takes place by using a pathway different for *S. aureus*. Another possibility could be that the structural properties of the Gram-positive bacteria *S. aureus* make difficult to observe the effects on its membrane, as the cell wall of Gram-positive bacteria is significantly thicker than Gram-negative bacteria.

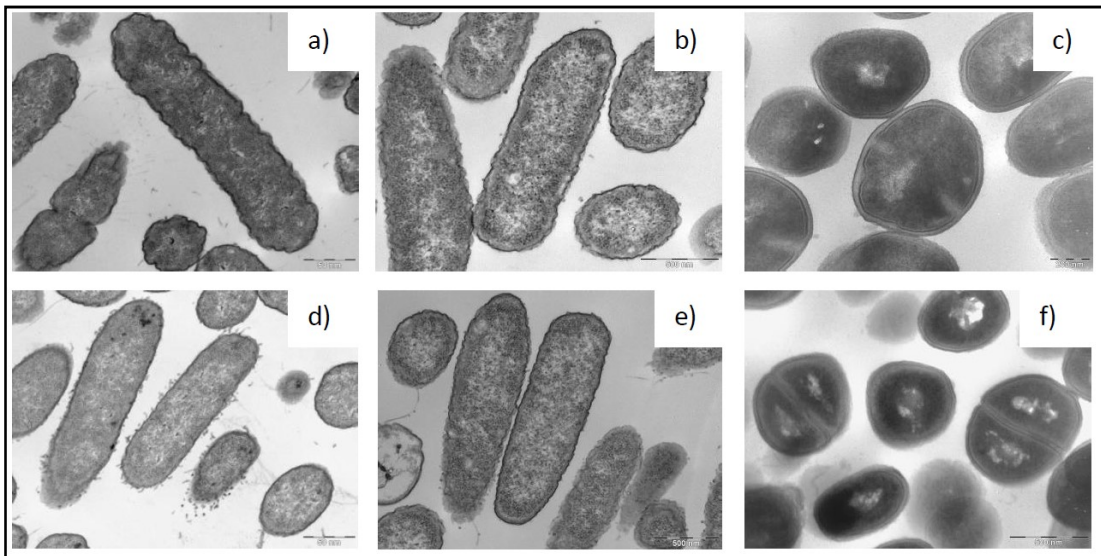


Figure 32. Images captured via TEM: a) Untreated *E. coli*; b) Untreated *P. aeruginosa*; c) Untreated *S. aureus*; d) *E. coli* treated with #A2 ($21 \mu\text{g}\cdot\text{mL}^{-1}$); e) *P. aeruginosa* treated with #A2 ($5 \mu\text{g}\cdot\text{mL}^{-1}$); f) *S. aureus* treated with #A3 ($11 \mu\text{g}\cdot\text{mL}^{-1}$).

3.3. SERIES B

3.3.1. *IN VITRO* ANTIMICROBIAL ACTIVITY

Similar to the Series A analogues, we wanted to start the study of the Series B peptides by measuring the MIC values against some bacteria.

Results of the assays performed for Series A peptides pointed towards analogues being mostly inactive against Gram-positive bacteria except for the molecules with long fatty acyl chains. Sequences in Series B peptides have all in common a short fatty acyl chain. Therefore, we decided to keep *S. aureus* out of the assays for Series B, and the only strains used for the MIC assay were *E. coli*, *P. aeruginosa*, and *A. baumannii* as Gram-negative bacteria. MIC determination was done by triplicate for each peptide and using bacteria in the pre-exponential phase; the obtained results are detailed in **Table 12**.

Table 12. MIC values in $\mu\text{g}\cdot\text{mL}^{-1}$ for peptides in Series B against *E. coli*, *P. aeruginosa* and *A. baumannii*.

Peptide	<i>E. coli</i>	<i>P. aeruginosa</i>	<i>A. baumannii</i>
PxE	0.5	2	2
B1	4	4	2
B2	4	2	>32
B3	2	2	4
B4	4	2	8
B5	1	2	2
B6	4	2	16
B7	2	2	8
B8	16	4	>32
B9	2	4	>32

Peptides from Series B show a high antibiotic activity towards Gram-negative bacteria in general. Specifically, analogues #B3, #B5, and #B7 have a MIC close to and sometimes equal to that of PxE. Therefore, these results suggest that peptides with 10-carbon fatty acyl chain DAdec (#B1, #B3, #B5, #B7) are more active than the peptides containing 8-carbon chains, especially for *A. baumannii*. These results are consistent with the ones observed from Series A.

Notably, the addition of the leucic acid, which triggers the formation of an ester within the molecule, instead of the Leu residue in position 7 of natural PxE, seems to improve the activity spectrum of the peptide analogues. This is particularly important when comparing the peptides with leucic acid, #B4/#B5, with those with Leu⁷, #B2/#B3. The inclusion of leucic acid greatly improved the antimicrobial activity of the analogues against *A. baumannii*, a bacteria species which was mostly unaffected by Series A peptides. Furthermore, this substitution also slightly increased the activity against *E. coli*.

On the other side, the substitution of Leu⁷ with Abu⁷ residue did not result in significant improvements in activity, as the respective antimicrobial activity between the pairs #B6/#B7 and #B2/#B3 is almost identical. However, the substitution of Leu⁷ with the Nva⁷ residue resulted in a significant decrease in antimicrobial activity for all the three bacteria species studied, as can be observed when comparing the pairs #B8/#B9 and #B2/#B3. These results suggest that the ramification on the Leu⁷ side chain is relevant for peptide activity in a way that losing only one of the end carbons impairs it. This effect was already observed in Series A analogues with Nle⁷ peptides. On the other side, the loss of both carbons in the ramification has no effect on the activity, as seen with MIC values of Abu⁷ analogues.

Finally, the analogue #B1 only difference with #B3 was the use of a normal Thr (threonine) instead of a Ttr (thiolate threonine) for the cyclization of the ring. This difference did slightly affect the analogue, as it was more active against *A. baumannii* than for the rest of bacteria tested in comparison with #B3.

As a summary, Series B peptides emulating the 8-carbon fatty acyl chain of PxE plus Dab residue with a DAdec yielded promising activity results against Gram-negative bacteria, especially when substituting the Leu in position 7 by a leucic acid. The activity shown, albeit very similar to PxE, has brought hope that an active analogue with less side-effects and potentially easy to mass-produce can be feasible. On the contrary, other changes to the residue 7 seemed to worsen the antimicrobial activity or brought no noticeable benefit for the bacteria species tested.

3.2.3. *IN VIVO* ASSAYS

As previously shown, the Series B peptides had promising activity profiles, with especial mention to the analogues #B2, #B3, #B4, and #B5. These analogues had the cyclization performed through a thiolate threonine, while some of them presented either an octanoyl or DAdec tail; and an amide or ester bond between residues 6 and 7.

Given the positive results obtained from some of the Series B peptides, it was decided to skip some of the previously assays performed for Series A. Therefore, *in vivo* assays were performed using analogues #B2, #B3, #B4, and #B5.

In vivo assays are the epitome of drug research. *In vitro* assays help streamlining research, providing very important data via a wide array of different techniques, which results in massive screening potential. However, for drugs or medicinal products to be considered as suitable for human use they must be tested in animal models first.

For that reason, the pre-clinical development process of drugs needs to include assays conducted on living animals. Amongst other assays, the most important ones are the pharmacokinetics (PK), the general toxicology study, and the safety pharmacology (focused on central nervous systems, cardiovascular, respiratory, and renal). Of the tests mentioned, the PK and the toxicology need to be conducted in at least two animal species: 1 rodent and 1 non-rodent animal [ICH guideline].

As the bulk of preclinical assays to be conducted is very expensive, it was decided to prioritize the ones that provided the most information: the PK, to assess how the organisms metabolize the peptide analogues and excrete them; and the nephrotoxicity, which is the main toxicity event triggered by polymyxin analogues. Once these two parameters are completely understood, then additional assessments can be performed.

Therefore, *in vivo* assays for pharmacokinetics and nephrotoxicity were conducted using peptides #B2, #B3, #B4 and #B5. These assays allowed to better understand the effect of the different analogues on living animals. Due the expertise needed for conducting these type of assays, *in vivo* experiments were

performed in collaboration with Dr. Javier González Linares in *Centre de Recerca en Toxicologia (CERETOX)*, in the *Parc Científic de Barcelona*.

3.2.3.1. Nephrotoxicity

The kidneys are crucial organs in the animal metabolism: blood is received in the kidneys, where it is filtrated to promote the removal of xenobiotics (a chemical substance within the organism that is not expected to be present within it) and excretion of compounds. The nephrotoxicity is the capability of a substance or compound to cause toxic effects in the kidneys and affect their function during this filtration work. The substances leading to nephrotoxicity can be toxic chemicals, medications, or even some components found in food (such as lead or mercury salts in fish) and they usually cause it due to accumulation in the kidneys [Weber et al., 2017].

Nephrotoxic compounds can be classified in several categories depending on how they affect the renal system:

- Cardiovascular effect

Drugs or substances that have an effect in increasing or decreasing the blood pressure. These compounds generally augment or decrease the diuresis capabilities of the kidneys (compounds known as diuretics or antidiuretics) or have an effect in the width of blood vessels (vasodilators and vasoconstrictors). Examples of such are β -blockers and angiotensin-converting enzyme inhibitors, respectively [Freemantle et al., 1999; Bangalore et al., 2017].

- Direct tubular effect

Substances that have a direct effect in renal tubules, which are the functional units of kidneys. Renal tubules have the function of modifying the composition of excreted liquid by reabsorbing useful substances and secreting unwanted ones [Chinard, 1964]. Substances in this group disrupt the tubular tissue, which impairs the kidney ability to modify the composition of urine. This group is further divided between compounds which disrupt the proximal convoluted

tubule (e.g., aminoglycoside antibiotics [Chinard, 1964]), those that affect the distal tubule (e.g., Nonsteroidal anti-inflammatory drugs such as ibuprofen [Bally et al., 2017]), and finally those that cause tubule obstruction (e.g., sulphonamides, due to low solubility, may crystallize in the tubules, obstructing them [Prien, 1945].

➤ Interstitial nephritis

Substances that cause inflammation of the kidney areas known as renal interstitium. Renal interstitium is made of different kinds of cells, extracellular matrix, and fluid surrounding renal tubules; and it is meant to act as scaffolding support for the tubules, as well as participate in fluid and electrolyte exchange [Zeisber & Kalluri, 2015]. Examples of compounds causing interstitial nephritis in an acute fashion include several antibiotics such as β -lactam and sulfonamides, as well as the anti-seizure medication phenytoin [Rossert, 2001; Pusey et al., 1983; Brewster & Rastegar, 2014]. On the other side, exposure over long time to compounds like lithium salts can cause chronic interstitial nephritis [Nielsen et al., 2008].

➤ Acute glomerulonephritis

Substances that cause inflammation and disruption of the glomeruli, which are the filtering units which initiate the nephron, containing the tubules. Lesions to the glomeruli are very rare and are usually linked to immune pathways instead of drug toxicity. Examples of this group include heroin [Dettmeyer et al., 2005].

➤ Diabetes insipidus

Substances that cause diabetes insipidus to organisms. Diabetes insipidus is known as an increased amount of urine and thirst, as high as 20 litres per day, and is caused by dysregulation on several hormone pathways, such as vasopressin or the hypothalamic thirst mechanism [Saborio et al., 2000]. Examples of such include demeclocycline and HIV-treating drug foscarnet [Goh, 2004; Navarro et al., 1996].

➤ Other nephrotoxic compounds

Other compounds do not fit with the categories described but are able to cause toxic effects to the kidneys, such as salts base on lead, mercury, and cadmium [Abyar et al., 2019], as well as some plant-based supplements like aristolochic acid [Shaw, 2010].

3.2.3.1.1. Nephrotoxicity assessment

For the assessment of the peptide nephrotoxicity of the analogues #B2, #B3, #B4 and #B5, mice were used as a rodent model. Peptides were administered, repeatedly, via subcutaneous injection for regular period times. These series of administrations, detailed in **section 5.4.4.1**, allowed maintaining the concentration of the analogues in the animal blood as long as possible in toxic levels. As a negative control saline solution was used, while Polimyxin (PxB) at high concentration was used as a positive control for nephrotoxicity, as it has long been described to exhibit such toxicity [Zavascki & Nation, 2017].

Blood extractions allowed the determination of biochemical parameters (blood urea and blood creatinine), while kidney extractions were used for histopathological analysis to observe under a microscope the effects of the colistin analogues. Some examples of the histopathological analysis are detailed in **Figure 33**.

While observing the microscope preparations of the kidneys obtained from the nephrotoxicity assay, many histopathological signs were identified in the tissue: cell vacuolization, tubular necrosis, urinary cylinders, cell desquamation, and oedema of tube cells. For each of these parameters, a value from 0 (inexistent) to 4 (predominant) was assigned, depending on how common they were at the samples of a given combination of compound and dose.

The mean between the different histopathological values for a given combination of compound and dose was calculated within the same animal. The mean value obtained in this manner is named Animal Score (AS), and it was representative of the nephrotoxicity shown by the specific animal. Afterwards, the mean between the AS of all the animals for a given condition was calculated, obtaining thus the Group Score (GS). GS is the relative representation of how

nephrotoxic a peptide at a given concentration is in comparison with other conditions.

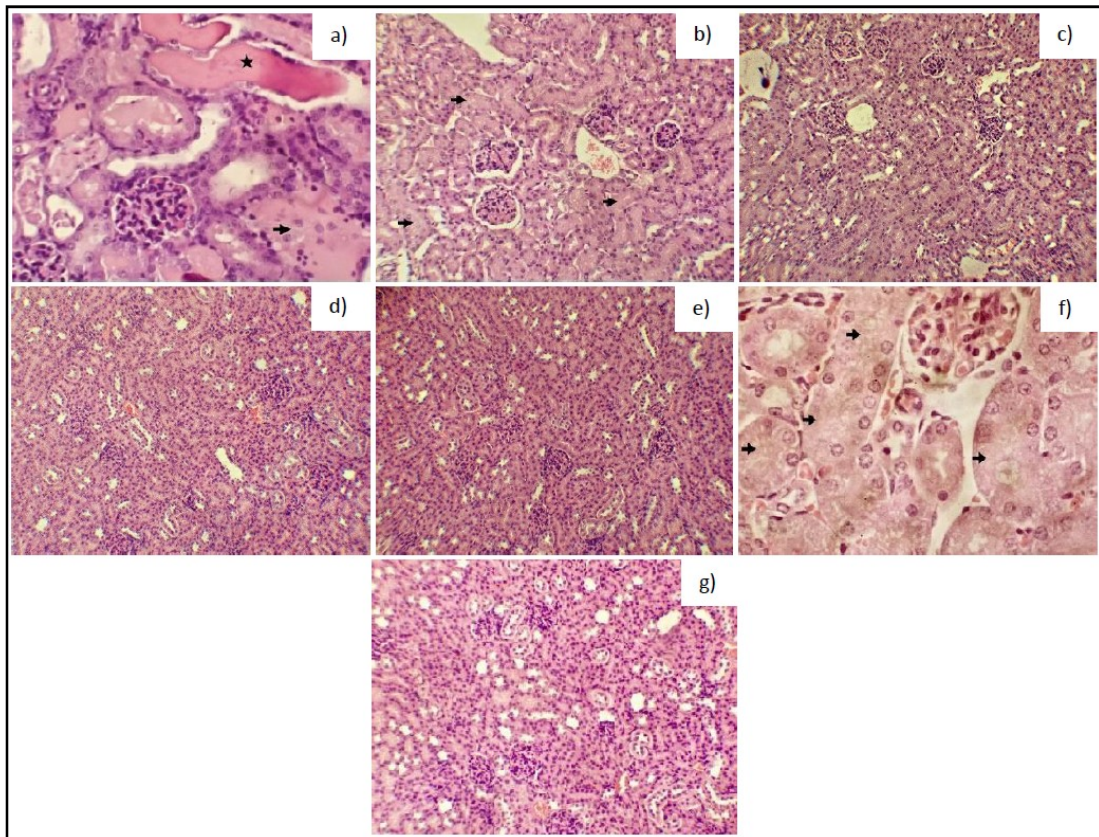


Figure 33. Representative pictures of bright field optical microscope of the kidney preparations dyed with hematoxylin/eosin. The animals had been previously treated as follows: a) Peptide #B2; b) Peptide #B3; c) Peptide #B3 at low concentration; d) Peptide #B4; e) Peptide #B5 at low concentration; f) PxB at high concentration; g) Saline solution. Arrow = Tubular cells oedemas; Star = Urinary cylinders.

In **Table 13**, GS obtained for all peptide and dose combinations are collected, as well as the mean values of blood urea and blood creatinine obtained after analysing. Unlike other conditions, though, during the repeated dosage with PxB at $20 \text{ mg}\cdot\text{kg}^{-1}$ concentration, the animals died or were euthanized before the end of the assay because of the effects of the compound. As the animals were unable to complete the treatment, the blood samples could not be obtained, and for that reason they are not presented.

Table 13. Results for the experiments of the nephrotoxicity study at the different concentrations assayed. ^aAlthough the planned total dose for PxB at high concentration was 120 mg·kg⁻¹, due to the death of the animals, the total administered dose was lower.

Compound	Dose (mg·kg ⁻¹)	Total Dose (mg·Kg ⁻¹)	Group score	Blood urea (mg·dL ⁻¹)	Blood creatinine (mg·dL ⁻¹)
B2	12	72	4.1	91.1	0.34
B3 (high c.)	12	72	1.0	47.8	0.19
B3 (low c.)	8	48	0.2	44.0	0.20
B4	12	72	0.0	31.7	0.17
B5	12	72	0.0	32.3	0.16
PxB (low c.)	12	72	3.4	42.6	0.24
PxB (high c.)	20	120 ^a	6.4	-	-
Saline	0	0	0.0	41.5	0.16

After reviewing the results from the nephrotoxicity assay, it can be observed that animals treated with saline (negative control) show no affectations to kidney tissue (GS = 0.0). In the same manner, the blood urea and creatinine for those animals are within normal values (41.6 and 0.16, respectively).

On the other side, PxB (positive control) greatly disrupted the renal tissues, as both low and high doses obtain a very high GS (3.4 and 6.4, respectively). Moreover, the high dose ended up with the animals dying even before they finished the series of administration, which is the only condition with this effect.

As for the peptides assayed, peptide #B2 disrupts the renal tissue on a similar level to PxB. This affectation of the kidneys also results in a great increase of the biomarkers for renal activity blood urea and creatinine (91.1 and 0.34 mg·dL⁻¹, respectively). Therefore, peptide #B2 does not improve the safety profile of polymyxins, at least regarding the nephrotoxicity.

On the other side, peptide #B3 at low concentration, as well as peptides #B4 and #B5, showed low levels of histopathologic affectation to the kidneys (GS), hinting that they could be potential antibiotic peptides with reduced or minimal nephrotoxicity. In addition, peptides #B4 and #B5 slightly modify one of the biochemical renal markers (blood urea, specifically) by reducing it.

This reduction in the levels of blood urea could be relevant because a similar decrease has been previously linked to severe affectation of the liver function due

to a decrease in its metabolization activity [Bigot et al., 2017]. The liver tends to be the first metabolization step for several drugs or compounds, so this could be a lead that perhaps the liver is affected by peptides #B4 and #B5. However, this hypothesis would need a hepatotoxicity assay with histopathological analysis before confirming it.

Finally, unlike peptides #B4 and #B5, the peptide #B3 was capable of maintaining the basal levels for both blood urea and creatinine. These results pointed towards #B3 being the best analogue candidate due to its great safety profile regarding nephrotoxicity.

3.2.3.2. Pharmacokinetics (PK)

Pharmacokinetics, usually abbreviated as PK, is the pharmacological study of the fate of substances administered to a living organism. When any xenobiotic compound, such as drugs, pesticides, or food additives, is administered, it is also processed (also known as metabolization) by the organism in different specific organs or tissues. This metabolization aims to modify the compounds so they are more easily removed from the body by the several excretion systems available (urine, sweat, exhalation, etc.) [Breuer et al., 2009].

PK describes how an organism modifies and alters a specific external compound after it has been administered. Substances are administered in a pharmaceutical formulation that eventually are liberated from (liberation). Afterwards, the liberated substances are absorbed by the organism they were administered to, accessing the blood circulation (absorption) and are distributed or disseminated across the fluids and tissues of the body (distribution). The organism recognises the type of substance absorbed and biotransform or inactivates it through a process known as metabolization. This metabolization aims to turn the substance into metabolites which are more easily to dispose of. Finally, the body excretes the metabolites through one or several excretion processes. The sum of all the different processes since the administration through the excretion are usually known as ADME, or LADME, and are the basis of the PK and are extensively studied during the phase of new drug discovery [Ruiz-Garcia et al., 2008].

All the processes included in LADME can be represented through the use of mathematical formulas to allow for a graphical representation. By using these models, it can be analysed and compared the characteristics of different molecules in order to choose the most suitable one for a given situation [Ruiz-Garcia et al., 2008].

3.2.3.2.1. PK assessment

To allow for the study of pharmacokinetics of #B2, #B3, #B4 and #B5 colistin analogues, an animal experiment with mice (rodent) was developed. In this case, animals were injected only once with the specific compound via subcutaneous, and after the administration, blood was extracted by using one animal per extracting point. As a control, Polymyxin B (PxB) was used. In total, 4 extraction points were conducted in order to plot the analyzed parameters as a function of concentration. Thus, extracted blood was analysed to measure the plasma concentration of every compound, and the different concentrations were plotted in a graphic to visualize the PK curves and obtain their different characteristic parameters. These parameters, shown in **Table 14**, are the following:

- Time of maximum concentration (T_{max}), expressed in hours

The time after administration in which the plasma concentration of the peptide attains the maximum concentration value.

- Maximum concentration (C_{max}), expressed in $\mu\text{g}\cdot\text{L}^{-1}$

The peak plasma concentration of a drug after administration. Once the peptide is administered subcutaneously to the animals, it is slowly absorbed into the blood flow. Parallel to that, the peptide in blood starts being metabolized and excreted by the liver and kidneys. When most of the administered peptide has already been absorbed, the absorption rate drops below the excretion rate, which creates a peak in the concentration per time graphic. That peak is the C_{max} .

- Area under the curve (AUC), expressed in $\mu\text{g}\cdot\text{h}\cdot\text{L}^{-1}$

The definite integral of the curve that describes the variation of a drug concentration in blood as a function of time. This parameter is

useful to compare different drugs or formulations on regards to the amount of tissue or plasma exposure. Therefore, if a drug is rapidly metabolized or excreted, or if it accumulates outside of the blood, the AUC will tend to be low. On the contrary, drugs that are rapidly absorbed or slowly metabolized usually have high AUC. Finally, as AUC represents the systemic exposure of a drug, a high AUC will correlate with a high efficacy for drugs that need to act on a systemic level.

Table 14. Pharmacokinetics parameters obtained for the analogue peptides and PxB.

Compound	Dose (mg·kg ⁻¹)	T _{max} (h)	C _{max} (µg·L ⁻¹)	AUC _{0-t} (µg·h·L ⁻¹)	n
B2	12	1.5	8.14	17.30	2
B3	12	2	12.48	29.44	2
B3	8	2	6.75	15.43	1
B4	12	2	2.41	7.33	1
B5	12	2	8.48	15.68	1
PxB	12	1.5	2.57	5.82	2
PxB	8	1	2.86	8.03	1

First of all, we can see that the PxB control has a really low maximum concentration and AUC. This is consistent with the PxB having a high accumulation in the kidneys and causing nephrotoxicity: as kidneys act as the filters of the blood, if they have a high ease to filter PxB, it is normal that it accumulates there, keeping the maximum concentration low. In the same manner, this also correlates with the nephrotoxic effects of PxB observed in the toxicity assays. On the other side, the low AUC in comparison with other analogues means that the organism of the animal has a low exposition to the peptide on a systemic level. The current results point towards this being a result of the accumulation of peptide in the kidneys. However, an analysis of the kidneys would be needed in order to confirm this hypothesis.

Second, we can see that the maximum concentrations are obtained using peptide #B3. This is true for both the high and low concentration. This also results in both having an extraordinarily high AUC. Having a high AUC means that the body of the animal is exposed to the specific peptide for longer time, which usually

correlates with both higher effect and toxicity. This is consistent with the nephrotoxicity previously described for high concentration of #B3.

On the other side, the analogue #B5 also shows an intermediate AUC value and maximum concentration, which would make it an interesting alternative, if it did not reduce the renal biomarkers tested in the nephrotoxicity assays.

Finally, analogues #B2 and #B4 could be ruled out because of different reasons. Peptide #B2 exhibited high nephrotoxic behaviour, even greater than PxB. Peptide #B4, however, combines a low AUC with the lowering effect on renal biomarkers which were already mentioned for peptide #B5.

In conclusion, all polymyxin modifications assayed seemed to increase the bioavailability (AUC) of the peptide. Amongst the analogues, however, we can appreciate that #B3 had the higher C_{max} and AUC value, pointing towards it being the most effective modification to increase the systemic exposure. These results correlate with the fact that #B3 was the analogue with less nephrotoxic potential in the previous assays. As nephrotoxic effect of polymyxins is usually caused by their accumulation in the kidneys, its reduction suggests that #B3 does not accumulate in the kidneys like other polymyxin analogues.

3.2.3.3. Efficacy

As discussed with the other *in vivo* assays, analogue #B3 exhibited a high bioavailability after its administration in mice, while presumably keeping the characteristic nephrotoxic effects of polymyxins at a minimum. Furthermore, the peptide analogue also exhibited an interesting efficacy towards the most prevalent Gram-negative bacteria. For this reason, the analogue #B3 was chosen as the best candidate for a proof-of-concept experiment in an animal infection model.

Proof of concept (or POC), also known as proof of principle, is the use of a method or experiment to demonstrate the feasibility of a hypothesis, drug, or machine. The main objective of this kind of experiments for drug development is to assess whether to continue working with a specific drug or not (known as point of go/no go). To make that decision, an experiment meant to test whether the analogue was able to reduce the effects of an infection caused by the same bacteria model object of study was conducted.

The basis of this proof-of-concept assay was to conduct an *in vivo* efficacy assay by using a pneumonia model of infection (mice infected with *Pseudomonas aeruginosa* Pa01 and Pa147) with the objective of comparatively assessing the efficacy of PxB, PxE and #B3 analogue. This assay was performed in IBIS (Instituto de Biomedicina de Sevilla), in its Infectious Disease Group led by Dr. M^a Eugenia Pachón Ibáñez. It has to be pointed out that all the bacteria-related assays performed in this section were performed using PxE, whilst *in vivo* assays were conducted using CMS, the PxE prodrug; differences between both molecules are detailed in **Figure 34**. CMS is less toxic than PxE since it is polyanionic, but does not present antimicrobial activity.

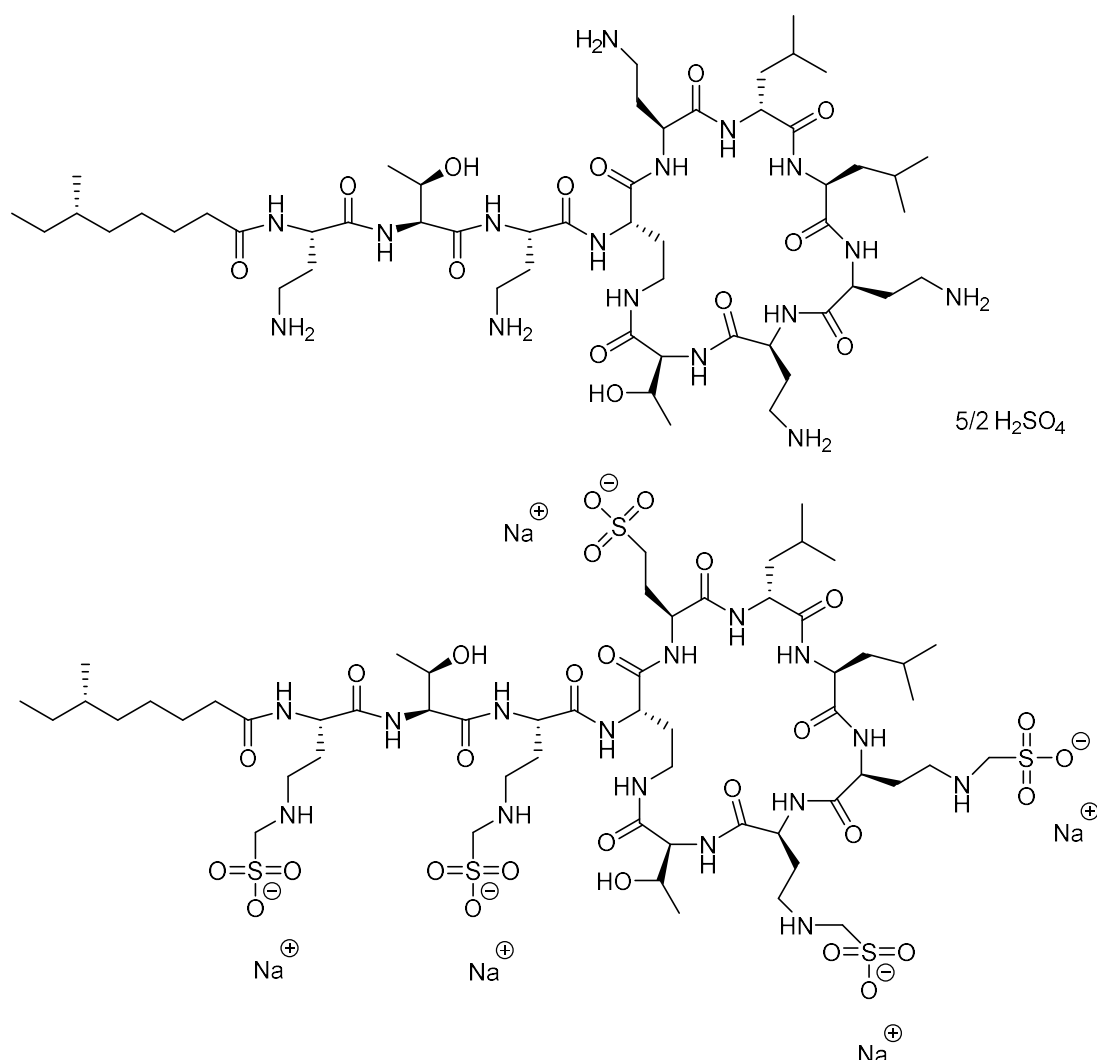


Figure 34. Structures of sodium colistimethate (bottom) and colistin A (polymyxin E1) (top). The molecular weight of colistinmethate is 1749.81 g·mol⁻¹, while for the free base it is 1169.48 g·mol⁻¹.

Determination of MIC and MBC

First of all, we needed to check whether the bacteria were sensible for the treatment with the peptides selected for the efficacy assay. As the bacteria strains used at the IBIS facilities were different than the ones used in our research group, an initial MIC determination of the compounds was carried out to confirm that selected strains were sensitive to them. Bacteria employed at the IBIS facilities were two different strains of *Pseudomonas aeruginosa* labelled Pa01 and Pa147. While Pa01 is a *P. aeruginosa* strain which is a global standard (ATCC 47085), Pa147 is a specific strain developed specifically to be sensible to colistin [Gil-Marqués et al., 2018; Cebrero, 2020].

To check both strains susceptibility to the peptides, the MIC and minimum bactericidal concentration (MBC) values for the analogue #B3 were determined, as well as for the control peptides PxB and PxE. Although the MIC assay had already been conducted previously, it was needed to repeat the experiment in the specific bacteria strains present at IBIS to demonstrate that #B3 was effective against them, as these are the strains that were to be used in the efficacy assays. Results for the MIC and MBC experiments can be found in **Table 15**.

Table 15. Results of the MIC and MBC assays performed at IBIS with *P. aeruginosa* strains Pa01 and Pa147.

Compound	MIC ($\mu\text{g}\cdot\text{mL}^{-1}$)		MBC ($\mu\text{g}\cdot\text{mL}^{-1}$)	
	Pa01	Pa147	Pa01	Pa147
B3	0.5	1	>4	>4
PxB	0.5	0.5	0.5	0.5
PxE	0.25	0.25	1	0.5

As it can be seen, #B3 analogue has a MIC value similar to that of PxB and PxE for the Pa01 strain, while slightly higher for the Pa147 strain. This suggests that the bacteria growth inhibition effect of #B3 is similar to PxB and PxE.

In order to decide whether the peptides could be considered effective against the bacteria, the MIC value had to be equal or lower to the MIC breakpoint for colistin according to the European Committee on Antimicrobial Susceptibility Testing (EUCAST) [EUCAST, 2018]. EUCAST is a well-known committee that from time to time assesses which is the concentration threshold within which bacteria

can be considered as resistant or sensible to a given compound. The MIC breakpoint for colistin is considered as 2 mg/L, we can consider that both strains are sensible to the #B3 analogue, as well as the PxB and PxE controls.

On the other side, #B3 has less bactericidal potential than PxB and PxE, as its MBC value is noticeable higher than the unaltered peptides. Therefore, there is a window between its MIC ($0.5\text{-}1\text{ mg}\cdot\text{L}^{-1}$) and MBC values ($4\text{ mg}\cdot\text{L}^{-1}$), which means that the peptide may be able to inhibit the growth of *P. aeruginosa* but not kill them unless administered at a much higher dose. Further research could help understand whether the #B3 analogue can still make for a good antimicrobial drug [Kłodzińska et al., 2018].

Characterization of lethal model

For the next step, the minimum lethal dose (MLD) for the two *P. aeruginosa* strains had to be determined. The MLD is the minimum dose of a bacterial inoculum needed to cause a 100% mortality using the experimental pneumonia model.

This data was already available at IBIS group, which had already determined the MLD of the two pneumonia strains when inoculated to mice in order to develop a murine pneumonia model [Gil-Marqués et al., 2018]. The previous experiments had demonstrated that $3.5\cdot 10^8\text{ cfu}\cdot\text{mL}^{-1}$ (colony-forming units per milliliter) were needed for the Pa01 strain to cause death on 100% of mice. On the other side, $3.23\cdot 10^9\text{ cfu}\cdot\text{mL}^{-1}$ were needed from the Pa147 strain. Therefore, when we refer to the pneumonia model going forward, we will mean mice treated with the MLD doses here stated.

Efficacy assay

Two pneumonia models, Pa01 and Pa147, that had already been characterized in the past [Gil-Marqués et al., 2018] were used in mice infected intratracheally with the previously calculated MLD dose for each strain. Afterwards, they were treated with the different compounds (PxB, CMS and #B3) via intraperitoneal injection and aseptic thoracotomies (a surgery opening the thorax cavity) were conducted on the animals to extract the lungs; the specific details of the protocol can be found in **section 5.4.4.3**.

From extracted lungs, a quantitative culture was performed. The presence of bacteria of at least 1 cfu deemed the culture as positive, and negative if no bacteria grew in the culture. Blood samples were also obtained and analysed for bacteraemia (bacteria infection in the blood). Finally, the mortality rate of the animals was also monitored for those mice dying or being euthanised before the endpoint.

Results for the efficacy studies done for the Pa01 strain can be seen in **Table 16**, while the time for animal death can be seen in **Table 17**.

Table 16. Results of the efficacy study performed with the bacteria strain Pa01. Control = untreated; Loading B3 = high initial dose of B3 peptides followed by recurrent doses for 24 hours. ^a Significantly better than the Control group; ^b Significantly better than the CMS group.

Group	Treatment	n	Dose (mg·kg ⁻¹ /8h)	Lung culture (cfu·g ⁻¹)	Bacteremia (%)	Mortality (%)
G1	Control	5	-	10.81 ± 0.64	100	100
G2	B3	5	12	7.32 ± 0.22 ^{a,b}	80	100
G3	Loading B3	4	36 + 12	7.12 ± 0.66 ^{a,b}	50	100
G6	PxB	6	12	6.85 ± 0.38 ^{a,b}	33	100
G7	CMS	5	20	9.21 ± 1.42 ^a	100	80

As we can appreciate in **Table 16**, none of the peptides administered was able to reduce the number of cfu in the lung lysates to undetectable levels. As expected, the control condition shows higher levels of bacteria (cfu·g⁻¹) in lungs within all the conditions, as well as the highest level of bacteraemia (bacteria in blood). On the contrary, both the administration of #B3 for 72 hours as well as the loading dose resulted in a significant reduction of cfu in lungs in comparison to both the control condition (p-value = 0.000 for both #B3 and the #B3 loading dose) and PxE (p-value = 0.012 for B3; p-value = 0.001 for #B3 loading dose). The reduction of bacteria in lungs is comparable to that caused by PxB, which is a promising result.

Table 17. Times for animal deaths after being inoculated the Pa01 strain and treated with the peptides. Control = untreated; Loading B3 = high initial dose of B3 peptides followed by recurrent doses for 24 hours.

Group	G1	G2	G3	G6	G7
Mice	Control (n=5)	B3 (n=5)	Loading B3 (n=4)	PxB (n=6)	CMS (n=5)
1	30 h	20 h	10 h	22 h	44 h
2	33 h	22 h	10 h	22 h	44 h
3	43 h	22 h	10 h	23 h	51 h
4	43 h	22 h	10 h	27 h	58 h
5	66 h	33 h		35 h	70 h
6				51 h	

However, looking at the mortality data (**Table 17**), it can be observed that neither #B3, #B3 on a loading dose, nor PxB reduced the mortality of the mice. In comparison, CMS had a reduced 80% mortality rate, which also is not significant enough due to the low group size. This suggests that an adjustment of the dosing should be made by increasing it for an improvement on bacteria clearance and survival. Another notable effect in mortality is that of the loading dose of #B3, which causes the death of all the animals roughly at 10 hours after administration, presumably by overdose. This means that, although the loading dose attains an efficacy similar to the #B3 analogue in the normal dosing, the increased concentration affects much more the survival of the animals. Autopsy of the animals may provide useful information on what the next steps should be and the optimization of the dosing.

On the other side, results for the efficacy studies done for the Pa147 strain are detailed in **Table 18**, while the time for animal death is shown in **Table 18**.

In **Table 18**, it can be appreciated that for the Pa147 strain, like with the Pa01 one, none of the peptides administered reduced the number of cfu in lungs to undetectable levels. As expected, the control condition shows higher levels of bacteria (cfu/g) in lungs within all the conditions, as well as the highest level of bacteraemia (bacteria in blood), but in this case the #B3 analogue in normal dosing also presented 100% bacteraemia. On the contrary, both administration of B3 for 72 hours as well as the loading dose resulted in a significant reduction of cfu in lungs in comparison to the control condition (p-value = 0.007 for B3; and

p-value = 0.011 the B3 loading dose). The reduction of bacteria load in lungs is comparable to that caused by PxB, which is the most efficient one.

Table 18. Results of the efficacy study performed with the bacteria strain Pa147. Control = untreated; Loading B3 = high initial dose of #B3 peptides followed by recurrent doses for 24 hours. ^a better than the control group.

Group	Treatment	n	Dose (mg·kg ⁻¹ /8h)	Lung culture (cfu·g ⁻¹)	Bacteremia (%)	Mortality (%)
G1	Control	5	-	9.52 ± 0.16	100	100
G2	B3	5	12	7.79 ± 0.46 ^a	100	100
G3	Loading B3	5	36+12	7.27 ± 0.59 ^a	40	100
G6	PxB	6	12	6.93 ± 1.37	50	100
G7	CMS	5	20	8.01 ± 3.38	80	80

After observing **Table 19**, it is again apparent that except for CMS, all the conditions ended up with a 100% mortality rate. This represents the same situation as for the Pa01 strain: presumably, the dose is too low, and a potential increase could be helpful in finding the optimal conditions for the treatment in mice. Another potential alternative which could be used in the future are the slow infusions. Slow infusion could keep the peptide concentration in blood relatively constant below toxic levels but over the threshold of activity. Therefore, this could maximize the effect of the molecules. Finally, like with Pa01 strain, the loading dose of #B3 also resulted in a fast death of all the animals. Again, the autopsy was not conducted but may have added some insight into the reasons for the death of the animals.

Table 19. Times for animal deaths after being inoculated the Pa147 strain and treated with the peptides. Control = untreated; Loading B3 = high initial dose of B3 peptides followed by recurrent doses for 24 hours.

Group	G1	G2	G3	G6	G7
Mice	Control (n=5)	B3 (n=5)	Loading B3 (n=4)	PxB (n=6)	CMS (n=5)
1	20 h	20 h	10 h	20 h	20 h
2	20 h	20 h	10 h	20 h	22 h
3	27 h	20 h	10 h	20 h	23 h
4	33 h	20 h	10 h	23 h	35 h
5	35 h	20 h	10 h	33 h	35 h
6				33 h	

In conclusion, colistin analogue #B3 shows some promising effects on bacteria clearance in the lungs, similar to the values of PxB, for both Pa01 and Pa147 bacteria strains. On the other hand, the treatment with #B3 does not improve the mortality rate nor the bacteraemia. The administration using a loading dose of #B3 of $36 \text{ mg}\cdot\text{L}^{-1}$ affects bacteria in a similar way to #B3 in a $12 \text{ mg}\cdot\text{kg}^{-1}$ dosing, while provoking the death of the animals much faster in comparison (10 hours). Therefore, the loading dose does not seem a good method to administer the #B3 analogue. The use of slow infusion could improve the effect of the #B3 analogue, but it cannot be assayed in mice due to their size, so efficacy assays with other animal species such as dogs or monkeys would be needed. Finally, while the autopsy of the animals is usually conducted in the toxicity assays instead of the efficacy ones, the autopsy of the animals deceased with the loading dose of #B3 condition would have been useful to determine whether the usual dose of #B3 could be increased without toxic effects. Analogue #B3 toxic effects seemed lower than those of PxB at similar dose, so it is to be expected that we can increase the dose of the peptide without increasing the toxicity, albeit further research is needed.

3.2.4. DISCUSSION

In the context of antibiotic resistance crisis that we are currently living, new therapeutic solutions are needed for the treatment of bacterial infections. In particular there is substantial concern worldwide with the mounting prevalence of infections caused by multidrug-resistant Gram negative bacteria such as *Pseudomonas aeruginosa*, *Acinetobacter baumannii* and *Klebsiella pneumoniae* [Boucheret et al., 2009]. As no new antibiotic families against Gram-negative bacteria have been developed for many decades, clinicians around the world have started to use polymyxins as a drug of last resort to treat multi-drug resistant Gram-negative infections. In addition, resistance to polymyxins is rare, and generally adaptive and thus reversible. Given that natural polymyxins are intrinsically nephrotoxic, newly synthesized analogues should aim to reduce the toxicity while maintaining the efficacy [Ventola, 2015; Cassir et al., 2014].

With this in mind, in this thesis we have designed and synthesized new molecules inspired in colistin and including several modifications that allow an easy scale-up of synthesis and purification. The synthesis has been done manually by conventional solid-phase chemistry, applying the most suitable conditions for each molecule. In order to streamline the synthesis, Cys and Ttr were introduced to replace Thr¹⁰ in the natural colistin, which allowed the formation of a disulfur bond, simplifying thus the cyclization process. Additionally, the use of Ttr allowed maintaining the natural Thr lateral chain, which is necessary for the hydrogen bond interactions with membranes for antimicrobial activity.

The antibacterial efficacy of polymyxins, expressed as the MIC, is well described in the literature and is usually around 0.5-4 $\mu\text{g}\cdot\text{mL}^{-1}$ both for PxB or PxE against Gram-negative bacteria *in vitro* [Rabanal & Cajal, 2017]. These values are similar to the ones we have obtained with Gram-negative bacteria *P. aeruginosa* and *A. baumannii*, with a MIC value of 2 $\mu\text{g}\cdot\text{mL}^{-1}$ for colistin. On the contrary, it seemed that the *E. coli* strain we used was more sensitive to the polymyxin family, exhibiting a MIC value of 0.5 $\mu\text{g}\cdot\text{mL}^{-1}$. Finally, as highlighted in several articles, we also detected that the Gram-positive bacteria *S. aureus* was mostly unaffected by polymyxin, with a MIC value above 32 $\mu\text{g}\cdot\text{mL}^{-1}$. While this is usually the case with

Gram-positive bacteria, it is worthy to highlight that some exceptional polymyxin analogues have been produced that exhibit a broad spectrum of activity, including both Gram-positive and Gram-negative bacteria [Rabanal et al., 2015; Rabanal & Cajal, 2017; Segovia & Sole, 2021].

The first series of peptides synthesized, Series A, aimed to identify the optimal length of the N-terminal fatty acyl chain for activity. Previous works about this topic have been published on polymyxin suggesting that a length between 7 and 9 carbons is the optimal one for activity [Velkov et al., 2010; O'Dowd et al., 2007]. However, while colistin and polymyxin are really similar in sequence and structure, they exhibit a key difference in position 6, where polymyxin B has a DPhe residue whereas colistin has a DLeu residue. We postulated that this small difference on a residue located in the hydrophobic domain of the cycle, which is important for the interaction with LPS, may also affect the optimal length of the fatty acyl chain. Thus, we expected to see analogues with very short or long fatty acyl chains exhibiting low activity and find a middle length with optimal results. On the other side, modifications on residues 6 and 7 were also assayed, as previous studies from our group identified that the inclusion of a Nle in these positions improved the antimicrobial profile of the molecule. A third type of modification was the substitution of DLeu⁶ by a DAoc residue, which increases the hydrophobicity in this position, and that may potentially enhance the antimicrobial activity.

When exposing the bacteria strains to the different analogues of Series A (#A1-7) and colistin, we observed that all of them were less active, since none of them was able to attain similar antimicrobial activity levels. While the MIC values for colistin were between 0.5 and 2 $\mu\text{g}\cdot\text{mL}^{-1}$ for the three different Gram-negative bacteria assayed, all of the analogues were inactive against *A. baumannii*. However, they showed good activity against *P. aeruginosa* and *E. coli*. However, these results provided the information that we were looking for: peptide #A3, which had a 10-carbon fatty acid chain, had the best efficacy profile, with MIC values of 8 and 4 $\mu\text{g}\cdot\text{mL}^{-1}$ for *E. coli* and *P. aeruginosa*, respectively. In contrast, analogues with a much shorter fatty acid chain, such as #A1 (6 carbons), had lower or none antimicrobial activity in the strains tested. Activity also decreased for analogues

with longer acyl chains. These results contrast with the previously reported optimal lengths for polymyxin B analogues, which are 7-9 carbons, and for that reason, further research was conducted on analogues in Series A [Velkov et al. 2010; Visser, 2003].

As expected, most analogues of Series A were not active on Gram-positive *S. aureus*, with the notable exceptions of analogues #A4 and #A6, both with 12 carbons in their fatty acid chain, with a MIC of $8 \mu\text{g}\cdot\text{mL}^{-1}$. While this result is uncommon, some cases have previously been published of some Gram-positive bacteria species being sensitive to polymyxin analogues [Trimble, 2016; Vega & Caparon, 2012]. In this specific case, it seems to be related to the longer fatty acid chain, but whether the 12-carbon chain helps the molecule interact with and disrupt the Gram-positive membrane, or it inhibits the bacterial growth via an alternative mechanism remains to be studied.

Finally, *A. baumannii* appeared to be resistant to all the synthetic analogues on this series. Resistance to polymyxins has already been described in *A. baumannii* via the Outer Membrane Protein (OMP) called AbOmpA [Choi, 2008; Kwon, 2017; Nie, 2020]. As the strain is sensitive to natural colistin, the mechanisms causing the resistance to the analogues in this specific case is unknown.

The results for the haemolysis assay indicated that peptides (e.g., #A4 and #A6) with long fatty acyl chains (C12) induced a great level of red blood cell lysis, which is an event that has been previously demonstrated for other molecules such as trisaccharides [Carvalho, 2015]. On the contrary, shorter fatty acyl chains did not cause such a marked haemolysis in rabbit blood. Furthermore, our results suggest that the substitution of Leu by Ile increased the haemolytic effect of analogues. However, such changes are evident at high concentrations, and not so relevant at MIC concentration ($2-8 \mu\text{g}\cdot\text{mL}^{-1}$).

We next studied the interaction of these analogues with model membranes that mimic the different bacterial membranes by using different biophysical assays that give complementary information. The biophysical assays with Langmuir monolayers of Series A were consistent with the selective binding to anionic membranes. All of the peptides showed very low affinity to bind and interact with POPC

monolayers, the eukaryotic plasma membrane model, mainly due to lack of electrostatic attraction between the cationic antibiotic and the zwitterionic POPC. This lack of affinity ensures a selective binding and reduces the toxicity toward mammalian cells [Zasloff, 2002]. Results showed that longer acyl chains facilitate the insertion of the peptide into the membrane, with the notable exception of analogue #A7, with the more compensated hydrophobic domains (short N-terminal acyl chain and longer hydrophobic lateral chains in positions 6 and 7 of the cycle) which behaves differently, showing no significant insertion into POPG monolayers, a model of Gram positive membranes. Parallel to that, all compounds showed good levels of affinity towards LPS monolayers, model of the bacterial OM, which is necessary for the antimicrobial activity of the analogues [Pristovsek&Kidric, 1999; 2004]. The analogue that induced higher increase in surface pressure, even above colistin, was #A7. Once we demonstrated the selective binding and insertion into anionic monolayers, we next analysed the effect on a more relevant system: unilamellar vesicles. In this case, all the analogues in series A caused the aggregation of anionic vesicles, forming clusters. Furthermore, no relevant differences were found when Gram-positive and Gram-negative membrane models were exposed to the peptide analogues in comparison with the natural colistin (PxE). However, it is relevant to highlight that peptides with long fatty acyl chain, such as #A6 (12 carbons), exhibited a higher affinity for Gram-positive membrane models (POPG) than peptides with shorter fatty acyl chains. No effect was seen on POPC vesicles, in agreement with the results obtained with monolayers of the same composition. This aggregation of vesicles is also observed in FRET assays with labelled vesicles, that indicated the mixing of lipids between the vesicles in contact, as also reported with PxB, colistin and other AMPs such as cecropins. At least at low peptide concentrations, below 0.5-1%, lipid mixing can not be attributed to leaky fusion. The absence of detectable leakage induced by the peptides at relevant concentrations needed for activity (MICs), suggest that the mechanism of action is not based on bilayer permeation by channel formation, but possibly due to the formation of contacts between the two apposed monolayers of the IM and OM of Gram-negative bacteria, and allowing the mixing of lipids from those membranes.

The most effective Series A analogues, #A2 (octanoyl) and #A3 (decanoyl), were used in a TEM assay. Sensitive bacteria *E. coli* and *P. aeruginosa*, as well as Gram-positive *S. aureus* were treated with both peptides at a sub-MIC concentration and later prepared for electronic microscopy observation.

Thus, we were able to observe intracellular stacks formed near the polar regions of the Gram-negative bacteria, and even some blebs protruding the membrane in the case of *E. coli*. These blebs are negatively charged membrane-derived oligosaccharides and are produced by Gram-negative bacteria as a response to the osmotic shock caused by membrane damage [Kennedy, 1982; Yeaman, 2003; Hartmann, 2010]. Both effects have been previously described as signs of membrane cell damage in Gram-negative bacteria. In the case of Gram-positive *S. aureus*, we are able to discern some minor spherical formations in the cell cytoplasm, as well as the nuclei with less contrast in comparison to the rest of the cell, which are signs of cell damage. Furthermore, it is clear that the cell envelope is affected to some degree, as the edges are less defined [Rabanal et al., 2015; Shimoda, 1995; Hartmann, 2010]. Therefore, this confirms that the lipopeptide-induced bacterial membrane effect occurs in a similar way as natural polymyxins.

Overall, peptides in the Series A could inhibit the cell growth Gram-negative bacteria, albeit with less efficacy in comparison to the wild type colistin. As previously described [Velkov et al., 2010], we were able to demonstrate that 8 to 10-carbon fatty acyl was the optimal length for colistin analogues against Gram-negative bacteria, as shorter ones were inactive, while longer fatty acids induced unacceptable levels of hemolysis. As demonstrated by the MIC values and biophysical assays, longer fatty acyl chains had significant activity against Gram-positive bacteria, consistent with previous works [Velkov et al., 2010]. Furthermore, the Nle⁷ modification did not improve the haemolytic profile of the molecule, contrary to what we had expected. Finally, the effect of the most active peptides (#A2 and #A3) was also observed via TEM with clear signs of antimicrobial effect. However, given that the Series A peptides had less activity and exhibited more haemolytic potential than colistin, it was decided to discontinue the research

of this line of compounds and instead use what we had learned to develop a new Series of analogues.

Series B incorporated the DAdec as a substitution for the N-terminal octanoyl + Dab¹ residue, which together with the 2-CTC resin and the Ttr as last residue facilitated the synthesis and cyclization procedures of the new analogues. As the modification of Leu⁷ for Nle to increase flexibility was not successful for Series A, we tested other alternatives in the form of leucic acid, Abu, and Nva, since these are also residues that are hydrophobic and that will confer more flexibility to the hydrophobic domain, possibly facilitating LPS-binding, or could even facilitate the metabolism [Brown et al., 2015; Hobbs, 1969; Kanazawa et al., 2009].

Contrary to Series A, Series B analogues exhibited really promising antimicrobial activities, comparable to colistin, for *P. aeruginosa* and *A. baumannii*, suggesting that the use of a Ttr instead of a Cys to cyclize the peptide was successful. This Ttr modification was able to reproduce the stereochemistry of natural colistin, something that was not taken into account in series A. Notably, peptides that had DAdec had more antimicrobial activity (lower MIC) than the analogues with the natural fatty acyl chain and Dab¹. Finally, analogues with leucic acid or, specially, a Leu in position 7 had the most activity in comparison with the other conditions such as Abu and Nva, which had more modest MIC values.

The promising results for some of the Series B analogues convinced us to focus our efforts on a series of *in vivo* assays with the most successful peptides. Thus, #B2, #B3, #B4, and #B5 were first assayed for nephrotoxicity in mice using polymyxin as a control instead of colistin. Polymyxin has been long described to behave in a similar way to colistin in the *in vivo* models, so the change of control did not affect the assays [Rabanal & Cajal, 2017; Sivanesan, 2017].

In the nephrotoxicity assay it became clear the limitations of polymyxin as a therapeutic, as it showed nephrotoxic signs as proved by histopathology of the kidney upon microscopy observation as previously described [Rabanal & Cajal, 2017] or even resulted in premature death of the animals due to toxicity. Regarding the peptides tested, one showed polymyxin-level kidney damage (#B2); while another two lacked proof of kidney damage but the biomarkers levels were

unnaturally low in comparison with the control, which has been previously associated to potential liver affectation (#B4 and B5) [Longo et al., 2011]. Notably, both #B4 and #B5 have an ester bond between residues 6 and 7 due to the substitution of Leu⁷ by a leucic acid. As drug metabolization (including esterases) is usually centralized in the liver, as well as the kidney, it may be the case that it is disrupting its function in some way [Lavis, 2008]. The #B3 analogue, which had already shown the best results for the antimicrobial *in vitro* assays, was also the one showing the least nephrotoxicity. Further assays would be needed to analyze the kidneys of euthanized mice and confirm that the analogues are also accumulating in the same manner as polymyxin. On the other side, it would be interesting to confirm the cause and effects of the #B4 and #B5 peptides lowering activity on the blood urea levels by causing liver damage.

Regarding the pharmacokinetics assays, the results were aligned with the nephrotoxicity as polymyxin did not achieve high blood concentrations and was rapidly removed from circulation, presumably due to kidney accumulation as previously reported [Nilsson et al., 2015; Velkov et al., 2016; Azad et al., 2015]. The analogues exhibit slightly higher blood exposure (AUC) and concentration than polymyxin, suggesting that they are being absorbed faster or not being retained as prominently at the kidneys. However, consistent with the nephrotoxicity assays, the #B3 analogue is again the one showing the highest degree of bioavailability.

Due to the high antimicrobial activity of #B3, and the potential toxicity effect of the other Series B peptides *in vivo*, we decided to focus our research in the former. Therefore, the #B3 analogue was used to perform *in vivo* efficacy assays in comparison with both polymyxin and colistin.

During the *in vitro* preparative assays before the efficacy assay, it was observed that, on the contrary to natural polymyxin B, the bactericidal concentration for #B3 was significantly higher than its inhibitory concentration which indicates that it works much better as a bacteriostatic rather than as a bactericidal. The efficacy assays were carried out on two different pneumonia models using *Pseudomonas aeruginosa* as the infective agent and provided promising results. While #B3 was not successful to reduce bacteraemia and mortality more than polymyxins,

the levels of lung culture (cfu) were statistically similar to those exhibited by natural polymyxins, which suggests that the newly synthesized compound is not inferior to them. Therefore, the DAdec and Ttr modifications included in #B3 did keep the *in vitro* antimicrobial potential.

Going forward, we want to focus our efforts in the #B3 analogue. Some additional *in vivo* tests may be needed, such as the quantification of peptide accumulated at the kidney or liver at the time of animal death, or the analysis of the cause of animal death in the *in vivo* efficacy studies. The membrane effects of the #B3 peptide should also be observed via TEM (electron microscopy), which would provide us with a clear picture of the peptide's effect on bacteria membrane.

4. CONCLUSIONS

The conclusions for the present thesis are as follows:

- Peptide analogues of colistin were successfully designed, synthesized and evaluated. Solid phase synthesis is a reliable method to produce pure compounds for *in vitro* and *in vivo* assays and can be scaled-up.
- Amongst the changes incorporated to the molecule we can highlight the extension or shortening of the fatty acyl chain; the substitution of the residues in position 6 and 7 without change in their charge.
- Peptide analogues with a very short (6 carbons) fatty acyl chain had a decreased activity due to lack of interaction with the LPS and Gram-negative membrane.
- On the other hand, very long (12 carbons) fatty acyl chain lost some of their Gram-negative membrane affinity in favour of Gram-positive affinity, which resulted in them exhibiting a significant increase in activity against Gram-positive bacteria. However, the extension of the fatty acyl chain caused a direct increase in the haemolytic activity of the compounds.
- Antimicrobial activity against bacteria of the synthesized colistin analogues triggers a cell death reaction similar to previously described polymyxins: exhibiting membrane protussions in Gram-negative bacteria; and causing the appearance of mesosomes within the cytoplasm of Gram-positive bacteria, as observed in peptides #A2 and #A3.
- Peptide cyclization was successfully simplified by substituting the Thr¹⁰ by Cys and Ttr to allow disulfur bond formation. Additionally, the use of Ttr instead of Thr allowed maintaining its natural lateral chain.
- The substitution of the N-terminal moiety by an DAdec residue enhances the antimicrobial activity of the resulting peptides (Series B), and allowed easing the synthesis while increasing the final yield. The confirmation that they do

not reduce the analogue activity will streamline the synthesis of future peptides.

- Analogue #B3 is the best analogue in the current thesis, as it shows similar activity against Gram-negative bacteria as that of colistin and polymyxin B. Furthermore, the pharmacokinetic and nephrotoxicity profiles of the peptide are the best amongst the ones assayed in this project, including polymyxin B. Finally, #B3 *in vivo* efficacy assays provided results similar to those of polymyxin B, proving that it was not inferior to it.

5. MATERIALS AND METHODS

5.1. CHEMICAL SYNTHESIS OF COLISTIN ANALOGUES

5.1.1. SOLVENTS

Table 20. Solvents, their quality and brand, used during peptide synthesis.

Solvent	Quality	Brand
Acetone	Synthesis	Scharlau
ACN	HPLC	Fischer Chemical
DCM ^(a)	Synthesis	VWR
DMF	HPLC	Fischer Chemical
EtAc	Synthesis	VWR
EtOAc	Synthesis	VWR
Et ₂ O ^(b)	Synthesis	Scharlau
EtOH	Synthesis	Scharlau
H ₂ O ^(c)	Milli-Q	Millipore
MeOH	HPLC	Fischer Chemical
THF	Synthesis	Scharlau

(a) The DCM is filtrated on an alumina column to remove impurities.

(b) The Et₂O was dried and conserved over Na.

(c) The H₂O was obtained by the filtration of deionised water using a Milli-Q Plus (Millipore) system to obtain water with a resistivity over 18 MΩ·cm⁻¹.

5.1.2. REAGENTS

Table 21. Reagents, their quality and brand, used during peptide synthesis.

Reagent	Quality	Brand
Resins: 2-CTC and BHA, Rink Linker and amino acids	99%	Bachem, Iris Biotech, Fischer Scientific, Fluorochem, Novachem or Polypeptide
Boc ₂ O	99%	Acros Organics
Decanoic acid	98%	Sigma-Aldrich
DIEA	99%	Sigma-Aldrich
DIPCDI	99%	Sigma-Aldrich
DMAP	99%	Sigma-Aldrich
DMSO	Synthesis	Carlo Erba
Dodecanoic acid	99%	Acros Organics
Fmoc-Cl	99%	Bachem
HATU	99%	Fluorochem
HCl	37% aq. solution	Scharlau

HFIP	99%	Acros Organics
HOAT	99%	Sigma-Aldrich
HOBt	99%	Fluka
KCN	99%	Sigma-Aldrich
K-Oxyma Pure	99%	Novabiochem
Na ₂ CO ₃	99%	Sigma-Aldrich
NaHCO ₃	99%	Sigma-Aldrich
Na ₂ SO ₄	99%	Fluorochem
Ninhydrin	99%, AR	Merck
Nonanoic acid	97%	Fluka
Octanoic acid	98%	Sigma-Aldrich
Phenol	99%	Sigma-Aldrich
Piperidine	99%	Sigma-Aldrich
Pyridine	99%	Panreac
TES	98%	Acros Organics
TFA	99%	Sigma-Aldrich
TFE	99%	Fischer Scientific
TIS	98%	Acros Organics

5.1.3. INSTRUMENTS

Table 22. Instruments, their model and brand, used during peptide synthesis.

Instrument	Model	Brand
Centrifuge	ROTOFIX 32 A	Hettich
Evaporator	R-200	BÜCHI
HPLC (analytical)	Serie 20 Prominence	SHIMADZU
HPLC (semi-preparative)	Delta Prep 3000	Waters
Lyophilizer	Alpha 1-2 LDplus	Christ
Mass spectrometer	Zq-Micromass	Waters
Weighting scale	AB204-5 and PJ360	Mettler Toledo

5.1.4. METHODS

5.1.4.1. Qualitative ninhydrin assay (Kaiser test)

The ninhydrin test, also known as Kaiser test, is a colorimetric, qualitative and highly sensitive test for primary amine detection. The basic reaction behind this test was first observed by Ruhemann [Ruhemann, 1911] in 1911; later in 1970 Kaiser

adapted the ninhydrin reaction to the solid-phase peptide synthesis (SPPS) [Kaiser et al., 1970], allowing the fast determination of the effectiveness of amino acid coupling.

For the application of this assay, the following reagents are required:

- Reagent A: 16.5 mg of KCN are dissolved in 25 mL of distilled water; then 1.0 mL of the previous solution is diluted with 49 mL of freshly distilled pyridine (from ninhydrin).

- Reagent B: 1.0 g of ninhydrin is dissolved in 20 mL absolute EtOH.

- Reagent C: 40 g of phenol are dissolved in 20 mL of warm absolute EtOH.

For conducting this test, a small amount of clean and dry resin beads are placed in a glass tube together with 2 drops of Reagent A, Reagent B and Reagent C, and finally the tube is heated at 110°C for 3 minutes. The color of the resulting solution determines the effectiveness of the coupling amino acid: an intense blue solution with blue beads indicates the presence of free primary amines and thus a recoupling is needed, whereas a colorless solution or faint blue with colorless beads indicates a complete coupling.

5.1.4.2. Solid phase peptide synthesis (SPPS)

The peptides were manually synthesized following standard Fmoc/^tBu procedures and using polypropylene syringes of different sizes (depending on the amount of resin used) equipped with a porous polyethylene filter. Manual stirring was applied using a Teflon rod, and the reagent and solvent excess, together with the byproducts, were flushed away by vacuum filtration. For the chemical synthesis of colistin analogues, resin BHA ($f = 0.69 \text{ mmol}\cdot\text{g}^{-1}$) and 2-CTC ($f = 1.56 \text{ mmol}\cdot\text{g}^{-1}$) were used.

5.1.4.2.1. Protection of amino acids

Most of the amino acids used during the present thesis were already purchased with the amino functional group protected. However, some special amino acids were not available in the protected forms, thus, they were acquired unprotected and the addition of the protective groups Boc and Fmoc was carried out following the standard procedures described below.

Boc amino acid protection

The amino acid protection with Fmoc was performed by slowly adding (drop by drop) 1 eq. of Boc₂O in THF/H₂O (1:1, v/v) at 0°C and under stirring to 1 eq. of amino acid in THF/H₂O (1:1, v/v); both solutions prepared with the minimum quantity of the solvent. The mixture was then pH adjusted with NaHCO₃ 10% solution to a final value of 9-10, and left to react for 40 minutes; after that time the reaction was left to react overnight at room temperature. The reaction was then monitored by thin layer chromatography using a mixture of chloromethane, methanol and ethyl acetate (89:10:1, v/v). After consumption of the free amine the solution was adjusted if needed to the previous pH and was extracted with Et₂O (3x10 mL). The aqueous phase was then acidified with HCl 37% until pH 4.5-5 and extracted with DCM (3x10 mL). The combined organic layers were dried with Na₂SO₄ and evaporated under low pressure, obtaining thus the protected amino acid. Purity of the AA-Boc was determined by HPLC analysis.

Fmoc amino acid protection

The amino acid protection with Fmoc was performed by slowly adding (drop by drop) 1.1 eq. of Fmoc-Cl in acetonitrile at 0°C and under stirring to 1 eq. of amino acid in acetonitrile; both solutions prepared with the minimum quantity of the solvent. The mixture was then pH adjusted with Na₂CO₃ 10% solution to a final value of 9-10, and left to react for 40 minutes; after that time the reaction was left to react for 2 hours at room temperature. The reaction was then monitored by thin layer chromatography using a mixture of chloromethane, methanol and ethyl acetate (89:10:1, v/v). After consumption of the free amine the solution was evaporated under low pressure and mQ water was added to the obtained product. The solution was adjusted to a pH of 10-11 with Na₂CO₃ and extracted with EtOAc (3x10 mL). The aqueous phase was then acidified with HCl 37% until pH 4-5 and extracted with EtOAc (3x10 mL). The combined organic layers were dried with Na₂SO₄ and evaporated under low pressure, obtaining thus the protected amino acid. Purity of the AA-Fmoc was determined by HPLC analysis.

5.1.4.2.2. Initial treatment of resins

Due to the compact storage form of resins it is highly recommended to perform an initial treatment before using it. This treatment is characteristic for each resin, and the main objective is its solvation and cleaning of impurities that it might contain.

BHA resin

The protocol of initial treatment for the BHA resin is described in the **Table 23**.

Table 23. Protocol of BHA resin conditioning.

Step	Reagent	Operation	Series	Time (min)
1	DCM	Washing	5	0.5
2	40% TFA / DCM	Washing and solvation	1	1
3	40% TFA / DCM	Washing and solvation	2	10
4	DCM	Washing	5	0.5
5	5% DEIA / DCM	Neutralization	3	2
6	DCM	Washing	5	0.5
7	DMF	Washing	5	0.5

2-CTC resin

The 2-CTC is a very acid labile resin, and therefore the initial treatment (**Table 24**) is performed only with DMF and DCM previously filtrated with basic alumina in order to remove the acid traces that it might contain.

Table 24. Protocol of 2-CTC resin conditioning.

Step	Reagent	Operation	Series	Time (min)
1	DCM	Washing	5	0.5
2	DCM	Washing and solvation	1	30
3	DCM	Washing	5	0.5
4	DMF	Washing	5	0.5

5.1.4.2.3. Elongation of peptide chain

The elongation of the peptide chain was carried out using different conditions depending on the resin used.

BHA resin

For the BHA resin, the elongation of the peptide chain included the addition of the first reference amino acid, the Rink Linker and the rest of amino acids of the

sequence of the peptide analogues. These couplings were performed using DIC as the activating agent and HOBt as an additive to minimize racemization. For each addition to the peptide chain, 3 eq. of all reagents were used for 1 hour, and in the cases where the coupling was not complete, it was repeated using 1.5 eq. instead for 30 more minutes. The protocol that describes the coupling steps is detailed in the **Table 25**.

Table 25. Protocol for peptide chain elongation used in the Fmoc/^tBu strategy for the BHA resin.

Step	Reagent	Operation	Series	Time (min)
1	DMF	Washing	5	0.5
2	20% piperidine in DMF	Deprotection	1	1
3	20% piperidine in DMF	Deprotection	2	10
4	DMF	Washing	5	0.5
5	3 eq. Fmoc-AA-OH [*] , 3eq. DIC, 3 eq. HOBt	Coupling	1	60
6	DMF	Washing	5	0.5
7	DCM	Washing	5	0.5
8	Ninhydrin assay	Control	1	3

2-CTC resin

In the case of the 2-CTC, the elongation of the peptide chain was conducted under different conditions depending on the nature of the bond performed. Thus, we can differentiate between the formation of an ester bond or an amide bond. Moreover, we can differentiate between the ester bond performed during the loading of the resin, as a result of the reaction of a carboxylic acid with the polymeric support, and the ester bond obtained when adding an acid to the carboxylic acid of the peptide chain.

Elongation via ester bond: loading of the resin

After the initial treatment of the resin, the first amino acid was coupled by the formation of an ester bond. This coupling was performed by adding directly to the resin 1.5 eq. of the amino acid and 3 eq. of DIEA for 1 hour.

Elongation via ester bond: coupling of the rest of amino acids

When the peptide chain has an alcohol, instead of the free amino functional group, the elongation must be performed by the formation of an ester bond.

This ester bond requires the activation of the carboxylic acid, which is accomplished by the formation of the anhydride symmetric acid, highly reactive.

In order to obtain the anhydride symmetric acid, 6 eq. of the amino acid were mixed with 3 eq. of DIC in the minimum amount of DCM; the mixture was stirred for 30 minutes, and finally the solvent was evaporated under N₂ airflow.

The esterification was performed by adding to the resin the 3 eq. of the anhydride symmetric acid, previously prepared, with 0.3 eq. of DMAP, used as catalyst, for 1 hour.

Elongation via amide bond

The addition to the peptide chain via amide bond of the rest of amino acids was performed by using one of the following combinations of coupling reagents and additives, depending on the synthesized analogue:

- 1) DIC, HOBt 2) HATU, HOBt, DIEA 3) DIC, K-Oxyme

HOBt was used as additive to minimize racemization. DIC, HATU and K-Oxyma were used as activating agents, DIEA was used in order to obtain base medium needed for HATU to react. For each one of the previous conditions used in the coupling of an amino acid, the protocol described in the **Table 26** was applied:

Table 26. Protocol for peptide chain elongation used in the Fmoc/^tBu strategy for the 2-CTC resin.

Step	Reagent	Operation	Series	Time (min)
1	DMF	Washing	5	0.5
2	20% piperidine in DMF	Deprotection	1	1
3	20% piperidine in DMF	Deprotection	2	10
4	DMF	Washing	5	0.5
5	1) 3 eq. of AA, DIC and HOBt; 2) 3 eq. of AA, HATU and HOBt, and 6 eq. of DIEA; 3) 3 eq. of AA, DIC and K-Oxyma	Coupling	1	60
6	DMF	Washing	5	0.5
7	DCM	Washing	5	0.5
8	Ninhydrin assay	Control	1	3

5.1.4.2.4. Coupling quantification of the first amino acid

After the coupling of the first amino acid, it was determined the real functionalization of the resin by treating a small amount of the resin with 20% piperidine in DMF for 20 minutes. The filtrate was then introduced in a volumetric flask, which was filled with DMF, and a bank of dilutions was prepared in order to obtain a theoretic absorbance between 0.5 and 1. A blank was prepared under the same conditions than the prepared sample, and finally absorbance was measured at 301 nm. Resin functionalization was determined using the following equation:

$$f = (A_s - A_b) \cdot X \cdot \epsilon^{-1} \cdot \rho^{-1} \cdot l^{-1}$$

where

f = functionalization of the resin ($\text{mmol} \cdot \text{g}^{-1}$)

A_s = Sample Absorbance

A_b = Blank Absorbance

X = dilution factor (mL)

ϵ = extinction coefficient of the Fmoc cleavage product in DMF ($7800 \text{ mol}^{-1} \cdot \text{dm}^3 \cdot \text{cm}^{-1}$)

l = length of the measurement cuvette

5.1.4.2.5. Cleavage, deprotection and cyclization of the peptides

During this thesis, two different strategies of cyclization of the peptides were carried out: the cyclization of peptides by disulfide bond using the two sulfide functional groups present in the analogues, and the cyclization of peptides by amide bond formation between a free amine group and a carboxylic acid. In order to perform successfully each one of the previous cyclizations, a specific protocol of cleavage, deprotection and cyclization must be carried out: these protocols are detailed below.

Cleavage, deprotection and cyclization by disulphide bond formation

Once the linear sequence of the peptide was complete, an acidolysis treatment was performed with TFA/TES/H₂O (95:3:2, v/v) for 60 minutes; separating the peptide from the resin and removing all the protective groups at the same time. After the cleavage, the resin was washed 3 times with TFA; the filtrates were

combined and evaporated using N₂ airflow. The crude of the peptide was precipitated with cold diethyl ether, centrifuged and the supernatant was removed by decantation. In order to remove the maximum number of impurities present in the crude, it was dissolved in acetonitrile/water (1:1) and lyophilized before cyclization.

The peptides were dissolved in water at the diluted concentration of 1.5 mg of peptide/mL of dissolution; then 3% of DMSO was added as the mild oxidant. The mixture was stirred constantly at room temperature for 24 to 48 hours depending on the progress of the cyclization, which was monitored by HPLC. Once the peptide was cyclized, the mixture was lyophilized.

Cleavage, deprotection and cyclization by amide bond formation

Once the linear sequence of the peptide was complete, a very soft acidolysis treatment was performed with DCM/HFIP/TFE/TES (65:20:10:5, v/v) for 60 minutes; separating the peptide from the resin and only removing the Mtt protective group. After the cleavage, the resin was washed 3 times with DCM; the filtrates were combined and evaporated using N₂ stream. The crude of the peptide was precipitated with cold water, centrifuged and the supernatant was removed by decantation. In order to remove the maximum number of impurities present in the crude, it was dissolved in acetonitrile/water (1:1) and lyophilized before cyclization.

The filtrates were combined and evaporated using N₂ airflow. The crude of the peptide was precipitated with cold diethyl ether, centrifuged and the supernatant was removed by decantation. In order to remove the maximum impurities present in the crude, it was dissolved in acetonitrile/water (1:1) and lyophilized before cyclization.

The peptides were dissolved in DMF at the diluted concentration of 10 mg of peptide/mL of dissolution; then 4 eq. of DIEA, 2 eq. of HATU and 2 eq. of HOAT were added. The mixture was stirred constantly at room temperature for 24 to 48 hours depending on the progress of the cyclization, which was monitored by HPLC.

Once the peptide was cyclized, the peptides were precipitated with cold water, centrifuged and the supernatant was removed by decantation; then the crude was lyophilized. In order to remove the rest of the protective groups, an acidolysis

treatment was performed with TFA/TES/H₂O (95:3:2, v/v) for 60 minutes. The solution was evaporated using N₂ airflow, and the crude was then dissolved in acetonitrile/water (1:1) and lyophilized.

5.1.4.3. High performance liquid chromatography (HPLC)

Purification of peptides was carried out by semi-preparative RP-HPLC, whereas analytical RP-HPLC was used to characterize them.

Semi-preparative RP-HPLC

This system consisted of a *Waters 600E* pump and controller, manual *Waters 712* injector, Ultraviolet-visible (UV-VIS) detector *Waters 484*, column Phenomex C18 1x25 cm of 5 µm diameter of particle, loop of 10 mL. The samples were eluted using lineal gradients of the following solvents:

A: H₂O – 0.1% TFA

B: ACN – 0.1% TFA

The conditions applied in HPLC analysis are described in **Table 27**.

Table 27. Semi-preparative RP-HPLC conditions.

Parameter	Value
Mobile phase flow rate (mL·min ⁻¹)	4.0
Detector wavelength (nm)	220

Prior to injection of a new compound, loop injector was cleaned with 15 mL of methanol followed by 15 mL of initial conditions solution.

Analytical RP-HPLC

This system consisted of two *LC-20AD* high pressure pumps, automatic *SIL-20A* injector, controller *CBM-20A*, detector *SPD-M20A*, column Nucleosil C18 0.4x25 cm of 5 µm diameter of particle, loop of 100 µm. The samples were eluted using lineal gradients of the following solvents:

A: H₂O – 0.045% TFA

B: ACN – 0.036% TFA

The conditions applied in HPLC analysis are described in **Table 28**.

Table 28. Analytical RP-HPLC conditions.

Parameter	Value
Mobile phase flow rate (mL·min ⁻¹)	1.0
Detector wavelength (nm)	220

5.1.4.4. Mass spectrometry

Characterization of peptides was also carried out by mass spectrometry by direct injection. The system consisted of a Waters Alliance 2695 HPLC conformed of a quaternary pressure pump, Micromas ZQ ESI-MS system.

The samples were eluted at a flow rate of 0.1-0.3 mL·min⁻¹ and using a 1:1 solution of the following solvents:

A: H₂O – 0.1% FA

B: ACN – 0.07% FA

Samples for the electrospray ionization (ESI) spectrometry analysis were prepared by dissolving a small amount of peptide in ACN/H₂O (1:1).

5.2. IN VITRO BACTERIAL BIOLOGICAL ASSAYS AND HEMOLYTIC ACTIVITY DETERMINATION

5.2.1. REAGENTS

Table 29. Reagents, their specifications and brand, used during in vitro biologic assays.

Reagents	Brand
Bacterial strains	ATCC
Colistin sulfate salt ^(a)	Sigma-Aldrich
H ₂ O ^(b)	Millipore
MHB	Oxoid
Polymyxin B sulfate salt	Sigma-Aldrich
Ringer 1/4	Oxoid
TSA	Oxoid
TSB	Oxoid
Tryptone water	Oxoid

(a) Colistin sulfate salt used contained $\geq 15,000$ IU·mg⁻¹.

(b) The H₂O was obtained by the filtration of deionised water using a Milli-Q Plus (Millipore) system to obtain water with a resistivity over 18 MΩ·cm⁻¹.

5.2.2. MATERIALS

Table 30. Material, their specifications and brand, used during in vitro biologic assays.

Material	Specifications	Brand
96-well plates	Sterile Polypropylene Flat-Shaped-Bottom plates	Thermo Scientific

5.2.3. INSTRUMENTS

Table 31. Instruments, their model and brand, used during in vitro biologic assays.

Instrument	Model	Brand
Centrifuge	Allegra 25R	Beckman Coulter
Microplate reader	HT	Synergy
Spectrophotometer	UV-1700 PC	Shimadzu

5.2.4. METHODS

5.2.4.1. Minimum Inhibition Concentration (MIC) determination

In vitro antibacterial activity was determined using sterile 96-well plates with different concentrations of *E. coli* (ATCC 25922), *P. aeruginosa* (ATCC 27853), *S. aureus* (ATCC25923) and *A. baumannii* (ATCC19606).

Bacterial strains were stored as cryogenic balls at -80°C, for this reason, before using them they needed to be cultured overnight in Trypticase Soy Broth (TSB) liquid medium at 37°C until bacterial growth was observed. After this initial step, bacteria could be cultured overnight in Trypticase Soy Agar (TSA) at 37°C in order to obtain visible bacterial colonies.

The day before the antimicrobial activity determination, bacterial colonies were cultured overnight in Mueller Hinton Broth (MHB) at 37°C. The same day of the assay, bacterial colonies were cultured again in MHB at 37°C for 4h, and the resultant solutions were adjusted to an optical density (OD) at 510 nm equal to 1, obtaining this way the inoculum solutions of bacteria on their exponential phase growth.

Using 96-well plates filled with MHB (50 µL in rows 2-11, 100 µL in row 12) and MHB twice concentrated (50 µL in row 1), serial 2-fold dilutions of peptides were obtained in rows 1-10 by adding 50 µL of peptide stock solution (512 µg·mL⁻¹) to row 1 and preparing the dilution range with an automated multichannel pipette. Finally, 50 µL of bacterial inoculum solution was added to rows 1-11, using row 12 as negative control (MHB) and row 11 as positive control (bacteria without peptide); each well thus contained 5x10⁵ cfu·mL⁻¹ of bacteria. The plate was cultured overnight at 37°C, and the MIC values were determined visually as the lowest peptide concentration that inhibited bacterial growth. Four determinations were performed for each peptide concentration.

5.2.4.2. Haemolysis determination

The haemolysis of erythrocytes induced by peptide was studied using a Spectrophotometer UV-VIS by measuring the absorbance of released haemoglobin (A_{sample}). For these measurements, rabbit red blood cells were washed by

centrifugation (10 min at 4.000 rpm) and the supernatant was replaced with buffer (80 mM NaCl 10 mM Tris, pH 7.4); this process was repeated three times or until the yellow coloration of supernatant was removed (which indicated an insufficient wash). Concentrated red blood cells, obtained on the last centrifugation step, were adjusted to an OD at 540 nm of 1 by the addition of buffer.

A range of peptide concentrations in the same buffer was prepared in 96-well plates by adding different amounts of peptide stock solution (0.5 mM or 2 mM) to 200 μ L of red blood cells solution previously prepared. Each peptide concentration was studied by triplicate, and negative and positive controls were included as buffer ($A_{0\%}$) and red blood cells with distilled water ($A_{100\%}$), respectively.

The plate was centrifuged (15 min at 5.000 rpm) and 100 μ L of supernatant were carefully placed in a new plate in order to read its absorbance at 540 nm. The haemolysis percentage (% h) was calculated relative to the red blood cell lysis by distilled water, according to the following equation:

$$\% h = 100 \cdot (A_{sample} - A_{0\%} / A_{100\%} - A_{0\%})$$

5.3. DETERMINATION OF THE MECHANISM OF ACTION

5.3.1. REAGENTS

Table 32. Reagents and their brand used during mechanism of action determination.

Reagents	Brand
ANTS	Invitrogen Molecular Probes
Bacterial strains	ATCC
CaCl ₂	Sigma-Aldrich
CHCl ₃	Fischer Scientific
Colistin sulfate salt ^(a)	Sigma-Aldrich
DPX	Invitrogen Molecular Probes
H ₂ O ^(b)	NA
LPS ^(c)	Sigma-Aldrich
MHB	Oxoid
NaCl	Sigma-Aldrich
Polymyxin B sulfate salt	Sigma-Aldrich
Tris	Sigma-Aldrich
Tryptone water	Oxoid
TSA	Oxoid
TSB	Oxoid
POPC	Invitrogen Molecular Probes
POPE	Invitrogen Molecular Probes
POPG	Invitrogen Molecular Probes
NBD-PE	Invitrogen Molecular Probes
Rh-PE	Invitrogen Molecular Probes
Triton X-100	Sigma-Aldrich

(a) Colistin sulfate salt used contained $\geq 15,000$ IU·mg⁻¹.

(b) The water used was distilled quality.

(c) Obtained from *Salmonella enteric* serotype Minnesota Re 595 (Re mutant).

5.3.2. MATERIALS

Table 33. Material, their specifications and brand, used during mechanism of action determination.

Material	Specifications	Brand
96-well plates	Sterile Polypropylene Flat-Shaped-Bottom plates	Thermo Scientific

5.3.3. INSTRUMENTS

Table 34. Instruments, their model and brand, used during mechanism of action determination.

Instrument	Model	Brand
Autoclave	ST DRY PV III	Autester
Centrifuge	ROTOFIX 32 A	Hettich
Electron microscope	JEM-1010	Jeol
Evaporator	Laborota 4000	Heidolph
Extruder	LIPEX	Northern Lipids Inc.
Monolayer system	KSV5000	Nima Technology
pH-meter	pH & ION-Meter GLP 22+	Crison
Particle Size Analyzer	Autosizer IIC	Malvern
Sonicator	G112SPIT	Lab Supplies
Spectrofluorimeter	Series 2 SLM-Aminco	AMINCO-Bowman
Spectrophotometer	UV-1700 PC	Shimadzu

5.3.4. METHODS

5.3.4.1. Preparation of liposomes

Unilamellar vesicles of POPG, POPE/POPG (6:4), or POPC, alone or with the fluorescently labelled phospholipids NBD-PE or Rh-PE, were prepared by evaporation of a mixture of the lipids and probes in CHCl_3 . The dried films were hydrated with Tris 10mM pH 7.4 to the desired final lipid concentration and then sonicated in a bath type sonicator until a clear dispersion was obtained (typically 3-5 min). To obtain large unilamellar vesicles, the lipid dispersions were extruded 21 times through a polycarbonate filter (Nucleopore) of 0.1 μm pore size using a mini-extruder device. All vesicles were used within 10 hours.

For the ANTS/DPX leakage assay, the dried films were hydrated in 12.5 mM ANTS, 45 mM DPX and 10 mM Tris pH 7.4. Moreover, they contained the probe Rh-PE 0.2 mol% in order to monitor the fluorescence before and after the separation of the unencapsulated material, which was carried out by gel-filtration on a Sephadex G-50 column eluted with 10 mM Tris 80 mM NaCl. First, the fluorescence of liposomes before columnation (F_0) was determined diluting 5 μL in 1.5 mL 10 mM Tris pH 7.4, with excitation and emission characteristic of Rh (563 nm and 585 nm, respectively). After columnation, liposomes with only

entrapped dye are diluted, and the fluorescence of 10 μL in 1.5 mL of buffer was measured (F).

The final lipid concentration (C) was calculated according to:

$$C = C_o \cdot (F / 10) \cdot (F_o / 5)$$

Vesicle size was determined by dynamic light scattering using a Malvern II-C Autosizer in order to assure that diameters were between 80-110 nm for sonicated and extruded vesicles, with a narrow size distribution (polydispersity < 0.1).

5.3.4.2. Kinetics of insertion into monolayers

Monolayer studies were performed at room temperature (24°C) on a monolayer system by using a cylindrical PTFE (Teflon®) trough (5 cm diameter) containing stirred aqueous phase (12 mL 10 mM Tris pH 7.4), and a Wilhelmy platinum plate connected to an electrobalance. The system was enclosed in a Plexiglas box to reduce surface contamination, and before each run the plate and the trough were cleaned with hot water at > 70°C to avoid carryover of lipid or peptide. Monolayers of POPG, POPE/POPG (6:4), POPC or LPS were formed by applying small drops of the lipid stock solutions in CHCl_3 on the aqueous subphase with a microsyringe (Hamilton Co., Reno, NV) to achieve a surface pressure of $32 \text{ mN}\cdot\text{m}^{-1}$. After 10 min, allowing for solvent evaporation, a known aliquot of peptide was added without disturbance of the monolayer via an inlet port, and the surface pressure was continuously monitored.

5.3.4.3. Aggregation of liposomes measured as light scattering intensity

The dynamic behaviour of liposomes as model membranes was measured as the change in the 90°C scattered light intensity with 1 nm slit-widths on a SLM-Aminco AB-2 spectrofluorimeter setting both excitation and emission at 360 nm. An aliquot of vesicles of the desired composition (total lipid concentration 106 μM) was added to the cuvette containing 1.5 mL of 10 mM Tris buffer at pH 7.4 with constant stirring, and then the peptide was added successively from a stock solution in water. The change in scattering was recorded continuously with 2 s resolution. The relative change in the intensity of the scattered light, δI , is defined as $(I - I_o)/I_o$,

where I_0 is the scattering without peptide, and I is the scattering in the presence of peptide.

5.3.4.4. Fluorescence assays for lipid mixing

Peptide-induced lipid mixing of vesicles of different composition was investigated in the same spectrofluorometer measuring the intensity of fluorescence resonance energy transfer from a NBD-PE donor population to an Rh-PE acceptor population. Measurements were carried out at 25°C in 1.5 mL 10 mM Tris buffer pH 7.4 with constant stirring by mixing an equimolar amount of vesicles containing 0.6% of donor NBD-PE with vesicles containing 0.6% of acceptor Rh-PE (total lipid concentration 106 μ M), followed by titration with peptide from a stock solution 0.25 mM. The excitation wavelength was set at 460 nm, corresponding to Rh, and the emission at 592 nm, corresponding to Rh, with slit widths at 4 nm.

Additionally, the peptide-induced fusion of vesicles was determined by FRET following the protocol described above but using in this case lipid vesicles co-labelled with 0.3% of both probes (13 μ M) and mixing them with an excess of unlabelled vesicles of the same composition (320 μ M). The dilution contribution due to lipopeptide addition was determined by titration of the same lipid final concentration of unlabelled vesicles. The maximum fluorescence values, in both FRET studies, were obtained by adding 50 μ L of CaCl₂ 2 M to the lipid mixing.

5.3.4.5. Leakage assay

To assess the leakage of coencapsulated ANTS and DPX vesicles due to their interaction with peptides, fluorescence measurements were carried out at 25°C in 1.5 mL 10 mM Tris buffer pH 7.4 on a PTI QM4 spectrophotometer with constant stirring by the titration of lipid vesicles (lipid concentration 115 μ M) with peptide stock solution 0.25 mM. The excitation wavelength was set at 350 nm, and the emission, at 530 nm with slit widths at 4 nm. The maximum fluorescence value was obtained by adding 10 μ L of triton X-100 to the lipid solution, and represented the 100% leakage, whereas the 0% leakage corresponded to the fluorescence of the fluorescence of the vesicles at time zero.

5.3.4.6. TEM

Transmission electron microscopy was performed using different concentrations of *E. coli* (ATCC 25922), *P. aeruginosa* (ATCC 9027) and *S. aureus* (ATCC 29213).

Bacterial strains were stored as cryogenic balls at -80°C, for this reason, before using them they needed to be cultured overnight in TSB liquid medium at 37°C until bacterial growth was observed. After this initial step, bacteria could be cultured overnight in TSA at 37°C in order to obtain visible bacterial colonies.

Sample preparation: antimicrobial treatment

The day before the antimicrobial activity determination, bacterial colonies were cultured overnight in MHB at 37°C. The same day of the assay, bacterial colonies were cultured again in MHB at 37°C for 4h, and the resultant solutions were adjusted to an OD at 510 nm equal to 0.2 (for *E. coli* and *S. aureus*) or 0.3 (for *P. aeruginosa*) obtaining this way the inoculum solutions of bacteria on their exponential phase growth.

The bacterial suspensions were treated with peptides at each MIC concentration and incubated during 2h at 37°C. Bacterial cells were obtained by centrifugation during 5 minutes at 2000 rpm.

Sample preparation: transmission electron microscopy preparation

The preparation of samples was carried out by fixing the pellet, obtained in the previous section, with 2.5% of glutaraldehyde in phosphate buffer solution for 2 hours at 4°C in gentle stirring. The samples were washed four times with the same buffer and post fixed with 1% osmium tetroxide in buffer containing 0.8% potassium ferricyanide at 4°C. The samples were dehydrated in acetone for 1 hour and infiltrated in a graded series of Epon resin for 2 days. The samples were then embedded in fresh Epon resin and polymerized at 60°C for 48 hours.

The ultrathin sections were obtained by the specialized technicians in the Centres Científics i Tecnològics of the University of Barcelona (CCiTUB) as follows: using a Leica Ultracut UCT ultramicrotome and mounted on Formvar-coated copper grids. Finally, the ultrathin sections were stained with 2% aqueous uranyl acetate and lead citrate, and examined using a *JEM-1010* electron microscope.

5.4. IN VIVO ASSAYS

5.4.1. REAGENTS

Table 35. Reagents and their brand used during *in vivo* assays.

Reagents	Brand
H ₂ O	ND
Polymyxin B	Sigma-Aldrich
Colistin sulfate salt	Sigma-Aldrich
Colistin methanesulfonate	Accord Healthcare, BCN
Physiological saline	ND
Isoflurane	ND
10% formalin buffer solution	ND
Paraffin	ND
Sodium thiopental	ND
Eosin	ND
Hematoxylin	ND

5.4.2. MATERIALS

Table 36. Material, their specifications and brand, used during *in vivo* assays.

Material	Specifications	Brand
Female swiss CD-1 mice	Animals between 20-24 g	JANVIER
Immunocompetent C57BL/6 female mice	Animals weighing 20 g	Charles River Laboratories
<i>P. aeruginosa</i>	Pa01 and Pa147 strains	ND
Columbia agar with 5% sheep blood	ND	ND

5.4.3. INSTRUMENTS

Table 37. Instruments, their model and brand, used during *in vivo* assays.

Instrument	Model	Brand
Autoclave	ND	ND
Microscope	Eclipse 300	Nikon
Microtome	RM2 145	Leica Biosystems

5.4.4. METHODS

5.4.4.1. Nephrotoxicity

The nephrotoxicity of the synthesized analogues was assessed in CD-1 mice after a sequential series of subcutaneous administration of the peptides to all animals.

This study was performed according to standard local regulations and guidelines by specialized technicians in the Animal Housing Unit (PCB-PRBB) located at the Parc Científic de Barcelona, registered as “User centre of experimental animals” in the Register of “Centres for Breeding, Suppliers and Users of Experimental Animals” of the Department of Environment of the Autonomic government Generalitat de Catalunya, with registration number: B-9900062.

This study was carried out under a series of strictly controlled conditions detailed in the following **Table 38**:

Table 38. Conditions of the nephrotoxicity study.

Condition	Value
Temperature*	20.3°C – 20.9°C
Humidity*	39.8% – 84.2%
Room air renovation cycles*	30 cycles / h
Photoperiod*	12 hours of light, 12 hours of darkness
Quarantine period	5 days
Feeding	Dry diet <i>ad libitum</i>
Drinking	Autoclaved mineral water <i>ad libitum</i>
Enrichment	Supply of Kleenex
Veterinary care and observations	Weighting of animals and initial veterinary inspection at arrival, daily observation by an animal care technician
Terminal procedures	Animals were anesthetized with isoflurane, pathology analyzed, and euthanized by rupture of the diaphragm

* Was monitored continuously.

After 5 days of acclimatization period, animals were randomly selected, marked for its identification with a permanent marker at the base of the tail, and distributed in different dosage groups as described in **Table 39**. A total of 51 animals were used.

Each animal was weighted, and a dosage according to the body weight was administered subcutaneously 6 times at 2-hours intervals. Each dose was prepared

the same day of the administration by suspending the appropriate compound in physiological saline (as vehicle) to a final volume corresponding to an administration of 5 mL·kg⁻¹. Negative control was performed using physiological saline.

20 hours after the last administration, animals were anesthetized with isoflurane, blood was extracted for biochemical parameters determination (urea and creatinine) and both kidneys were extracted and weighted for histopathological analysis, finally animals were euthanized by rupture of the diaphragm.

Extracted kidneys were fixed in 10% formalin buffer solution and routinely embedded in paraffin. Subsequently, blocks were cut at 5 μ in a Leica RM2 145 microtome, stained with hematoxylin and eosin and blind scored in a Nikon Eclipse 300 microscope.

Table 39. Summary of animals used with the concentration administered nephrotoxicity study.

Compound	Dose (mg·kg ⁻¹)	Total Dose (mg·Kg ⁻¹)	Animal number
B2	12	72	8
B3	12	72	8
B3	12	72	8
B4	12	72	3
B5	12	72	3
PxB	12	72	8
PxB	20	120	5
Saline	0	0	8

5.4.4.2. Pharmacokinetics

The pharmacokinetics of the synthesized analogues was assessed in CD-1 mice after a subcutaneous administration of the peptides to all animals.

This study was performed by the same Animal Experimental Unit described in the nephrotoxicity section and under the conditions detailed in **Table 38**.

After 5 days of acclimatization period, animals were randomly selected, marked for its identification with a permanent marker at the base of the tail, and distributed in different dosage groups as described in **Table 40**. A total of 40 animals were used.

Each animal was weighted, and a dosage according to the body weight was administered subcutaneously only once. Each dose was prepared the same day of the administration by suspending the appropriate compound in physiological saline (as vehicle) to a final volume corresponding to an administration of 5 mL·kg⁻¹.

Table 40. Summary of animals used, concentration and products administered in pharmacokinetic study.

Compound	Dose (mg·kg ⁻¹)	Extraction times (h)	Animal number
B2	12	1, 2, 4 and 6	4
B2	12	1, 2, 4 and 8	4
B3	8	1, 2, 4 and 6	4
B3	12	1, 2, 4 and 6	4
B3	12	1, 2, 4 and 8	4
B4	12	1, 2, 4 and 6	4
B5	12	1, 2, 4 and 6	4
PxB	8	1, 2, 4 and 6	4
PxB	12	1, 2, 4 and 6	4
PxB	12	1, 2, 4 and 8	4

1, 2, 4 and 8 hours after the administration, animals were anesthetized with isoflurane, blood was extracted for biochemical parameters determination, and finally animals were euthanized by rupture of the diaphragm. A single animal was used per extraction point.

5.4.4.3. Efficacy

The efficacy of the best analogue, B3, was assessed in experimental pneumonia models of infection caused by clinical strains of *P. aeruginosa*.

This study was performed according to standard local regulations and guidelines by specialized technicians in the animal facility of the Institute of Biomedicine of Seville (IBiS). Due the nature of the study, safety measures were put in place to ensure safety of all personnel involved.

The efficacy study was carried out under a series of strictly controlled conditions detailed in the following **Table 41**:

Table 41. Conditions of the efficacy study.

Condition	Value
Temperature*	20.0°C – 24.0°C
Humidity*	≤ 55.0 %
Room air renovation cycles*	12-25 cycles / h
Photoperiod*	12 hours of light, 12 hours of darkness
Feeding	Dry diet <i>ad libitum</i>
Drinking	Autoclaved mineral water <i>ad libitum</i>
Veterinary care and observations	Weighting of animals and initial veterinary inspection at arrival, daily observation by an animal care technician
Terminal procedures	Animals were euthanized with sodium thiopental (for the survival mice)

* Was monitored continuously.

Prior the efficacy assay, a MIC and MBC determination was conducted with *P. aeruginosa* Pa01 and Pa147 strains in order to check their susceptibility against synthesized analogues object of the study.

MIC determination

The MIC of the studied compounds was defined as the lowest concentration of each compound able to avoid bacterial growth in a visible way, and was determined in triplicate by broth microdilution method, using Mueller Hinton broth II. MIC results were interpreted according to the EUCAST breakpoints.

MBC determination

The MBC values were calculated from the previous MIC studies, taking into consideration that MBC is defined as the lowest concentration of antimicrobial that reduces the initial inoculums by 99.9%.

In vivo efficacy study: MLD determination

For both Pa01 and Pa147 *P. aeruginosa* strains, the minimal lethal dose was calculated as the dose of bacterial inoculums capable of causing 100% mortality using the experimental pneumonia model. This determination was carried out by instilling intratracheally to 5 randomly selected animals, for each of the strains, the dose previously calculated.

In vivo efficacy study: pneumonia model

The efficacy study was conducted using a previously characterized murine pneumonia model [Gil-Marqués et al., 2018].

The first day of the experimentation, animals were anesthetized and infected intratracheally using 50 μL of the MLD calculated for each strain. After 2 hours of the post-infection, animals were randomly selected, marked for its identification, and distributed in different dosage groups for each *P. aeruginosa* strain as described in **Table 42** and **Table 43**.

It can be observed that for the best analogue, the peptide #B3, a loading dose group was added in order to assess the effect of an initial high dose administration.

Table 42. Summary of animals used, concentration and products administered in efficacy study using Pa01 pneumonia experimentation model.

Pa01 strain groups			
Compound	Dosing pattern (mg·kg ⁻¹ /8h)	Treatment time (h)	Animal number
B3	12+12+12+12+12+12	72	5
B3	36+12+12	24	4
PxB	12+12+12+12+12+12	72	6
CMS	20+20+20+20+20+20	72	5
Saline	0	72	5

Table 43. Summary of animals used, concentration and products administered in efficacy study using Pa147 pneumonia experimentation model.

Pa147 strain groups			
Compound	Dosing pattern (mg/kg/8h)	Treatment time (h)	Animal number
B3	12+12+12+12+12+12	72	5
B3	36+12+12	24	5
PxB	12+12+12+12+12+12	72	6
CMS	20+20+20+20+20+20	72	5
Saline	0	72	5

Each animal was treated with the appropriate compound via intraperitoneal injection with the corresponding dose every 8 hours; the treatment was planned to

last 72 hours, except for the loading dose group, which was reduced to 24 hours due the high initial amount of peptide injected. A total of 25 animals were used for the Pa01 *P. aeruginosa* strain, whereas for the Pa147 experimental pneumonia model 26 animals were used.

During all the treatments, each animal was closely monitored, mortality was recorded, and samples were extracted and processed immediately after the death of mice. Survivor mice were euthanized with sodium thiopental after 72 hours for the regular groups or 24 hours for the loading dose group. Aseptic thoracotomies were carried out, and blood samples were obtained for qualitative blood cultures; results were expressed as positive (≥ 1 cfu present in the plate) or negative. Lungs were aseptically extracted, weighted, and homogenized in sterile saline before quantitative cultures (\log_{10} cfu·g⁻¹) in Columbia agar with 5% sheep blood plates.

5.5. EXPERIMENTAL PART

Colistin analogues were synthesized as explained in the **section 5.1.1**. The analogues were usually synthesized using an initial amount of resin between 35 and 250 mg, approximately. Two different resins were used depending on the analogue to synthesize: BHA with a functionalization of $0.69 \text{ mmol}\cdot\text{g}^{-1}$ and 2-CTC with a functionalization of $1.56 \text{ mmol}\cdot\text{g}^{-1}$. However, after the incorporation of the first amino acid, the functionalization was determined in each synthesis, following the protocol detailed in **section 5.1.4.2.4**.

After the cleavage, the peptides were cyclized by disulfide bond or by an ester bond, both procedures described in **section 5.1.4.2.5**. In **Table 44** it is specified the strategy followed for each peptide: which resin was used, the conditions of the cleavage, and how the peptide was cyclized. In the case of the analogue B1, a full deprotection was needed once the cyclization was completed.

Table 44. Summary of resins used during the synthesis of each analogue, together with the cleavage conditions and the cyclization strategy followed; in the case of the cyclization by an amide bond, a second full deprotection was needed.

Peptide	Resin used	Cleavage	Cyclization strategy	Full deprotection
A1	BHA	TFA/TES/H ₂ O	Disulfur bond	---
A2	BHA	TFA/TES/H ₂ O	Disulfur bond	---
A3	BHA	TFA/TES/H ₂ O	Disulfur bond	---
A4	BHA	TFA/TES/H ₂ O	Disulfur bond	---
A5	BHA	TFA/TES/H ₂ O	Disulfur bond	---
A6	BHA	TFA/TES/H ₂ O	Disulfur bond	---
A7	BHA	TFA/TES/H ₂ O	Disulfur bond	---
B1	2-CTC	DCM/HFIP/TFE/TES	Amide bond	TFA/TES/H ₂ O
B2	2-CTC	TFA/TES/H ₂ O	Disulfur bond	---
B3	2-CTC	TFA/TES/H ₂ O	Disulfur bond	---
B4	2-CTC	TFA/TES/H ₂ O	Disulfur bond	---
B5	2-CTC	TFA/TES/H ₂ O	Disulfur bond	---
B6	2-CTC	TFA/TES/H ₂ O	Disulfur bond	---
B7	2-CTC	TFA/TES/H ₂ O	Disulfur bond	---
B8	2-CTC	TFA/TES/H ₂ O	Disulfur bond	---
B9	2-CTC	TFA/TES/H ₂ O	Disulfur bond	---

Table 45 summarizes the synthesis conducted for each analogue, whereas **Table 46** details the characterization performed by HPLC and mass spectrometry.

Some analogues (#A5-#A7) were already available since they had been synthesised previously by other members of our research group, thus, all the information regarding their synthesis was not available; however, their purity was determined before using them in the different assays.

Table 45. Summary of the details of the synthesis for all the peptides, including the crude and pure peptide amount, as well as the yield.

Peptide	Initial resin weight (mg)	Resin loading (mg·mmol ⁻¹)	Crude peptide weight (mg)	Synthesis yield (%)	Pure peptide weight (mg)	Purity (by HPLC) (%)	Final yield (%)
A1	37.4	1.1	50.0	70	16.6	> 99	24
A2	39.0	1.1	55.0	73	14.3	> 99	19
A3	49.9	1.1	58.0	60	15.1	> 99	16
A4	49.9	1.1	63.0	64	13.8	> 99	14
A5	--	--	--	--	--	> 98	--
A6	--	--	--	--	--	> 98	--
A7	--	--	--	--	--	> 99	--
B1	260.0	0.9	275.0	70	86.2	> 98	22
B2	131.0	0.8	92.0	51	44.0	> 99	24
B3	131.0	0.8	145.0	82	85.9	> 99	49
B4	135.0	0.5	60.4	51	24.3	> 99	21
B5	135.0	0.5	64.1	56	30.9	> 99	27
B6	130.0	0.5	55.0	50	12.4	> 99	11
B7	130.0	0.5	50.0	47	13.0	> 99	12
B8	200.0	0.5	130.8	76	47.0	> 99	27
B9	200.0	0.5	115.7	69	38.0	> 99	22

Table 46. Summary of characterization by HPLC and mass spectrometry for each analogue.

Peptide	HPLC gradient	Retention time (min)	Mass spectrometry ($m \cdot z^{-1}$)
A1	5-95% B in 30 min	12.4	$[M+H]^+ = 1147.8$, $[M+2H/2]^{2+} = 574.5$
	15-30% B in 30 min	14.4	
A2	5-95% B in 30 min	14.4	$[M+H]^+ = 1175.9$, $[M+2H/2]^{2+} = 588.7$
	25-40% B in 30 min	7.0	
A3	5-95% B in 30 min	17.8	$[M+H]^+ = 1204.1$, $[M+2H/2]^{2+} = 602.8$
	20-35% B in 30 min	14.7	
A4	5-95% B in 30 min	17.9	$[M+H]^+ = 1232.1$, $[M+2H/2]^{2+} = 616.8$
	20-35% B in 30 min	22.9	
A5	5-95% B in 30 min	16.1	$[M+H]^+ = 1204.0$, $[M+2H/2]^{2+} = 602.7$
	20-35% B in 30 min	--	
A6	5-95% B in 30 min	17.7	$[M+H]^+ = 1231.7$, $[M+2H/2]^{2+} = 616.6$
	20-35% B in 30 min	--	
A7	5-95% B in 30 min	17.7	$[M+H]^+ = 1190.0$, $[M+2H/2]^{2+} = 595.8$
	20-35% B in 30 min	--	
B1	5-95% B in 30 min	27.5	$[M+H]^+ = 1098.7$, $[M+2H/2]^{2+} = 550.1$
	20-35% B in 30 min	21.1	
B2	5-95% B in 30 min	14.7	$[M+H]^+ = 1176.9$, $[M+2H/2]^{2+} = 589.2$
	20-35% B in 30 min	16.1	
B3	5-95% B in 30 min	15.4	$[M+H]^+ = 1120.1$, $[M+2H/2]^{2+} = 560.7$
	20-35% B in 30 min	21.2	
B4	5-95% B in 30 min	15.7	$[M+H]^+ = 1178.2$, $[M+2H/2]^{2+} = 589.8$
	20-35% B in 30 min	22.3	
B5	5-95% B in 30 min	16.4	$[M+H]^+ = 1120.4$, $[M+2H/2]^{2+} = 560.9$
	20-35% B in 30 min	26.5	
B6	5-95% B in 30 min	--	$[M+H]^+ = 1134.6$, $[M+2H/2]^{2+} = 568.8$
	20-35% B in 30 min	11.0	
B7	5-95% B in 30 min	--	$[M+H]^+ = 1077.8$, $[M+2H/2]^{2+} = 539.7$
	20-35% B in 30 min	15.9	
B8	5-95% B in 30 min	--	$[M+H]^+ = 1162.6$, $[M+2H/2]^{2+} = 582.1$
	20-35% B in 30 min	14.0	
B9	5-95% B in 30 min	--	$[M+H]^+ = 1105.9$, $[M+2H/2]^{2+} = 550.1$
	20-35% B in 30 min	19.2	

The synthesis of analogue #B3 was conducted under three different conditions in order to optimize it. **Table 47** details how much time was needed to couple each amino acid depending on the coupling reagents used, whereas **Table 48** includes the information regarding the synthesis performed.

Table 47. Summary of the time needed for the coupling of each amino acid depending on the reagents used to perform the elongation of the peptide chain.

Amino acid coupled	Duration of the coupling (min)		
	DIC/HOBt	HATU/HOBt/DIEA	DIC/K-Oxy
Ttr	60	60	60
Dab	60	60	60+30
Dab	60	60	60+30
Leu	60	60	60+30
Leu	60	60	60+30
Dab	60	60	60+30
Cys	60	60+30	60+30
Dab	60	60	60+30
Thr	60	60	60+30
D-Adec	60	60	60

Table 48. Summary of the details of the synthesis of the analogue #B3 for the three coupling conditions used.

Peptide B3	Initial resin weight (mg)	Resin loading (mg·mmol ⁻¹)	Crude peptide weight (mg)	Synthesis yield (%)	Pure peptide weight (mg)	Purity (by HPLC) (%)	Final yield (%)
DIC/HOBt	1000	0.5	659	78	287	> 99	34
HATU/HOBt /DIEA	1000	0.5	620	73	205	> 99	24
DIC/K-Oxy	1000	0.5	560	67	253	> 99	30

6. REFERENCES

Abyar, S., Khandar, A. A., Selehi, R., Hosseini-Yazdi, S. A., Alizadeh, E., Mahkam, M., Jamalpoor, A., White, J. M., Shojaei, M., Aizpurua-Olaizola, O., Maserreuw, R., Janssen, M. J. (2019). In vitro nephrotoxicity and anticancer potency of newly synthesized cadmium complexes. *Scientific Reports*, 9(1), 14686.

Adzitey, F. (2015). Antibiotic classes and antibiotic susceptibility of bacterial isolates from selected poultry; a mini review. *World's Veterinary Journal*, 6(1), 36-41.

Ageitos, J. M., Sánchez-Pérez, A., Calo-Mata, P., Villa, T. G. (2017). Antimicrobial peptides (AMPs): Ancient compounds that represent novel weapons in the fight against bacteria. *Biochemical Pharmacology*, 133, 117-138.

Ainsworth, G.C., Brown, A. M., Brownlee, G. (1947). 'Aerosporin', an Antibiotic Produced by *Bacillus aerosporus* Greer. *Nature*, 160(4060), 262-263.

Ambroggio, E. E., Separovic, F., Bowie, J., Fidelio, G. D. (2004). Surface behaviour and peptide-lipid interactions of the antibiotic peptides, Maculatin and Citropin. *Biochimica et Biophysica Acta*, 1664(1), 31-37.

Andrade, S., Ramalho, M. J., Loureiro, J. A., Pereira, M. C. (2021). Liposomes as biomembrane models: Biophysical techniques for drug-membrane interaction studies. *Journal of Molecular Lipids*, 334, 116141.

Angelova, M. I., Dimitrov, D. S. (1986). Liposome electroformation. *Faraday Discussion of the Chemical Society*, 81, 303-311.

Azad, M. A. K., Akter, J., Rogers, K. L., Nation, R. L., Velkov, T., Li, J. (2015). Major pathways of polymyxin-induced apoptosis in rat kidney proximal tubular cells. *Antimicrobial Agents and Chemotherapy*, 59(4), 2136-2143.

Baciu, M., Sebai, S. C., Ces, O., Mulet, X., Clarke, J. A., Shearman, G. C., Law, R. V., Templer RH, Plisson, C., Parker, C. A., Gee, A. (2006). Degradative transport of cationic amphiphilic drugs across phospholipid bilayers. *Philosophical Transactions. Series A, Mathematical, Physical and Engineering Sciences*, 364(1847), 2597-614.

Balls, A. K., Hale, W. S., Harris, T. H. (1942). A Crystalline Protein Obtained from a Lipoprotein of Wheat Flour. *Cereal Chemistry*, 19, 279-288.

Bally, M., Dendukuri, N., Rich, B., Nadeau, L., Helin-Salmivaara, A., Garbe, E., Brophy, J. M. (2017). Risk of acute myocardial infarction with NSAIDs in real world use: bayesian meta-analysis of individual patient data. *BMJ (Clinical Research ed.)*, 357, j1909.

Bangalore, S., Fakhri, R., Wandel, S., Toklu, B., Wandel, J., Messerli, F. H. (2017). Renin angiotensin system inhibitors for patients with stable coronary artery disease without heart

failure: systematic review and meta-analysis of randomized trials. *BMJ (Clinical Research ed.)*, 356, j4.

Bangham, A. D., Horne, R. W. (1964). Negative staining of phospholipids and their structural modification by surface-active agents as observed in the electron microscope. *Journal of Molecular Biology*, 8(5), 660-668.

Barnett, M., Bushby, S. R., Wilkinson, S. (1964). SODIUM SULPHOMETHYL DERIVATIVES OF POLYMYXINS. *British Journal of Pharmacology and Chemotherapy*, 23(3), 552-574.

Bartholomew, J. W., Mittwer, T. (1952). The gram stain. *Bacteriological Reviews*, 16(1), 1-29.

Beining P. R., Huff E., Prescott B., Theodore T. S. (1975). Characterization of the lipids of mesosomal vesicles and plasma membranes from *Staphylococcus aureus*. *Journal of Bacteriology*, 121, 137–143.

Belvins, S. M., Bronze, M. S. (2010). Robert Koch and the 'golden age' of bacteriology. *International Journal of Infectious Diseases*, 14(9), e744-e751.

Benedict, R. G., Langlykke, A. F. (1947). Antibiotic activity of *Bacillus polymyxa*. *Journal of Bacteriology*, 54(1).

Bercellini, W. (2015). Immune Hemolysis: Diagnosis and Treatment Recommendations. *Seminars in Hematology*, 52(4), 304-312.

Beris, P., Picard, V. (2015). Non-immune Hemolysis: Diagnostic Considerations. *Seminars in Hematology*, 52(4), 287-303.

Bigot, A., Tchan, M. C., Thoreau, B., Blasco, H., Maillot, F. (2017). Liver involvement in urea cycle disorders: a review of the literature. *Journal of Inherited Metabolic Disease*, 40(6), 757-769.

Bines, J. E., Israel, E. J. (1991). Hypoproteinemia, anemia, and failure to thrive in an infant. *Gastroenterology*, 101(3), 848-856.

Boakes, S., Jorgensen, J. H., Boakes, S., Collins, M. S., McElmeel, M., Cushion, M. T., Patterson, T. F. (2015). Poster F-735, 55th Interscience Conference on Antimicrobial Agents and Chemotherapy, San Diego, CA, USA.

Boucher, H. W., Talbot, G. H., Bradley, J. S., Edwards, J. E., Gilbert, D., Rice, L. B., Scheld, M., Spellberg, B., Bartlett, J. (2009). Bad bugs, no drugs: no ESKAPE! An update from the Infectious Diseases Society of America. *Clinical infectious diseases : an official publication of the Infectious Diseases Society of America*, 48(1), 1-12.

Breuer, E., Chorghade, M. S., Fischer, J., Golomb, G. (2009). Glossary of terms related to pharmaceuticals (IUPAC Recommendations 2009). *Pure and Applied Chemistry*, 81(5), 971-999.

Brewster, U. C., Rastegar, A. (2014). Acute Interstitial Nephritis. National Kidney Foundation Primer on Kidney Diseases, 6th Edition, 312-317.

Brockman, H. (1999). Lipid monolayers: why use half a membrane to characterize protein-membrane interactions?. *Current Opinion in Structural Biology*, 9(4), 438-443.

Brown, P., Boakes, S., Duperchy, E., Simonovic, M., Abdulle, O., Divall, N., Stanway, S. J., Wilson, A., Moss, S. F., Dawson, M. J. (2015). Poster F-739, 55th Interscience Conference on Antimicrobial Agents and Chemotherapy, San Diego, CA, USA.

Brown, P., Dawson, M., Simonovic, M., Boakes, S., Duperchy, E. (2014). Duperchy, patent application WO2014/188178.

Brown, P., Dawson, M., Simonovic, M., Boakes, S., Duperchy, E., Stanway, S. J., Wilson, A., Moss, S. F. (2015). Patent application WO2015/135976.

Bush, K. (2012). Antimicrobial agents targeting bacterial cell walls and cell membranes. *Scientific and Technical Review*, 31(1), 43-56.

Cajal, Y., Berg, O. G., Jain, M. K. (1995). Direct vesicle-vesicle exchange of phospholipids mediated by polymyxin B. *Biochemical and Biophysical Research Communications*, 210(3), 746-752.

Cajal, Y., Ghanta, J., Easwaran, K., Surolia, A., Jain, M. K. (1996). Specificity for the exchange of phospholipids through polymyxin B mediated intermembrane molecular contacts. *Biochemistry*, 35(18), 5684-5695.

Carvalho, L., Morales, J. C., Pérez-Victoria, J. M., Pérez-Victoria, I. (2015). Hemolytic activity and solubilizing capacity of raffinose and melezitose fatty acid monoesters prepared by enzymatic synthesis. *European journal of pharmaceutics and biopharmaceutics: official journal of Arbeitsgemeinschaft fur Pharmazeutische Verfahrenstechnik e.V*, 92, 139-145.

Cassir, N., Rolain, JM., Brouqui, P. (2014). A new strategy to fight antimicrobial resistance: the revival of old antibiotics. *Frontiers in Microbiology*, 5(551).

CDC website. (2022). <https://www.cdc.gov/drugresistance/covid19.html>

Cebrero, T. C. (2020). Respuesta inmunitaria celular y eficacia del tratamiento con células de memoria e IgM en la neumonía experimental por *Pseudomonas aeruginosa* y *Acinetobacter baumannii*. Tesis doctoral, Universidad de Sevilla.

Chinard, F. P. (1964). KIDNEY, WATER AND ELECTROLYTES. *Annual Review of Physiology*, 26, 187-226.

Choi, C. H., Hyun, S. H., Lee, J. Y., Lee, J. S., Lee, Y. S., Kim, S. A., Chae, J. P., Yoo, S. M., Lee, J. C. (2008). Acinetobacter baumannii outer membrane protein A targets the nucleus and induces cytotoxicity. *Cellular Microbiology*, 10(2), 309-319.

Chopra, I., Roberts, M. (2001). Tetracycline Antibiotics: Mode of Action, Applications, Molecular Biology, and Epidemiology of Bacterial Resistance. *Microbiology and Molecular Biology Reviews*, 65(2), 232-260.

Choquet-Kastylevsky, G., Vial, T., Descotes, J. (2002). Allergic adverse reactions to sulfonamides. *Current Allergy and Asthma Reports*, 2(1), 16-25.

Coates, A. RM., Halls, G., Hu, Y. (2011). Novel classes of antibiotics or more of the same? *British Journal of Pharmacology*, 163(1), 184-194.

Corbett, D., Wise, A., Langley, T., Skinner, K., Trimby, E., Birchall, S., Dorali, A., Sandiford, S., Williams, J., Warn, P., Vaara, M., Lister, T. (2017). Potentiation of Antibiotic Activity by a Novel Cationic Peptide: Potency and Spectrum of Activity of SPR741. *Antimicrobial Agents and Chemotherapy*, 61(8), e00200-e00217.

Corrêa, J. A. F., Evangelista, Al. G., Nazareth, T. M., Luciano, F. B. (2019). Fundamentals on the Molecular Mechanism of Action of Antimicrobial Peptides. *Acta Materialia*, 8, 100494.

Cruz, G. F., de Araujo, I., Torres, M. D. T., de la Fuente-Nunez, C., Oliveira Jr., V. X, Ambrosio, F. N., Lombello, C. B., Almeida, D. V., Silva, F. D., Garcia, W. (2020). Photochemically-Generated Silver Chloride Nanoparticles Stabilized by a Peptide Inhibitor of Cell Division and Its Antimicrobial Properties. *Journal of Inorganic and Organometallic Polymers and Materials*, 30, 2464–2474.

Demchick, P., Koch, A. L. (1996). The permeability of the wall fabric of Escherichia coli and Bacillus subtilis. *Journal of Bacteriology*, 178(3), 768-773.

Dettmeyer, R. B., Preuß, J., Wollersen, H., Madea, B. (2005). Heroin-associated nephropathy. *Expert Opinion on Drug Safety*, 4(1), 19-28. |

De Visser, P. C., Kriek, N. M. A. J., van Hooft, P. A. V., Van Schepdael, A., Filippov, D. V., van der Marel, G. A., Overkleeft, H. S., van Boom, J. H., Noort, D. (2003). Solid-phase synthesis of polymyxin B1 and analogues via a safety-catch approach. *The Journal of Peptide Research: Official Journal of the American Peptide Society*, 61(6), 298-306.

Dodge, J. T., Philips, G. B. (1967). Composition of phospholipids and of phospholipid fatty acids and aldehydes in human red cells. *Journal of Lipid Research*, 8(6), 667-675.

Doktorova, M., Heberle, F. A., Eicher, B., Standaert, R. F., Katsaras, J., London, E., Pabst, G., Marquardt, D. (2018). Preparation of asymmetric phospholipid vesicles for use as cell membrane models. *Nature Protocols*, 13(9), 2086-2101.

Dubos, R. J. (1939). STUDIES ON A BACTERICIDAL AGENT EXTRACTED FROM A SOIL BACILLUS : II. PROTECTIVE EFFECT OF THE BACTERICIDAL AGENT AGAINST EXPERIMENTAL PNEUMOCOCCUS INFECTIONS IN MICE. *Journal of Experimental Medicine*, 70(1), 11-17.

Dubos, R. J., Hotchkiss, R. D. (1941). THE PRODUCTION OF BACTERICIDAL SUBSTANCES BY AEROBIC SPORULATING BACILLI. *Journal of Experimental Medicine*, 73(5), 629-640.

Duwe, A. K., Rupar, C. A., Horsman, G. B., Vas, S. I. (1986). In vitro cytotoxicity and antibiotic activity of polymyxin B nonapeptide. *Antimicrobial Agents and Chemotherapy*, 30(2), 340-341.

El-Faham, A. (2000). Addition of HOXt (X = A or B) improves the efficiency of phenol-based coupling reagents during peptide synthesis. *Letters in Peptide Science*, 7, 113-121.

Escribá, P. V. (2006). Membrane-lipid therapy: a new approach in molecular medicine. *Trends in Molecular Medicine*, 12(1), 34-43.

Etebu, E., Arikekpar, I. (2016). Antibiotics: Classification and mechanisms of action with emphasis on molecular perspectives. *International Journal of Applied Microbiology and Biotechnology Research*, 4, 90-101.

EUCAST website. (2022). https://www.eucast.org/clinical_breakpoints/

Falagas, M. E., Kasiakou, S. K. (2006). Toxicity of polymyxins: a systematic review of the evidence from old and recent studies. *Critical Care (London, England)*, 10(1), R27.

Fomnya, H. J., Ngulde, S. I., Amshi, K. A., Bilbonga, G. (2021). Antibiotics: Classifications and mechanism of resistance. *International Journal of Applied Microbiology and Biotechnology Research*, 9(3), 38-50.

Forrest, R. D. (1982). Early history of wound treatment. *Journal of the Royal Society of Medicine*, 75(3), 198-205.

Franken, L. E., Grünewald, K., Boekema, E. J., Stuart, M. C. A. (2020). A Technical Introduction to Transmission Electron Microscopy for Soft-Matter: Imaging, Possibilities, Choices, and Technical Developments. *Small (Weinheim and der Bergstrasse, Germany)*, 16(14), e1906198.

Frank, U., Tacconelli, E. (2012). The Daschner Guide to In-Hospital Antibiotic Therapy. European standards. Available online at: <http://www.springer.com/978-3-642-18401-7>. 300p.

Freceer, V., Ho, B., Ding, J. L. (2004). De novo design of potent antimicrobial peptides. *Antimicrobial Agents and Chemotherapy*, 48(9), 3349-3357.

Freemantle, N., Young, J. C. P., Mason, J., Harrison, J. (1999). Beta Blockade after myocardial infarction: systematic review and meta regression analysis. *BMJ (Clinical Research ed.)*, 318(7200), 1730-1737.

Fuerst, J. A. (2005). Intracellular compartmentation in planctomycetes. *Annual Review of Microbiology*, 59, 299-328.

Fuoco, D. (2012). Classification Framework and Chemical Biology of Tetracycline-Structure-Based Drugs. *Antibiotics (Basel)*, 1(1), 1-13.

Gaines, G. L. (1966). Insoluble monolayers at liquid-gas interfaces [by] George L. Gaines, Jr. New York, Interscience Publishers.

Gallardo-Godoy, A., Hansford, K.A., Muldoon, C., Becker, B., Elliott, A. G., Huang, J. X., Pelingon, R., Butler, M. S., Blaskovich, M. A. T., Cooper, M. A. (2019). Structure-Function Studies of Polymyxin B Liponapeptides. *Molecules*, 24(3), 553.

Gest, H. (2009). Homage to Robert Hooke (1635-1703): new insights from the recently discovered Hooke Folio. *Perspectives in Biology and Medicine*, 52(3), 392-399.

Gil-Marqués, M. L., Pachón-Ibáñez, M. E., Pachón, J., Smani, Y. (2018). Effect of Hypoxia on the Pathogenesis of *Acinetobacter baumannii* and *Pseudomonas aeruginosa* In Vitro and in Murine Experimental Models of Infection. *Infection and Immunity*, 68(10), e00543-e00548.

Goh, K. P. (2004). Management of hyponatremia. *American Family Physician*, 69(10), 2387-2394.

Gonzalez-Perez, D., Ratcliffe, J., Tan, S. K., Wong, M. C. M., Yee, Y. P., Nyabadza, N., Xu, J. H., Wong, T. S., Tee, K. L. (2021). Random and combinatorial mutagenesis for improved total production of secretory target protein in *Escherichia coli*. *Scientific Reports*, 11(1), 5290.

Gordeev, M. F. (2018). Polymyxin soft drug MRX-8 with potential to address the class nephrotoxicity. 3rd International Conference on Polymyxins, (Madrid).

Gordeev, M. F., Liu, J., Wang, Z., Yuan, Z. (2016). Antimicrobial polymyxins for treatment of bacterial infections. Patent Application WO2016/100578.

Gottschalk, S., Ifrah, D., Lerche, S., Gottlieb, C. T., Cohn, M. T., Hiasa, H., Hansen, P. R., Gram, L., Ingmer, H., Thomsen, L. E. (2013). The antimicrobial lysine-peptoid hybrid LP5 inhibits DNA replication and induces the SOS response in *Staphylococcus aureus*. *BMC Microbiology*, 13, 192.

Greco, I., Molchanova, N., Holmedal, E., Jenssen, H., Hummel, B. D., Watts, J. L., Håkansson, J., Hansen, P. R., Svenson, J. (2020). Correlation between hemolytic activity, cytotoxicity and systemic in vivo toxicity of synthetic antimicrobial peptides. *Scientific Reports*, 10(1), 13206.

Gregoriadis, G. (1984). Preparation of Liposomes. *CRC, Boca Ratón (Florida)*.

Griffin, J. H., Judice, J. K. (2002). Multivalent polymyxin antibiotics. Patent Application US6380356B1.

Groves, M. L., Peterson, R. F., Kiddy, C. A. (1965). Poliomorphism in the red protein isolated from milk of individual cows. *Nature*, 207(5000), 1007-1008.

Gruszecki, W. I., Gagos, M., Herec, M., Kernén, P. (2003). Organization of antibiotic amphotericin B in model lipid membranes. A mini review. *Cellular & Molecular Biology Letters*, 8, 161–170.

Hancock, R. E. (1997). Antibacterial peptides and the outer membranes of gram-negative bacilli. *Journal of Medical Microbiology*, 46(1), 1-3.

Hancock, R. E. (1998). Cationic peptides: a new source of antibiotics. *Trends in Biotechnology*, 16(2), 82-88.

Hancock, R. E., Chapple, D. S. (1999). Peptide antibiotics. *Antimicrobial Agents and Chemotherapy*, 43(6), 1317-1323.

Hartman, M., Berditsch, M., Hawecker, J., Ardakani, M. F., Gerthsen, D., Ulrich, A. S. (2010). Damage of the Bacterial Cell Envelope by Antimicrobial Peptides Gramicidin S and PGLa as Revealed by Transmission and Scanning Electron Microscopy. *Antimicrobial Agents and Chemotherapy*, 54(8), 3132-3142.

Helsel, M. E., Franz, K. J. (2015). Pharmacological activity of metal binding agents that alter copper bioavailability. *Dalton Transactions*, 44(19), 8760-8770.

Henry, R., Crane, B., Powell, D., Lucas, D. D., Li, Z., Aranda, J., Harrison, P., Nation, R. L., Adler, B., Harper, M., Boyce, J. D., Li, J. (2015). The transcriptomic response of *Acinetobacter baumannii* to colistin and doripenem alone and in combination in an in vitro pharmacokinetics/pharmacodynamics model. *The Journal of Antimicrobial Chemotherapy*, 70(5), 1303-1313.

Henry, R. J. (1943). THE MODE OF ACTION OF SULFONAMIDES. *Bacteriology Reviews*, 7(4), 175-262.

Hernández, V. A., Karlsson, G., Edwards, K. (2011). Intrinsic Heterogeneity in Liposome Suspensions Caused by the Dynamic Spontaneous Formation of Hydrophobic Active Sites in Lipid Membranes. *Langmuir*, 27(8), 4873-4883.

He, S. W., Zhang, J., Li, N. Q., Zhou, S., Yue, B., Zhang, M. (2017). A TFPI-1 peptide that induces degradation of bacterial nucleic acids, and inhibits bacterial and viral infection in half-smooth tongue sole, *Cynoglossus semilaevis*. *Fish & Shellfish Immunology*, 60, 466-473.

Hirsch, J. G. (1956). Phagocytin: a bactericidal substance from polymorphonuclear leucocytes. *Journal of Experimental Medicine*, 103(5), 589-611.

Hobbs, D. C. (1996). Lower alkanoyl esters of polymyxin antibiotics. Patent US3450687A.

Huan, Y., Kong, Q., Mou, H., Yi, H. (2020). Antimicrobial Peptides: Classification, Design, Application and Research Progress in Multiple Fields. *Frontiers in Microbiology*, 11, 582779.

ICH guideline M3(R2) on nonon non-clinical safety studies for the conduct of human clinical trials and marketing authorisation for pharmaceuticals Step 5. (2022). www.ema.europa.eu/en/

Imura, Y., Choda, N., Matsuzaki, K. (2008). Magainin 2 in action: distinct modes of membrane permeabilization in living bacterial and mammalian cells. *Biophysical Journal*, 95(12), 5757-5765.

James, D. (1971). *The Birth of Penicillin and the Disarming of Microbes*, by Ronald Hare, London, George Allen & Unwin, 1970, pp. 236, illus., £3.15. *Medical History*, 15(4), 410.

Kahre, T., Teder, M., Panov, M., Metspalu, A. (2004). Severe CF manifestation with anaemia and failure to thrive in a 394delTT homozygous patient. *Journal of Cystic Fibrosis*, 3(1), 58-60.

Kaiser, E., Colecott, R.L., Bossinger, C.D. Cook, P.I. (1970). Color test for detection of free terminal amino groups in the solid-phase synthesis of peptides. *Analytical Biochemistry*, 34(2), 595-598.

Kanazawa, K., Sato, Y., Ohki, K., Okimura, K., Uchida, Y., Shindo, M., Sakura, N. (2009). Contribution of each amino acid residue in polymyxin B(3) to antimicrobial and lipopolysaccharide binding activity. *Chemical & Pharmaceutical Bulletin*, 57(3), 240-244.

Katsuma, N., Sato, Y., Ohki, K., Okimura, K., Ohnishi, K., Sakura, N. (2009). Development of des-fatty acyl-polymyxin B decapeptide analogs with *Pseudomonas aeruginosa*-specific antimicrobial activity. *Chemical & Pharmaceutical Bulletin*, 57(4), 332-336.

Kennedy, E. P. (1982). Osmotic regulation and the biosynthesis of membrane-derived oligosaccharides in *Escherichia coli*. *Proceedings of the National Academy of Sciences of the United States of America*, 79(4), 1092-1095.

Kłodzińska, S. N., Priemel, P. A., Rades, T., Nielsen, H. M. (2018). Combining diagnostic methods for antimicrobial susceptibility testing - A comparative approach. *Journal of Microbiological Methods*, 144, 177-185.

Klose, J., El-Faham, A., Henklein, P., Carpino, L. A., Bienert, M. (1999). Addition of HOAt dramatically improves the effectiveness of pentafluorophenyl-based coupling reagents. *Tetrahedron Letters*, 40(11), 2045-2048.

Kragol, G., Lovas, S., Varadi, G., Condie, B. A., Hoffmann, R., Otvos Jr., L. (2001). The antibacterial peptide pyrrolicorin inhibits the ATPase actions of DnaK and prevents chaperone-assisted protein folding. *Biochemistry*, 40(10), 3016-3026.

Kresge, N., Simoni, R. D., Hill, R. L. (2004). Selman Waksman: the Father of Antibiotics. *Journal of Biological Chemistry*, 279(48), 101-102.

Krieg, N. R., Staley, J. T., Brown, D. R., Hedlund, B. P., Paster, B. J., Ward, N. L. Ludwig, W., Whitman, W. B. (2010). *Bergey's Manual of Systematic Bacteriology*. Springer, Athens, GA (USA).

Kwon, H. I., Kim, S., Oh, M. H., Na, S. H., Kim, Y. J., Jeon, Y. H., Lee, J. C. (2017). Outer membrane protein A contributes to antimicrobial resistance of *Acinetobacter baumannii* through the OmpA-like domain. *The Journal of Antimicrobial Chemotherapy*, 72(11), 3012-3015.

Landman, D., Georgescu, C., Martin, D. A., Quale, J. (2008). Polymyxins revisited. *Clinical Microbiology Reviews*, 21(3), 449-465.

Lane, N. (2015). The unseen world: reflections on Leeuwenhoek (1677) 'Concerning little animals'. *Philosophical Transactions of The Royal Society B*, 370.

Laouini, A., Jaafar-Maalej, C., Limayem-Blouza, I., Sfar, S., Charcosset, C., Fessi, H. (2012). Preparation, Characterization and Applications of Liposomes: State of the Art. *Journal of Colloid Science and Biotechnology*, 1(2), 147-168.

Lasic, D. D. (1988). The mechanism of vesicle formation. *The Biochemical Journal*, 256(1), 1-11.

Lavis, L. D. (2008). Ester bonds in prodrugs. *ACS Chemical Biology*, 3(4), 203-206.

Le, C. F., Fang, C. M., Sekaran, S. D. (2017). Intracellular Targeting Mechanisms by Antimicrobial Peptides. *Antimicrobial Agents and Chemotherapy*, 61(4), e02340-14.

Ledger, E. V., Sabnis, A., Edwards, A. M. (2022). Polymyxin and lipopeptide antibiotics: membrane-targeting drugs of last resort. *Microbiology (Reading, England)*, 168(2).

Levitt, R. E., Ostrow, J. D. (1980). Hemolytic jaundice and gallstones. *Gastroenterology*, 78(4), 821-830.

Li, H., Zhao, T., Sun, Z. (2017). Analytical techniques and methods for study of drug-lipid membrane interactions. *Reviews in Analytical Chemistry*, 37(1), 20170012.

Li, L., Sun, J., Xia, S., Tian, X., Cheserek, M. J., Le, G. (2016). Mechanism of antifungal activity of antimicrobial peptide APP, a cell-penetrating peptide derivative, against *Candida albicans*: intracellular DNA binding and cell cycle arrest. *Applied Microbiology and Biotechnology*, 100(7), 3245-3253.

Lipkin, R. B., Lazaridis, T. (2015). Implicit Membrane Investigation of the Stability of Antimicrobial Peptide β -Barrels and Arcs. *Journal of Membrane Biology*, 248(3), 469-486.

Li, Z., Cao, Y., Yi, L., Liu, J. H., Yang, Q. (2019). Emergent Polymyxin Resistance: End of an Era? *Open Forum Infectious Diseases*, 6(10), ofz368.

Longo, N., Ardon, O., Vanzo, R., Schwartz, E., Pasquali, M. (2011). Disorders of creatine transport and metabolism. *American Journal of Medical Genetics. Part C, Seminars in Medical Genetics*, 157C(1), 72-78.

Lúcio, M., Lima, J. L. F. C., Reis, S. (2010). Drug-membrane interactions: significance for medicinal chemistry. *Current Medicinal Chemistry*, 17(17), 1795-1809.

Machado, R. F., Gladwin, M. T. (2010). Pulmonary hypertension in hemolytic disorders: pulmonary vascular disease: the global perspective. *Chest*, 137(6 Suppl), 30S-38S.

Madigan, M. T., Martinko, J. M., Parker, J. (2002). Brock biology of microorganisms (10th edition). *Prentice Hall/Pearson Education*, Upper Saddle River, NJ (USA).

Malanovic, N., Lohner, K. (2016). Gram-positive bacterial cell envelopes: The impact on the activity of antimicrobial peptides. *Biochimica et Biophysica Acta (BBA) - Biomembranes*, 1858(5), 936-946.

Magee, T. V., Brown, M. F., Starr, J. T., Ackley, D. C., Abramite, J. A., Aubrecht, J., Butler, A., Crandon, J. L., Dib-Hajj, F., Flanagan, M. E., Granskog, K., Hardink, J. R., Huband, M. D., Irvine, R., Kuhn, M., Leach, K. L., Li, B., Lin, J., Luke, D. R., MacVane, S. H., Miller, A. A., McCurdy, S., McKim, J. M. Jr., Nicolau, D. P., Nguyen, T. T., Noe, M. C., O'Donnell, J. P., Seibel, S. B., Shen, Y., Stepan, A. F., Tomaras, A. P., Wilga, P. C., Zhang, L., Xu, J., Chen, J. M. (2013). Discovery of Dap-3 polymyxin analogues for the treatment of multidrug-resistant Gram-negative nosocomial infections. *Journal of Medicinal Chemistry*, 56(12), 5079-5093.

Mardirossian, M., Grzela, R., Giglione, C., Meinel, T., Gennaro, R., Mergaert, P., Scocchi, M. (2014). The host antimicrobial peptide Bac71-35 binds to bacterial ribosomal proteins and inhibits protein synthesis. *Chemistry & Biology*, 21(12), 1639-1647.

Mardirossian, M., Pérébasquine, N., Benincasa, M., Gambato, S., Hofmann, S., Huter, P., Müller, C., Hilpert, K., Innis, C. A., Tossi, A., Wilson, D. N. (2018). The Dolphin Proline-Rich Antimicrobial Peptide Tur1A Inhibits Protein Synthesis by Targeting the Bacterial Ribosome. *Cell Chemical Biology*, 25(5), 530-539.

Matos, C., Moutinho, C., Lobão, P. (2012). Liposomes as a model for the biological membrane: studies on daunorubicin bilayer interaction, *The Journal of Membrane Biology*, 245(2), 69-75.

Mazzei, T., Mini, E., Novelli, A., Periti, P. (1993). Chemistry and mode of action of macrolides. *Journal of Antimicrobial Chemotherapy*, Suppl C, 1-9.

Menninger, J. R. (1995). Mechanism of inhibition of protein synthesis by macrolide and lincosamide antibiotics. *Journal of Basic and Clinical Physiology and Pharmacology*, 6(3-4), 229-250.

Mora-Ochomogo, M., Lohans, C. T. (2021). β -Lactam antibiotic targets and resistance mechanisms: from covalent inhibitors to substrates. *RSC Medicinal Chemistry*, 12, 1623-1639.

Morein S., Andersson A., Rilfors L., Lindblom G. (1996). Wild-type Escherichia coli cells regulate the membrane lipid composition in a "window" between gel and non-lamellar structures. *Journal of Biological Chemistry*, 271, 6801-6809.

Mortensen, N. P., Fowlkes, J. D., Sullivan, C. J., Allison, D. P., Larsen, N. B., Molin, S., Doktycz, M. J. (2009). Effects of colistin on surface ultrastructure and nanomechanics of Pseudomonas aeruginosa cells. *Langmuir*, 25(6), 3728-3733.

Mozafari, M. R. (2005). Liposomes: an overview of manufacturing techniques. *Cellular & Molecular Biology Letters*, 10(4), 711-719.

Mukhopadhyay, J., Sineva, E., Knight, J., Levy, R. M., Ebright, R. H. (2004). Antibacterial peptide microcin J25 inhibits transcription by binding within and obstructing the RNA polymerase secondary channel. *Molecular Cell*, 14(6), 739-751.

Navarro, J. F., Quereda, C., Quereda, C., Gallego, N., Antela, A., Mora, C., Ortuno, J. (1996). Nephrogenic diabetes insipidus and renal tubular acidosis secondary to foscarnet therapy. *American Journal of Kidney Diseases: the Official Journal of the National Kidney Foundation*, 27(3), 431-434.

Needham, D., Evans, E. (1988). Structure and mechanical properties of giant lipid (DMPC) vesicle bilayers from 20 degrees C below to 10 degrees C above the liquid crystal-crystalline phase transition at 24 degrees C. *Biochemistry*, 27(21), 8261-8269.

Nie, D., Hu, Y., Chen, Z., Li, M., Hou, Z., Luo, X., Mao, X., Xue, X. (2020). Outer membrane protein A (OmpA) as a potential therapeutic target for *Acinetobacter baumannii* infection. *Journal of Biomedical Science*, 27(1), 26.

Nielsen, J., Kwon, T.-H. Christense, B. M., Frøkiaer, J., Nielsen, S. (2008). Dysregulation of renal aquaporins and epithelial sodium channel in lithium-induced nephrogenic diabetes insipidus. *Seminars in Nephrology*, 28(3), 227-244.

Nikaido, H. (2003). Molecular basis of bacterial outer membrane permeability revisited. *Microbiology and Molecular Biology Reviews*, 67(4), 593-656.

Nikaido, H., Nakae, T. (1980). The Outer Membrane of Gram-negative Bacteria. *Advances in Microbial Physiology*, 20, 163-250.

Nilsson, A. Goodwin, R. J. A., Swales, J. G., Gallagher, R., Shankaran, H., Sathe, A., Pradeepan, S., Xue, A., Keirstead, N., Sasaki, J. C., Andren, P. E., Gupta, A. (2015). Investigating nephrotoxicity of polymyxin derivatives by mapping renal distribution using mass spectrometry imaging. *Chemical Research in Toxicology*, 28(9), 1823-1830.

O'Dwod H., Kim, B., Margolis, P., Wang, W., Wu, C., Lopez, S. L., Blais, J. (2007). Preparation of tetra-Boc-protected polymyxin B nonapeptide. *Tetrahedron Letters*, 48(11), 2003-2005.

Oh, J. T., Cajal, Y., Dhurjati, P. S., Van Dyk, T. K., Jain, M. K. (1998). Cecropins induce the hyperosmotic stress response in *Escherichia coli*. *Biochimica et Biophysica Acta*, 1415(1), 235-245.

Oh, J. T., Cajal, Y., Skowronska, E. M., Belkin, S., Chen, J., Van Dyk, T. K., Sasser, M., Jain, M. K. (2000). Cationic peptide antimicrobials induce selective transcription of *micF* and *osmY* in *Escherichia coli*. *Biochimica et Biophysica Acta*, 1463(1), 43-54.

Oh, J. T., Van Dyk, T. K., Cajal, Y., Dhurjati, P. S., Sasser, M., Jain, M. K. (1998). Osmotic stress in viable *Escherichia coli* as the basis for the antibiotic response by polymyxin B. *Biochemical and Biophysical Research Communications*, 246(3), 619-623.

Okada, M., Natori, S. (1983). Purification and characterization of an antibacterial protein from haemolymph of *Sarcophaga peregrina* (flesh-fly) larvae. *Biochemical Journal*, 211(3), 727-734.

Okimura, K., Ohki, K., Yuki, S., Kuniharu, O., Yoshiki, U., Naoki, S. (2007). Chemical Conversion of Natural Polymyxin B and Colistin to Their N-Terminal Derivatives. *Bulletin of the Chemical Society of Japan*, 80(3), 543-552.

Olson, F., Hunt, C. A., Szoka, F. C., Vail, W. J., Papahadjopoulos, D. (1979). Preparation of liposomes of defined size distribution by extrusion through polycarbonate membranes. *Biochimica et Biophysica Acta*, 557(1), 9-23.

Omardien, S., Drijfhout, J. W., Zaat, S. A., Brul, S. (2018). Cationic Amphipathic Antimicrobial Peptides Perturb the Inner Membrane of Germinated Spores Thus Inhibiting Their Outgrowth. *Frontiers in Microbiology*, 9, 2277.

Pankey, G. A., Sabath, L. D. (2004). Clinical relevance of bacteriostatic versus bactericidal mechanisms of action in the treatment of Gram-positive bacterial infections. *Clinical Infectious Diseases*, 38(6), 864-870.

Peetla, C., Stine, A., Labhasetwar, V. (2009). Biophysical interactions with model lipid membranes: applications in drug discovery and drug delivery. *Molecular Pharmaceutics*, 6(5), 1264-1276.

Peterson, J. W., Baron, S. (1996). Bacterial Pathogenesis (4th edition). *University of Texas Medical Branch at Galveston*, Galveston, TX (USA).

Pham, T. D. M., Ziora, Z. M., Blaskovich, M. A. T. (2019). Quinolone antibiotics. *Medicinal Chemistry Communications*, 10, 1719-1739.

Porro, M. (1993). Synthetic Peptides for Detoxification of Bacterial Endotoxins and Treatment of Septic Shock. World Patent Application WO 93/14115.

Porro, M., Terme, S. (1993). Synthetic Peptides for Detoxification of Bacterial Endotoxins and Treatment of Septic Shock. World Patent Application WO 93/14115.

Porro, M., Terme, S. (1995). Peptides for Neutralizing the Toxicity of Lipid A. World Patent Application WO 95/03327.

Porro, M., Terme, S., Vaara, M. (1996). Compositions Containing an Antibiotic and a Peptide Potentiating This Antibiotic. World Patent Application WO 96/38163.

Prien, E. (1945). The Mechanism of Renal Complications in Sulfonamide Therapy. *The New England Journal of Medicine*, 232, 63-68.

Pristovesk, P., Kidric, J. (1999). Solution structure of polymyxins B and E and effect of binding to lipopolysaccharide: an NMR and molecular modeling study. *Journal of Medicinal Chemistry*, 42(22), 4604-4613.

Pristovsek, P., Kidric, J. (2004). The search for molecular determinants of LPS inhibition by proteins and peptides. *Current Topics in Medicinal Chemistry*, 4(11), 1185-1201.

Pusey, C. D., Saltissi, D., Bloodworth, L., Rainford, D. J., Christie, J. L. (1983). Drug associated acute interstitial nephritis: clinical and pathological features and the response to high dose steroid therapy. *The Quarterly Journal of Medicine*, 52(206), 194-211.

Quale, J., Shah, N., Kelly, P., Babu, E., Backer, M., Rosas-Garcia, G., Salamera, J., George, A., Bratu, S., Landman, D. (2012). Activity of polymyxin B and the novel polymyxin analogue CB-182,804 against contemporary Gram-negative pathogens in New York City. *Microbial Drug Resistance (Larchmont, N.Y.)*, 18(2), 132-136.

Rabanal, F., Cajal, Y. (2017). Recent advances and perspectives in the design and development of polymyxins. *Natural Products Reports*, 34(7), 886-908.

Raetz, C. R. H., Whitfield, C. (2002). Lipopolysaccharide endotoxins. *Annual Review of Biochemistry*, 71, 635-700.

Ralph, E. D. (1978). The bactericidal activity of nitrofurantoin and metronidazole against anaerobic bacteria. *Journal of Antimicrobial Chemotherapy*, 4(2), 177-184.

Redelmeier, T. E., Hope, M. J., Cullis, P. R. (1990). On the mechanism of transbilayer transport of phosphatidylglycerol in response to transmembrane pH gradients. *Biochemistry*, 29, 3046–3053.

Reygaert, W. C. (2018). An overview of the antimicrobial resistance mechanisms of bacteria. *AIMS Microbiology*, 4(3), 482-501.

Rhouma, M., Beaudry, F., Thériault, W, Letellier, A. (2016). Colistin in Pig Production: Chemistry, Mechanism of Antibacterial Action, Microbial Resistance Emergence, and One Health Perspectives. *Frontiers in Microbiology*, 7, 1789.

Rossert, J. (2001). Drug-induced acute interstitial nephritis. *Kidney International*, 60(2001), 804-817.

Routledge, S. J., Linney, J. A., Goddard, A. D. (2019). Liposomes as models for membrane integrity. *Biochemical Society Transactions*, 47(3), 919-932.

Ruhemann, S. (1911). CXL11.-Triketohydrindene Hydrate. Part I V. Hydrindantin and its Analogues. *Journal of the Chemical Society*, 99(792), 1306-1486.

Ruiz-García, A., Bermejo, M., Moss, A., Casbo, V. G. (2008). Pharmacokinetics in Drug Discovery. *Journal of Pharmaceutical Sciences*, 97(2), 654-690.

Rustici, A., Velucchi, M., Faggioni, R., Sironi, M., Ghezzi, P., Quataert, S., Green, B., Porro, M. (1993). Molecular mapping and detoxification of the lipid A binding site by synthetic peptides. *Science*, 259(5093), 361-365.

Saborio, P., Tipton, G. A., Chan, J. C. (2000). Diabetes insipidus. *Pediatrics in Review*, 21(4), 122-129.

Sakura, N., Itoh, T., Uchida, Y., Ohki, K., Okimura, K., Chiba, K., Sato, Y., Sawanishi, H. (2004). The Contribution of the N-Terminal Structure of Polymyxin B Peptides to Antimicrobial and Lipopolysaccharide Binding Activity. *Bulletin of the Chemical Society of Japan*, 77(10), 1915-1924.

Salvioli G., Rioli G., Lugli R., Salati R. (1978). Membrane lipid composition of red blood cells in liver disease: regression of spur cell anaemia after infusion of polyunsaturated phosphatidylcholine. *Gut*, 19, 844-850.

Sampson, T. R., Liu, X., Schroeder, M. R., Kraft, C. S., Burd, E. M., Weiss, D. S. (2012). Rapid killing of *Acinetobacter baumannii* by polymyxins is mediated by a hydroxyl radical death pathway. *Antimicrobial Agents and Chemotherapy*, 56(11), 5642-5649.

Santer, M. (2009). Richard Bradley: A Unified, Living Agent Theory of the Cause of Infectious Diseases of Plants, Animals, and Humans in the First Decades of the 18th Century. *Perspectives in Biology and Medicine*, 52(4), 566-578.

Segovia, R., Solé, J., Marqués, A. M., Cajal, Y., Rabanal, F. (2021). Unveiling the Membrane and Cell Wall Action of Antimicrobial Cyclic Lipopeptides: Modulation of the Spectrum of Activity. *Pharmaceutics*, 13(12), 2180.

Selsted, M. E., Novotny, M. J., Morris, W. L., Tang, Y. Q., Smith, W., Cullor, J. S. (1991). Indolicidin, a novel bactericidal tridecapeptide amide from neutrophils. *Journal of Biological Chemistry*, 267(7), 4292-4295.

Shaw, D. (2010). Toxicological risks of Chinese herbs. *Planta Medica*, 76(17), 2012-2018.

Shenkarev, Z. O., Balandin, S. V., Trunov, K. I., Paramonov, A. S., Sukhanov, S. V., Barsukov, L. I., Arseniev, A. S., Ovchinnikova, T. V. (2011). Molecular Mechanism of Action of β -Hairpin Antimicrobial Peptide Arenicin: Oligomeric Structure in Dodecylphosphocholine Micelles and Pore Formation in Planar Lipid Bilayers. *Biochemistry*, 50(28), 6255-6265.

Shetty, N., Tang, J. W., Andrews, J. (2010). Infectious Disease: Pathogenesis, Prevention and Case Studies. *Emerging Infectious Diseases*, 16(1), 172-173.

Shimoda, M., Ohki, K., Shimamoto, Y., Kohashi, O. (1995). Morphology of defensin-treated *Staphylococcus aureus*. *Infection and Immunity*, 63(8), 2886-2891.

Silvius, J. R. (2005). Partitioning of membrane molecules between raft and non-raft domains: insights from model-membrane studies. *Biochimica et Biophysica acta*, 1746(3), 193-202.

Sines, G., Sakellarakis, Y. A. (1987). Lenses in Antiquity. *American Journal of Archaeology*, 91(2), 191-196.

Singer, S. J., Nicolson, G. L. (1972). The fluid mosaic model of the structure of cell membranes. *Science*, 175(4023), 720-731.

Sivanesan, S., Roberts, K., Wang, J., Chea, S. E., Thompson, P. E., Li, J., Nation, R. L., Velkov, T. (2017). Pharmacokinetics of the Individual Major Components of Polymyxin B and Colistin in Rats. *Journal of Natural Products*, 80(1), 225-229.

Slatore, C. G., Tilles, S. A. (2004). Sulfonamide hypersensitivity. *Immunology and Allergy Clinics of North America*, 24(3), 477-490.

Spížek, J., Řezanka, T. (2017). Lincosamides: Chemical structure, biosynthesis, mechanism of action, resistance, and applications. *Biochemical Pharmacology*, 133, 20-28.

Steiner, H., Hultmark, D., Engström, Å., Bennich, H., Boman, H. G. (1981). Sequence and specificity of two antibacterial proteins involved in insect immunity. *Nature*, 292, 246-248.

Strandberg, E., Tiltak, D., Ieronimo, M., Kanithasen, N. (2007). Influence of C-terminal amidation on the antimicrobial and hemolytic activities of cationic-helical peptides. *Pure and Applied Chemistry*, 79(4), 717-728.

Subbalakshmi, C., Sitaram, N. (1998). Mechanism of antimicrobial action of indolicidin. *FEMS Microbiology Letters*, 160(1), 91-96.

Su, L. Y., Willner, D. L., Segall, A. M. (2009). An antimicrobial peptide that targets DNA repair intermediates in vitro inhibits *Salmonella* growth within murine macrophages. *Antimicrobial Agents and Chemotherapy*, 54(5), 1888-1899.

Szoka, F., Papahadjopoulos, D. (1978). Procedure for preparation of liposomes with large internal aqueous space and high capture by reverse-phase evaporation. *Proceedings of the National Academy of Sciences of the United States of America*, 75(9), 4194-4198.

Takaoka, R., Kurosaki, H., Nakao, H., Ikeda, K. and Nakano, M. (2018). Formation of asymmetric vesicles via phospholipase D-mediated transphosphatidylation. *Biochimica et Biophysica Acta (BBA) - Biomembranes*, 1860, 245–249.

Talaro, K. P., Chess, B. (2008). Foundations in microbiology: basic principles. *McGray-Hill*, 8th edition.

Tian, C., Tétreault, E., Huang, C. K., Dahms, T. E. S. (2006). Electrostatic interactions of colicin E1 with the surface of *Escherichia coli* total lipid. *Biochimica et Biophysica Acta*, 1758(6), 693-701.

Trimble, M. J., Mlynářčík, P., Kolář, M., Hancock, R. E. W. (2016). Polymyxin: Alternative Mechanisms of Action and Resistance. *Cold Spring Harbor Perspectives in Medicine*, 6(10): a025288.

Tsubery, H., Ofek, I., Cohen, S., Fridkin, M. (2000). Structure activity relationship study of polymyxin B nonapeptide. *Advances in Experimental Medicine and Biology*, 479, 219-222.

Tsubery, H., Ofek, I., Cohen, S., Fridkin, M. (2000). Structure-function studies of polymyxin B nonapeptide: implications to sensitization of gram-negative bacteria. *Journal of Medicinal Chemistry*, 43(16), 3085-3092.

Tsubery, H., Ofek, I., Cohen, S., Fridkin, M. (2000). The functional association of polymyxin B with bacterial lipopolysaccharide is stereospecific: studies on polymyxin B nonapeptide. *Biochemistry*, 39(39), 11837-11844.

Tsubery, H., Yaakov, H., Cohen, S., Giterman, T., Matityahou, A., Fridkin, M., Ofek, I. (2005). Neopeptide antibiotics that function as opsonins and membrane-permeabilizing agents for gram-negative bacteria. *Antimicrobial Agents and Chemotherapy*, 49(8), 3122-3128.

Turaman, C. (2021). The Potential Uses of Insect Biochemicals in Medical Therapeutics. *American Journal of Pharmacology & Therapeutics*, 6(1), 9-18.

Vaara, M. (1991). The outer membrane permeability-increasing action of linear analogues of polymyxin B nonapeptide. *Drugs Under Experimental and Clinical Research*, 17(9), 437-443.

Vaara, M. (1992). Agents that increase the permeability of the outer membrane. *Microbiological Reviews*, 56(3), 395-411.

Vaara, M., Fox, J., Loidl, G., Siikanen, O., Apajalahti, J., Hansen, F., Frimodt-Møller, N., Nagai, J., Takano, M., Vaara, T. (2008). Novel polymyxin derivatives carrying only three positive charges are effective antibacterial agents. *Antimicrobial Agents and Chemotherapy*, 52(9), 3229-3236.

Vaara, M., Siikanen, O., Aajalahti, J., Fox, J., Frimodt-Møller, N., He, H., Poudyal, A., Li, J., Nation, R. L., Vaara, T. (2010). A novel polymyxin derivative that lacks the fatty acid tail and

carries only three positive charges has strong synergism with agents excluded by the intact outer membrane. *Antimicrobial Agents of Chemotherapy*, 54(8), 3341-3346.

Vaara, M., Vaara, T. (1983). Sensitization of Gram-negative bacteria to antibiotics and complement by a nontoxic oligopeptide. *Nature*, 303(5917), 526-528.

Van Bambeke, F., Glupczynski, Y., Mingeot-Leclercq, M. P., Tulkens, P. M. (2010). Infectious Diseases, *Elsevier*, 3rd edition, chapter 130: Mechanisms of action.

Vance, D. E., Vance, J. (1996). Biochemistry of Lipids, Lipoproteins and Membranes. *Elsevier Science*, Amsterdam (Netherlands).

Van-Hoek, A. H. A. M., Mevius, D., Guerra, B., Mullany, P., Roberts, A. P., Aarts, H. J. M. (2011). Acquired antibiotic resistance genes: An overview. *Frontiers in Microbiology*, 2, 203.

Vega, L. A., Caparon, M. G. (2012). Cationic antimicrobial peptides disrupt the *Streptococcus pyogenes* ExPortal. *Molecular Microbiology*, 85(6), 1119-1132.

Velkov, T., Roberts, K. D., Nation, R. J., Thompson, P. E., Li, J. (2013). Pharmacology of polymyxins: new insights into an 'old' class of antibiotics. *Future Microbiology*, 8(6), 711-724.

Velkov, T., Roberts, K. D., Nation, R. L., Wang, J., Thompson, P. E., Li, J. (2014). Teaching 'old' polymyxins new tricks: new-generation lipopeptides targeting gram-negative 'superbugs'. *ACS Chemical Biology*, 9(5), 1172-1177.

Velkov, T., Roberts, K. D., Thompson, P. E., Li, J. (2016). Polymyxins: a new hope in combating Gram-negative superbugs? *Future Medicinal Chemistry*, 8(10), 1017-1025.

Velkov, T., Thompson, P. E., Nation, R. L., Li, J. (2010). Structure—Activity Relationships of Polymyxin Antibiotics. *Journal of Medicinal Chemistry*, 53(5), 1898-1916.

Ventola, C. L. (2015). The antibiotic resistance crisis: part 1: causes and threats. *Pharmacy and Therapeutics*, 40(4), 277-283.

Virtanen, J. A., Cheng, K. H., Somerharju, P. (1998). Phospholipid composition of the mammalian red cell membrane can be rationalized by a superlattice model. *Proceedings of the National Academy of Sciences of the United States of America*, 95(9), 4964–4969.

Visser, P. C., Kriek, N. M. A. J., van Hooft, P. A. V., Van Schepdael, A., Filippov, D. V., van der Marel, G. A., Overkleeft, H. S., van Boom, J. H., Noort, D. (2008). Solid-phase synthesis of polymyxin B1 and analogues via a safety-catch approach. *The Journal of Peptide Research*, 61(6), 298-306.

Vogler, K., Studer, R. O. (1966). The chemistry of the polymyxin antibiotics. *Experientia*, 22(6), 345-354.

Vogler, K., Studer, R. O., Lanz, P., Lergier, W., Bohni, E. (1961). Total synthesis of two cyclodecapeptides exerting polymyxin-like activity. *Experientia*, 17, 223-224.

Wainwright, M. (1989). Moulds in ancient and more recent medicine. *Mycologist*, 3(1), 21-23.

Weber, E. J., Himmelfarb, J., Kelly, E. J. (2017). Concise Review: Current and Emerging Biomarkers of Nephrotoxicity. *Current Opinion in Toxicology*, 2017(4), 16-21.

Wehrstedt, K. D., Wandrey, P. A., Heitkamp, D. (2005). Explosive properties of 1-hydroxybenzotriazoles. *Journal of Hazardous Materials*, 126(1-3), 1-7.

Weinstein, J., Afonso, A., Moss Jr, E., Miller, G. H. (1998). Selective chemical modifications of polymyxin B. *Bioorganic & Medicinal Chemistry Letters*, 8(23), 3391-3396.

Wertheim, H., Van Nguyen, K., Hara, G. L., Gelband, H., Laxminarayan, R., Mouton, J., Cars, O. (2013). Global survey of polymyxin use: A call for international guidelines. *Journal of Global Antimicrobial Resistance*, 1(3), 131-134.

Wiederhold, N. P., Duperchy, E., Brown, P., Payne L. J., Dawson, M. J. (2015). Poster, F-734, 55th Interscience Conference on Antimicrobial Agents and Chemotherapy, San Diego, CA, USA.

Wiegand, I., Hilpert, K., Hancock, R E W. (2008). Agar and broth dilution methods to determine the minimal inhibitory concentration (MIC) of antimicrobial substances. *Nature Protocols*, 3(2), 163-175.

Wimley, W. C. (2015). Determining the Effects of Membrane-Interacting Peptides on Membrane Integrity. *Methods in molecular biology (Clifton, N.J.)*, 1324, 89-106.

Williams, K. J. (2009). The introduction of 'chemotherapy' using arsphenamine – the first magic bullet. *Journal of the Royal Society of Medicine*, 102(8), 343-348.

Witzke, N. M., Heding, H. (1976). Broad-spectrum derivatives of polymyxin B and colistin. *The Journal of Antibiotics*, 29(12), 1349-1350.

Wollman, A. J. M., Nudd, R., Hedlund, E. G., Leake, M. C. (2015). From Animaculum to single molecules: 300 years of the light microscope. *Open Biology*, 5(4), 150019.

Yadavalli, S. S., Carey, J. N., Leibman, R. S, Chen, A. I., Stern, A. M., Roggiani, M., Lippa, A. M., Goulian, M. (2016). Antimicrobial peptides trigger a division block in Escherichia coli through stimulation of a signalling system. *Nature Communications*, 7, 12340.

Yaeman, M. R., Yount, N. Y. (2003). Mechanisms of antimicrobial peptide action and resistance. *Pharmacological Reviews*, 55(1), 27-55.

Yim, H. H., Villarejo, M., (1992). osmY, a new hyperosmotically inducible gene, encodes a periplasmic protein in Escherichia coli. *Journal of Bacteriology*, 174(11), 3637-3644.

Yu, Z., Guo, C., Qiu, J. (2015). Precursor Amino Acids Inhibit Polymyxin E Biosynthesis in Paenibacillus polymyxa, Probably by Affecting the Expression of Polymyxin E Biosynthesis-Associated Genes. *BioMed Research International*, 2015, 690830.

Yu, Z., Qin, W., Lin, J., Fang, S., Ciu, J. (2015). Antibacterial mechanisms of polymyxin and bacterial resistance. *BioMed Research International*, 2015, 679109.

Zasloff, M. (2002). Antimicrobial peptides of multicellular organisms. *Nature*, 415, 389-395.

Zavascki, A. P., Nation, R. L. (2017). Nephrotoxicity of Polymyxins: Is There Any Difference between Colistimethate and Polymyxin B? *Antimicrobial Agents of Chemotherapy*, 61(3), e02319-e02316.

Zeisberg, M., Kalluri, R. (2015). Physiology of the Renal Interstitium. *Clinical Journal of the American Society of Nephrology: CJASN*, 10(10), 1831-1840.

Zeya, H. I., Spitznagel, J. K. (1963). ANTIBACTERIAL AND ENZYMIC BASIC PROTEINS FROM LEUKOCYTE LYSOSOMES: SEPARATION AND IDENTIFICATION. *Science*, 142(3595), 1085-1087.

Zhang, L., Dhillon, P., Farmer, S., Hancock, R. E. (2000). Interactions of bacterial cationic peptide antibiotics with outer and cytoplasmic membranes of Pseudomonas aeruginosa. *Antimicrobial Agents and Chemotherapy*, 44(12), 3317-3321.

Zhang, L., Rozek, A., Hancock, R. E. (2001). Interaction of cationic antimicrobial peptides with model membranes. *The Journal of Biological Chemistry*, 276(38), 35714-35722.

Zhang, R., Shen, Y., Walsh, T. R., Wang, Y., Hu, F. (2020). Use of polymyxins in Chinese hospitals. *The Lancet Infectious Diseases*, 20(10), 1125-1126.

Zhu, J., Hu, C., Zeng, Z., Deng, X., Zeng, L., Xie, S., Fang, Y., Alezra, V., Wan, Y. (2021). Polymyxin B-inspired non-hemolytic tyrocidine A analogues with significantly enhanced activity against gram-negative bacteria: How cationicity impacts cell specificity and antibacterial mechanism. *European Journal of Medicinal Chemistry*, 221, 113488.

Zimmerberg, J., Vogel, S. S., Chernomordik, L. V. (1993). Mechanism of membrane fusion. *Annual Review of Biophysics and Biomolecular Science*, 22(1), 433-466.

Zgurskaya, H. I., López, C. A., Gnanakaran, S. (2015). Permeability Barrier of Gram-Negative Cell Envelopes and Approaches To Bypass It. *ACS Infectious Diseases*, 1(11), 512-522.